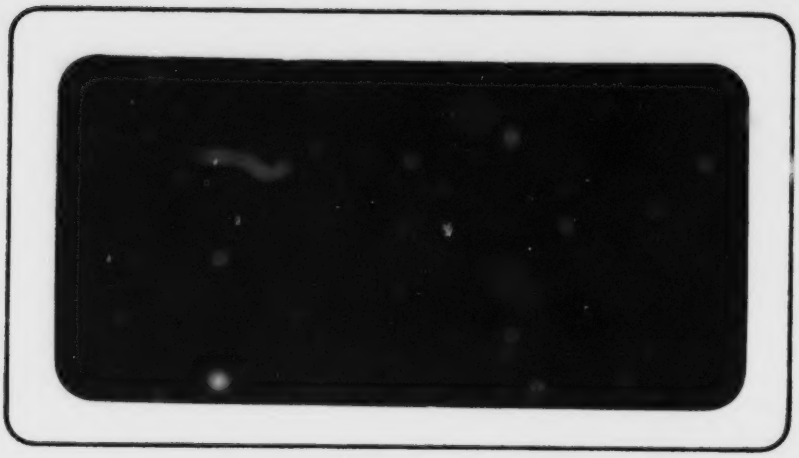

MACDONALD DETTWILER AND ASSOCIATES LTD.

Suite 210 – 955 Green Valley Crescent
Ottawa, Ontario, Canada K2C 3V4
Telephone (613) 226-2701 / Telefax (613) 226-2271

CA1
DTC800-
89
F27

427189

41.D

TP 9602E

FEASIBILITY STUDY OF A WIND SHEAR/ MICROBURST DETECTION, ANALYSIS, AND ADVANCE WARNING SYSTEM FOR CANADIAN AIRPORTS

FINAL REPORT

Prepared for

Transportation
Development Centre
Policy and Coordination Group
Transport Canada

by

MacDonald Dettwiler and Associates Ltd.
955 Green Valley Crescent, Suite 210
Ottawa, Ontario, Canada K2C 3V4
Telephone (613) 226-2701 Telefax 226-2271

MARCH 1989

TP 9602E

FEASIBILITY STUDY OF A WIND SHEAR/MICROBURST DETECTION, ANALYSIS AND ADVANCE WARNING SYSTEM FOR CANADIAN AIRPORTS

FINAL REPORT

by

Dr. Geoff Austin, Douglas Ballantyne, Karl Snider
MacDonald Dettwiler and Associates Ltd.

Reference: WI-RP-MDA-SY-0001

MARCH 1989

DISCLAIMER

The contents of this report reflect the views of MacDonald Dettwiler and Associates Ltd. and not necessarily the official view or opinions of Transport Canada.

LANGUAGE NOTICE

Un sommaire en français de ce rapport est inclus avant la Table des matières.

Transport Canada / Transports Canada

PUBLICATION DATA FORM

1. Transport Canada Publication No.	2. Project No.	3. Recipient's Catalogue No.
TP 9602E	6791	

4. Title and Subtitle

Feasibility Study of a Wind Shear/Microburst Detection, Analysis, and Advance Warning System For Canadian Airports

5. Publication Date

March 1989

6. Performing Organization Document No.

WI-RP-MDA-SY-001

7. Author(s)

Dr. Geoff Austin, Douglas Ballantyne, Karl Snider

8. Transport Canada File No.

D1455-186

9. Performing Organization Name and Address

MacDonald Dettwiler and Associates Ltd.
955 Green Valley Crescent, Suite 210
Ottawa, Ontario
K2C 3V4

10. DSS File No.

11SD.T8200-6-6547-A

11. DSS or Transport Canada Contract No.

T8200-6-6547/01/SD

12. Sponsoring Agency Name and Address

Transportation Development Centre (TDC)
200 René-Lévesque Boulevard, West
West Tower, Suite 601
Montréal, Québec H2Z 1X4

13. Type of Publication and Period Covered

Final

14. Project Officer

H. Posluns

15. Supplementary Notes (Funding programs, titles of related publications, etc.)

16. Abstract

Transport Canada's requirements for a wind shear/microburst detection system are established. The meteorological causes of wind shear are described, including a detailed discussion of microbursts. Current wind shear/microburst detection technologies are described and assessed. A system consisting of Doppler radar and low level sensors is proposed to meet Transport Canada's requirements. The authors conclude that a wind shear/microburst detection system is feasible for less than $1,000,000 per installation. Recommendations include further investigation of microburst occurrence in Canada and development of a prototype system.

17. Key Words	18. Distribution Statement
Wind Shear, Aviation, Airports, Microbursts	Limited number of copies available from the Transportation Development Centre

19. Security Classification (of this publication)	20. Security Classification (of this page)	21. Declassification (date)	22. No. of Pages	23. Price
Unclassified	Unclassified		187	

TDC/CDT 79-005
Rev 88

Canada

Transports Canada Transport Canada

FORMULE DE DONNÉES POUR PUBLICATION

1. N° de la publication de Transports Canada	2. N° de l'étude	3. N° de catalogue du destinataire
TP 9602E	6791	

4. Titre et sous-titre	5. Date de la publication
Feasibility Study of a Wind Shear/Microburst Detection, Analysis, and Advance Warning System for Canadian Airports	Mars 1989
	6. N° du document de l'organisme exécutant: WI-RP-MDA-SY-001
7. Auteur(s): Dr. Geoff Austin, Douglas Ballantyne, Karl Snider	8. N° de dossier — Transports Canada: D1455-186
9. Nom et adresse de l'organisme exécutant: MacDonald Dettwiler and Associates Ltd. 955 Green Valley Crescent, Suite 210 Ottawa, Ontario K2C 3V4	10 N° de dossier — ASC: 11SD.T8200-6-6547-A
	11. N° de contrat — ASC ou Transports Canada: T8200-6-6547/01-SD
12. Nom et adresse de l'organisme parrain: Centre de développement des transports (CDT) 200 ouest, boulevard René-Lévesque Tour ouest, suite 601 Montréal, Québec H2Z 1X4	13. Genre de publication et période visée: Final
	14. Agent de projet: H. Posluns

15. Remarques additionnelles (Programmes de financement, titres de publications connexes, etc.)

16. Résumé

Transport Canada a fait connaitre ses exigences en ce qui concerne le système de détection des microrafales et de l'effet de cisaillement du vent. Le présent document décrit le causes météorologiques de l'effet du cisaillement; on y trouve également une description détaillée des microrafales, ainsi qu'unee description et une évaluation des technologies actuelles de détection des microrafales et de l'effet de cisaillement du vent. On y propose un système consistant en un radar Doppler et des détecteurs à basse altitude pour satisfaire aux exigences de Transport Canada. Les auteurs concluent qu'il est possible de mettre au point un système de détection des microrafales et de l'effet de cisaillement du vent pour moins de 1 000 000 $ par installation. On recommande des études plus avançées sur l'incidence de microrafales au Canada, ainsi que sur las mise au point d'un prototype du système.

17. Mots clés	18. Diffusion
L'effet de cisaillement du vent, Microrafales, Aviation, Aéroports	Le Centre de développement des transports dispose d'un nombre limité d'exemplaires.

19. Classification de sécurité (de cette publication)	20. Classification de sécurité (de cette page)	21. Déclassification (date)	22. Nombre de pages	23. Prix
non classifiée	non classifiée		187	

CDT/TDC 79-005 Rev 88

Canada

EXECUTIVE SUMMARY

Problem Statement

Hazardous wind shear conditions have been linked to the meteorological phenomena known as microbursts. Microbursts, and the associated wind shear conditions, are difficult to predict with the detection technology currently available at Canadian airports.

The purpose of this study was to examine the feasibility of a wind shear/microburst detection system for use at Canadian airports.

User Requirements

Six user requirements for the wind shear/microburst detection system were established by Transport Canada. These requirements included cost, coverage and functionality of a wind shear/microburst detection system. In brief, the requirements define a system costing less than $1,000,000 which would detect wind shear within a 15 km radius, to an altitude of 1000 m.

Meteorological Aspects

Wind shear is the vector difference between two observed wind vectors, divided by the distance between the two points of measurement. A wind shear of sufficient magnitude over a sufficient distance will pose a hazard to aviation.

Microbursts have been identified as a primary cause of hazardous wind shear. Microbursts are strong downdraughts, of short duration, which induce an outflow of damaging winds on, or near, the ground. Both wet and dry microbursts are possible. Wet microbursts are usually accompanied by heavy precipitation, whereas with dry microbursts the rain or water content has evaporated before reaching the earth's surface.

Microbursts are usually associated with convective storms, particularly thunderstorms.

The microburst studies documented in the literature have all taken place in the United States, therefore the incidence and type of microbursts which may occur in Canada are not known by direct observation of the phenomena. The probability of microbursts occurring at Canadian airports can be deduced in part by examination of meteorological information such as thunderstorm days at Canadian airports.

Technical Review

When attempting to detect the wind shear present in microbursts, the surveillance system may be in fact observing:

- the wind shear itself, by direct measurement of relative wind velocities;
- the microburst, by measurement of meteorological parameters correlated with microbursts (e.g. temperature change, pressure change, etc.);
- the existence of the weather formation (e.g. detecting wet microbursts via radars return from the raindrops).

Possible detection technologies include:

- visual observation
- anemometers, weather vanes, and microbarographs
- wind profilers
- airborne sensors
- Doppler radar
- rawinsondes
- acoustic radars (sodars)
- satellite instrumentation
- lidars

Technology Assessment

Doppler radar appears to be the most suitable technology for the detection of microbursts. Doppler radar can be used to measure relative wind velocity (by measuring the Doppler shift), and can detect refractive index changes due to temperature and humidity variations. The use of Doppler radar to detect microbursts and associated wind shear is currently being studied in the U.S.

Anemometers, weather vanes and microbarographs provide surface meteorological measurement. These sensors are currently used in Low Level Wind Shear Alert Systems (LLWAS). These sensors provide vital data for the measurement and detection of low level wind shear.

As a result of the technology assessment, the recommended approach for a conceptual design is a hybrid system containing both Doppler radar and LLWAS technology.

Conceptual Design

The recommended detection system is an integrated LLWAS and Doppler radar. The LLWAS will consist of six to eleven remote weather stations and a central base station. Each of the remote stations is monitored once every 10 seconds transferring information relating to temperature,

pressure, wind speed and direction, and relative humidity. Each station's sensed values are compared to the airport average and, if a threshold is exceeded, an alarm is raised. The Doppler radar sensor is used in the detection of the impending microburst as it descends from above.

The radar data is transferred to the display processor where it is correlated with the LLWAS information. A range azimuth presentation is displayed on a colour monitor depicting the various wind velocities by means of colour definition. If a wind shear/microburst condition is detected, an aural and visual alarm is generated and its relative location is indicated.

Cost Analysis

A system production cost analysis was performed with an estimate developed for each major sub-group. These sub-group costs are summarized in the following:

Doppler Radar	
Antenna Group	$236,000
Transmitter/Receiver Group	$300,000
Signal Processor Group	$ 70,000
Facility Shelter	$ 18,000
LLWAS	
11 Station System	$310,000
Total	$934,000
Non-recurring Engineering (NRE)	810,000

The NRE includes software development for the signal processor and the display processor, system integration, antenna and RF feed re-design, and preliminary system evaluation and testing. The major NRE expense is $560,000 relating to the development of the transmitter/receiver prototype. This would include a deliverable item that could be integrated with the Doppler processor for complete system testing and evaluation.

Conclusions

1. Future work in this area would benefit from an analysis of wind shear/microburst data collected at Canadian airports.

2. The microburst phenomenon is not easily characterized by a definitive set of meteorological parameters.

3. Several technologies exist for measuring and monitoring various meteorological parameters but there is no single technology capable

of meeting Transport Canada's requirements for wind shear/microburst detection.

4. Doppler radar and LLWAS systems provide the best complimentary capabilities to solve this requirement.

5. The proposed wind shear/microburst detection system can be built with a large complement of off-the-shelf components from Canadian companies.

6. It appears feasible to install a wind shear detection system at an airport for $1,000,000. Initially, however, approximately $1,000,000 in non-recurring engineering costs would be required to develop such a system.

Recommendations

1. Install an LLWAS system at a Canadian airport for collecting meteorological data on wind shear/microbursts. This will help to determine the extent of the wind shear problem in Canada.

2. Develop and evaluate (laboratory and in-situ) a prototype integrated Doppler radar/LLWAS.

3. Define suitable wind shear detection algorithms for use in a detection system, with consideration given to expert systems and developments in the NEXRAD and TDWR systems.

SOMMAIRE

Énoncé du problème

Des conditions dangereuses de cisaillement du vent ont été reliées aux phénomènes météorologiques connus sous le nom de microrafales. Il est difficile, à l'aide de la technologie de détection présentement disponible dans les aéroports canadiens, d'élaborer des prévisions sur les microrafales et les conditions de cisaillement qui y sont reliées.

La présente étude vise à considérer la viabilité de la mise au point d'un système de détection des microrafales et de l'effet du cisaillement du vent qui pourra être mis en service dans les aéroports canadiens.

Exigences des utilisateurs

Transport Canada a dressé une liste de six exigences pour les utilisateurs d'un système de détection des microrafales et de l'effet du cisaillement du vent. Ces exigences incluent le coût, la portée et l'utilité fonctionnelle d'un tel système. En bref, ces exigences prévoient un système qui coûte moins de 1 000 000 $, et qui soit capable de détecter des effets de cisaillement dans un rayon de 15 km et à une altitude maximale de 1 000 mètres.

Aspects météorologiques

L'effet de cisaillement du vent est la différence angulaire entre deux vecteurs de vents divisée par la distance entre les deux points de mesure. Les effets de cisaillement du vent dépassant un certain niveau d'intensité, relevés sur distance donnée, présentent des dangers pour l'aviation.

Il a été déterminé que les microrafales sont les causes principales des effets dangereux de cisaillement du vent. Les microrafales sont de forts courants descendants, de courte durée, qui provoquent des rafales de vents dangereuses au niveau du sol, ou juste au-dessus. Les microrafales peuvent être accompagnées ou non de précipitations. Lorsqu'elles le sont, les précipitations sont abondantes. Dans le cas contraire, le contenu en eau s'est évaporé.

En règle générale, les microrafales accompagnent les tempêtes d'origine convectionnelle, plus particulièrement les orages.

Toutes les études publiées sur les microrafales ont été faites aux États-Unis. C'est-à-dire que les types et les incidences de microrafales pouvant se produire au Canada n'ont pas été observés directement. On peut déduire en partie les probabilités de microrafales au Canada en examinant des données météorologiques, par exemple, en étudiant les jours d'orages aux aéroports canadiens.

Étude technique

En tentant de détecter l'effet de cisaillement présent dans les microrafales, le système de détection pourrait en fait être en train d'observer:

- l'effet de cisaillement du vent lui-même, par la mesure directe des vitesses relatives des vents;
- la microrafale elle-même, en mesurant les paramètres météorologiques qui y sont reliés (entre autres, les changements de température et de pression atmosphérique);
- l'existence de la formation atmosphérique (par exemple, la détection de microrafales accompagnées de précipitations au moyen des réflexions d'ondes radar sur les goutelettes de pluie).

Les techniques de détection suivantes sont envisageables:

- l'observation visuelle;
- les anémomètres, girouettes et microbarographes;
- les instruments de mesure de profil du vent;
- les détecteurs aériens;
- les radar Doppler;
- les sondes radiovent;
- les radars acoustiques (sodars)
- les instruments à bord de satellites;
- les lidars.

Évaluations des technologies

Les radars Doppler semblent représenter la technologie la plus appropriée pour la détection de microrafales. Ces appareils peuvent mesurer les vitesses relatives des vents (en mesurant le décalage appelé effet Doppler) et ils peuvent également mesurer les changements d'index de réfraction attribuables aux variations de température et d'humidité. On étudie actuellement aux États-Unis la possibilité d'utiliser les radars Doppler pour détecter les microrafales et les effets de cisaillement du vent qui y sont reliés.

Les anémomètres, girouettes et microbarographes permettent de mesurer les paramètres météorologiques à la surface du sol. Ces détecteurs sont mis en service à l'heure actuelle dans les systèmes d'alerte de cisaillement du vent à basse altitude. Ces détecteurs produisent des données vitales en ce qui concerne la mesure des vélocités des vents et la détection.

Après avoir évalué toutes les technologies disponibles, il est recommandé d'envisager la conception d'un système qui pourrait intégrer les radars Doppler et les technologies reliées aux systèmes d'alerte de cisaillement du vent à basse altitude.

Conception du projet

Le système de détection recommandé est un système qui intègre les technologies des systèmes LLWAS et de radar Doppler. La portion LLWAS du système comporte l'installation de six a onze stations météorologiques éloignées l'une de l'autre et une station de base centrale. Chacune des stations distantes est interrogée à toutes les 10 secondes et transmet des données sur la température, la pression atmospérique, la vitesse du vent et sa direction, et l'humidité relative. Les données recueillies par chaque station sont comparées à la moyenne recueillie à l'aeroport et une alarme est généréé si ces données dépassent un seuil prédéterminé. Le détecteur radar Doppler aide à la détection de la microrafale imminente, au moment où elle est en train de descendre.

Les données en provenance du radar sont transférées au processeur d'affichage, où elles sont mises en corrélation avec les données en provenance des composants. Un écran couleur permet l'affichage d'un ensemble azimut-distance, qui attribue des couleurs différentes aux diverses vitesses des vents. Le système donne la position de toute condition de microrafale et l'effet de cisaillement du vent détectée, et il génère des alarmes sonore et visuelle à cet effet.

Analyse des coûts

Voici le résumé des frais estimatifs de production de chaque sous-groupe principal:

Radar Doppler	
Groupe antenne	236 000 $
Groupe émetteur-récepteur	300 000 $
Groupe de traitement de signal	70 000 $
Abri des installations	18 000 $
LLWAS	
Système de 11 stations	310 000 $
Total	934 000 $
Frais d'ingénierie non récurrents	810 000 $

Les frais d'ingénierie non récurrents comprennent la mise au point du processeur de signal et du processeur d'affichage, l'intégration du système, la modification de la conception de l'antenne ainsi que de l'alimentation RF, de même que l'évaluation et les essais préliminaires du système. La plus grande dépense, soit 560 000 $, est attribuable à la mise au point du prototype de l'émetteur-récepteur et elle couvre la livraison de l'article, qu'il sera possible d'intégrer au processeur Doppler aux fins d'évaluation et des essais complets du système.

Conclusions

1. Les travaux futurs bénéficieraient de l'analyse de données sur les microrafales et l'effet de cisaillement du vent recueillies aux aéroports canadiens.

2. Le phénomène des microrafales ne se caractérise pas facilement par un ensemble fixe et définitif de paramètres météorologiques.

3. Il existe plusieurs technologies propres à la mesure et à la vérification des divers paramétres météorologiques, mais il n'en existe pas une qui soit capable à elle seule de satisfaire aux exigences de Transport Canada en ce qu'il s'agit de la détection des microrafales et de l'effet de cisaillement du vent.

4. Les systèmes radar Doppler et LLWAS utilisés ensemble offrent les meilleures possibilités pour résoudre ce problème.

5. Le système de détection des microrafales et de l'effet du cisaillement du vent proposé peut être construit à l'aide de composants commerciaux qu'il est facile de se procurer auprès de firmes canadiennes.

6. Il semble possible d'installer un système de détection des microrafales et de l'effet de cisaillement du vent dans les aéroports canadiens au coût de 1 000 000 $. Cependant, il faut prévoir environ 1 000 000 $ supplémentaires en frais d'ingénierie non récurrents pour mettre au point un tel système.

Recommandations

1. Installer un système LLWAS dans un aéroport canadien aux fins de réunir des données météorologiques sur les microrafales et l'effet de cisaillement du vent. Cela permettra de déterminer l'étendue du problème que présente l'effet de cisaillement du vent au Canada.

2. Mettre au point et évaluer (en laboratoire et sur le terrain) un prototype de système de détection intégré radar Doppler/LLWAS.

3. Mettre au point les algorithmes appropriés pour un système de détection des microrafales et de l'effet de cisaillement du vent, en tenant compte des derniers développements en matière de systèmes experts, ainsi que des systèmes NEXRAD et TDWR.

TABLE OF CONTENTS

1. INTRODUCTION 1
   1.1 Purpose 1
   1.2 Scope 1
   1.3 Limitations 1
   1.4 Study Overview 1
      1.4.1 User Requirements 1
      1.4.2 Technical Specifications 1
      1.4.3 Technology Evaluation 2
      1.4.4 Conceptual Design 2
      1.4.5 Costing 2
      1.4.6 Conclusions 2

2. USER REQUIREMENTS 3
   2.1 General Requirements 3
   2.2 Operational/Functional Requirements 3
   2.3 Technical Constraints 4
   2.4 Environmental Constraints 8
      2.4.1 Class 1 Surface Mobile 8
      2.4.2 Class 2 Outdoor (Exposed) 8
      2.4.3 Class 3 Fixed Sheltered (Unheated) 8
      2.4.4 Class 4 Fixed Sheltered (Heated) 8
      2.4.5 Class 5 Fixed Sheltered (Heated and Cooled) 8
      2.4.6 Class 6 Fixed Sheltered (Conditioned) 8

3. TECHNICAL SPECIFICATIONS 12
   3.1 Meteorological Review 12
      3.1.1 Definitions 12
      3.1.2 The Normal Atmosphere 15
      3.1.3 The Causes of Low Level Wind Shear 22
      3.1.4 Climatology of Thunderstorms 36
   3.2 Wind Shear Parameters 39
      3.2.1 Normal Strong Wind 39
      3.2.2 Obstacle Wind Shear 42
      3.2.3 Gust Fronts, Downbursts, Macrobursts, and Microbursts 42
      3.2.4 Severity of Shear 42

3.3 Microburst Parameters 44
3.3.1 Diurnal Characteristics 47
3.3.2 Duration 47
3.3.3 Size 47
3.3.4 Wind Speed 47
3.3.5 Air Temperature 48
3.3.6 Pressure 48
3.3.7 Dew-Point Temperature 48
3.3.8 Rainfall 48
3.3.9 Dust and Bugs 50
3.4 Review of Detection Technology 50
3.4.1 Visual Observation 52
3.4.2 Anemometers, Weather Vanes, and Microbarographs .. 52
3.4.3 Wind Profilers 56
3.4.4 Airborne Sensors 59
3.4.5 Doppler Radar 65
3.4.6 Rawinsondes 68
3.4.7 Acoustic Radar (SODAR - SOund Detection And Ranging) 71
3.4.8 Satellite Instrumentation 76
3.4.9 Lidars (LIght Detection and Ranging) 78
3.5 Derived Requirements 81
3.5.1 LLWAS Specifications 81
3.5.2 Wind Profiler Specifications 82
3.5.3 Sodar Specifications 83
3.5.4 Doppler Radar Specifications 84
3.5.5 Rawinsonde Specifications 87
3.5.6 Airborne Sensor Specifications 88
3.5.7 Lidar Specifications 88
3.5.8 Generic Specifications 89

4. TECHNOLOGY EVALUATION 91
4.1 Introduction 91
4.2 General Discussions 92
4.3 Review and Analysis 96
4.3.1 Visual Observation 96
4.3.2 Anemometers, Weather Vanes and Microbarographs ... 98
4.3.3 Wind Profilers 98
4.3.4 Airborne Sensors 101
4.3.5 Doppler Radar 101
4.3.6 Rawinsondes 102
4.3.7 Sodars 102
4.3.8 Satellite Instrumentation 106
4.3.9 Lidars 106
4.4 Recommendation for an Appropriate Technology 109

5. CONCEPTUAL DESIGN FOR A WIND SHEAR DETECTION SYSTEM 110
5.1 System Overview 110
5.2 LLWAS Subsystem Description 110
5.2.1 Sensors and Associated Protection Devices 110
5.2.2 Data Collection and Processing Unit 113

5.2.3 Central Processing Unit 114
5.3 Doppler Radar Subsystem Description 114
5.3.1 General Discussion 114
5.3.2 Parameter Selection 115
5.3.3 Antenna Scan Rate and Pattern Selection 128
5.3.4 Functional Components 131
5.4 Conceptual Design Summary 137
5.5 Overall Recommendations 137

6. COST ANALYSIS 139
6.1 LLWAS Costs 139
6.2 Doppler Radar Costs 139
6.2.1 Antenna Group 142
6.2.2 Transmitter Receiver Group 143
6.2.3 Signal Processor Group 144
6.2.4 Facility Shelter 145
6.3 Canadian Industry Capability 145
6.4 Cost Summary 145

7. CONCLUSIONS AND RECOMMENDATIONS 149

REFERENCES 150

GLOSSARY 154

BIBLIOGRAPHY 156

LIST OF FIGURES

Figure 3-1	Geometrical construction for the sum and difference between two wind vectors $\overline{v}_1$ and $\overline{v}_2$	14
Figure 3-2	Graphic illustration of the parameters used in the derivation of the gradient wind equation	16
Figure 3-3	Theoretical wind profiles due to surface friction and geostrophic wind aloft - surface boundary layer	19
Figure 3-4	Theoretical change in wind speed and direction with height - Ekman layer wind profile	20
Figure 3-5	Wind flow around surface frontal systems	21
Figure 3-6	Obstacle wind flows: typical situations where fixed objects near runways can produce wind shear	24
Figure 3-7	Major wind patterns in a typical gust front	28
Figure 3-8	Gust front development over time	29
Figure 3-9	Surface winds associated with a particular microburst	31
Figure 3-10	Microburst wind analysis - 3 dimensional visualization of the structure of a microburst	33
Figure 3-11	Time history of a microburst as deduced from TV image analysis	34
Figure 3-12	Simplified air flow diagram, showing the rotational nature of microburst air flow	35
Figure 3-13	Boundary layer wind shear	40
Figure 3-14	Gust front eddies due to rough terrain - simplified view	41
Figure 3-15	Microburst wind analysis	43
Figure 3-16	Actual meteorological parameter measurement for a documented microburst occurrence	46
Figure 3-17	Pressure profiles across various portions of a microburst	49
Figure 3-18	Stages of a descending microburst	54

Figure 3-19	LOLA (Low Level Alert System)	55
Figure 3-20	Wind profiler system	57
Figure 3-21	American wind profiler network grid sites	58
Figure 3-22	Continuous atmospheric profiler radar system (CAPSONDE) antenna coverage pattern	60
Figure 3-23	Continuous atmospheric profiler radar system (CAPSONDE) typical Yagi antenna array	61
Figure 3-24	Functional block diagram of Safe Flight's airborne wind shear detection system	63
Figure 3-25	Sundstrand's airborne wind shear detection system	64
Figure 3-26	Rawinsonde operation principle	69
Figure 3-27	Meteorological presentation from rawinsonde data	70
Figure 3-28	Doppler Sodar configuration	72
Figure 3-29	Alternate Sodar configuration	73
Figure 3-30	Sodar data presentation	74
Figure 3-31	AeroVironment Inc. Sodar	75
Figure 3-32	Megasodar glidepath system	77
Figure 3-33	General configuration of a Lidar system	80
Figure 4-1	MLS signal coverage	93
Figure 4-2	External sensor coverage	94
Figure 4-3	Internal sensor coverage	95
Figure 4-4	Glidepath elevation at 15 km range	97
Figure 4-5	Integrated Sodar and LLWAS detection systems	105
Figure 5-1	Atmospheric coefficients for oxygen and water vapour combined at standard sea-level temperature and pressure	116
Figure 5-2	Attenuation versus frequency	119
Figure 5-3	Radar resolution cell to determine the radar cross section of rain	125

Figure 5-4	Typical microburst subtended angle	129
Figure 5-5	Radar processing system block diagram	134
Figure 6-1	Proposed wind shear detection system	140
Figure 6-2	Possible remote station locations at the Ottawa International Airport	141
Figure 6-3	Block diagram of DSP application development module (Motorola)	146

LIST OF TABLES

Table 2-1	Existing Frequency Assignments	5
Table 2-2	Class 1 and 2 Environmental Requirements	10
Table 2-3	Class 3 and 4 Environmental Requirements	11
Table 2-4	Class 5 and 6 Environmental Requirements	11
Table 3-1	Distribution and Causes of U.S. Wind Shear Accidents and Incidents (1959 - 1983)	23
Table 3-2	Monthly and Annual Mean Number of Days with Thunderstorms at Selected Canadian Airports	37
Table 3-3	Monthly and Annual Mean Number of Days with Thunderstorms at Selected American Airports	38
Table 3-4	Typical Microburst Parameters	45
Table 4-1	LLWAS Capabilities Review	99
Table 4-2	Wind Profiler Capabilities Review	100
Table 4-3	Doppler Radar Capabilities Review	103
Table 4-4	Sodar Capabilities Review	104
Table 4-5	Lidar Capabilities Review	107
Table 4-6	Atmospheric Propagation	108
Table 5-1	Elevation Above Sea Level (ASL) of Major Canadian Airports	112
Table 5-2	Atmospheric Attenuation over 35 km Two-way Path	117
Table 5-3	Rain Attenuation with Respect to Frequency One-way Propagation	120
Table 5-4	Range Velocity Ambiguities	123
Table 5-5	Pulses on Target	130
Table 5-6	Antenna Electrical Characteristics	132
Table 6-1	Canadian Suppliers and Vendors	147
Table 6-2	Cost Summary	148

LIST OF ABBREVIATIONS, ACRONYMS, AND SYMBOLS

A/D	Analog to Digital
ADF	Automatic Direction Finder
ALWAS	Advanced LLWAS
ASCII	American Standard Code for Information Interchange
ASL	Above Sea Level
C	Celsius
CDT	Central Daylight Time
CFAR	Constant False Alarm Rate
CLAWS	Classify, Locate and Avoid Wind Shear
cm	Centimetre
CPU	Central Processing Unit
CW	Continuous Wave
COHMEX	Cooperative Huntsville Meteorological Experiment
dBz	Measure of Radar Reflectivity
DFT	Discrete Fourier Transform
DME	Distance Measuring Equipment
ELT	Emergency Locator Transmitter

EMC	Electromagnetic Compatibility
FAA	Federal Aviation Administration
FFT	Fast Fourier Transform
FLOWS	Federal Aviation Administration - Lincoln Laboratory Operational Weather Studies
FM	Frequency Modulation
ft	Feet
g	Gravitational Constant (approximately 9.8 m/s^2)
GHz	GigaHertz
GOES	Geosynchronous Operational Environmental Satellite
GPWS	Ground Proximity Warning System
Hz	Hertz
H.F.	High Frequency
IC	Integrated Circuit
ICAO	International Civil Aviation Organization
ILS	Instrument Landing System
IR	Infrared
JAWS	Joint Airport Weather Studies
kHz	KiloHertz
km/h	Kilometres per hour
Knots	Nautical miles per hour
kt	Knot
kw	Kilowatts
LIDAR	Light Detection and Ranging
LLWAS	Low Level Wind Shear Alert System
LNA	Low Noise Amplifier

LOLA	Low Level Alert
μm	Micrometre
m	Metre
MaPS	Magnetron Phase Stabilizer
m/s	Metres per second
mb	Millibars
MDS	Minimum Discernable Signal
MHz	MegaHertz
MIST	Microburst and Severe Thunderstorm experiments
MLS	Microwave Landing System
mm/Hg	Millimetres of Mercury
mpm	Metres per minute
msec	Millisecond
μsec	Microsecond
MTBF	Mean Time Between Failures
Mw	Megawatts
NIMROD	Northern Illinois Meteorological Research on Downburst
NCAR	National Centre for Atmospheric Research
NEXRAD	Next Generation Weather Radar
NOAA	National Oceanic and Atmospheric Administration
NRE	Non-recurring Engineering
nsec	nanosecond
PAM	Portable Automated Mesonet
PC	Personal Computer
Pt	Point
Pk	Peak

pps	Pulses per second
PRF	Pulse Repetition Frequency
RAMP	Radar Modernization Project
RF	Radio Frequency
RH	Relative Humidity
rpm	Revolutions per minute
Rx	Receive
sec	Second
SODAR	Sound Detection and Ranging
SSR	Secondary Surveillance Radar
STALO	Stable Local Oscillator
TACAN	Tactical Air Navigation Aid (UHF Omni Range)
TDWR	Terminal Doppler Weather Radar
Temp	Temperature
TC	Transport Canada
TDC	Transportation Development Centre
Tx	Transmit
U.S.	United States (of America)
UHF	Ultra High Frequency
$w/m^2/h$	Watts per square metre per hour
w	Watts
V	Volts
VHF	Very High Frequency
VOR	VHF Omni Range

1. INTRODUCTION

1.1 Purpose

The purpose of this feasibility study was to determine possible technical approaches for the detection, analysis, and advance warning of wind shear conditions, specifically microbursts, in and around Canadian airports. A review of wind shear and microbursts was required to provide the necessary information for assessing the technical approaches. Once a feasible approach was determined, a conceptual design of a wind shear/microburst detection system for Canadian airports was developed.

1.2 Scope

This study predominantly consisted of literature review, analysis, evaluation, and design. The design is based upon equipment specifications provided by the manufacturers and vendors. No original research was undertaken in the areas of meteorological theory, algorithm development, or detection theory.

1.3 Limitations

The feasibility study has been limited to the detection of microbursts as a cause of wind shear. The review of meteorological parameters in Section 3 confirms that microbursts are a primary cause of hazardous wind shear.

The technical approaches examined have been limited by the user requirements described in Section 2.

1.4 Study Overview

The study consisted of two phases, with each phase containing several distinct activities. These activities are described in the following subsections.

1.4.1 User Requirements

The user requirements analysis involved discussions with various agencies of Transport Canada. The requirements, as established, are described in Section 2 of this document.

1.4.2 Technical Specifications

To determine the technical specifications for a wind shear/microburst detection system, a literature review was undertaken. The physical

causes of wind shear and a meteorological description of microbursts are contained in Section 3.

Section 3 also contains a high-level review of available wind shear/microburst detection technologies.

A set of generic specifications were derived from the meteorological parameters and capabilities of current technology.

1.4.3 Technology Evaluation

The technological alternatives enumerated in Section 3 were compared against the derived requirements. This evaluation was performed on two levels:

- implementations of similar technologies were compared (e.g. radar type "a" versus radar type "b");
- different technologies were compared (e.g. radar versus sodar).

The technologies best suited to the detection of wind shear at Canadian airports were incorporated into the conceptual design. The results of this evaluation are documented in Section 4.

1.4.4 Conceptual Design

During the conceptual design, the technology selections made during the assessment were examined in greater detail. The various parameters of availability, cost, performance, and functionality were taken into account to produce a single conceptual design of a wind shear/microburst detection system.

Conflicts between the various user requirements were identified and addressed during this phase, and recommendations were made where these conflicts could not be resolved. The conceptual design is described in Section 5 of this document.

1.4.5 Costing

A cost analysis of the conceptual design is contained in Section 6 of this document. This cost analysis includes estimated and actual costs for the various system components defined in the conceptual design. While every attempt has been made to ensure that the costs provided are accurate at the time of printing, these costs should be treated as estimates only.

1.4.6 Conclusions

Section 7 contains the conclusions and recommendations resulting from this study.

2. USER REQUIREMENTS

The user requirements have been intentionally restricted in order to ensure that this feasibility study considers all potential solutions. The following sections include both user requirements and user constraints. The user requirements have been compiled by the Aviation Group of Transport Canada; specifically the Air Navigation Systems Requirements and Facility Engineering and Systems Development Branches.

2.1 General Requirements

One general requirement has been identified with respect to the per airport cost of an installed wind shear/microburst detection system.

- The cost of an installed wind shear/microburst detection system should not exceed an order of magnitude of One Million Dollars ($1,000,000) (Canadian funds) per airport.

2.2 Operational/Functional Requirements

Five operational/functional requirements have been identified. They are listed below.

1. The wind shear/microburst detection system should be capable of detecting and reporting wind shear/microburst occurrences out to fifteen (15) kilometers from the centre of the airport and to an altitude of 1,000 metres.

2. The wind shear/microburst detection system should be able to detect wind shear/microbursts and provide, as a minimum, the location of any wind shear/microburst detected.

3. The wind shear/microburst detection system should provide sufficient warning, of wind shear/microbursts, such that:

   - Pilots are able to effectively utilize this information to operate their aircraft in a safe manner.

   - Air Traffic Controllers are able to effectively utilize this information in the provision of advisories and the management of their control area.

4. The wind shear/microburst detection system must provide "positive" or "negative" detection status.

   - Positive detection status: A hazardous wind shear/microburst condition is present within the area of coverage.

- Negative detection status: A hazardous wind shear is NOT present within the area of coverage.

5. The design of the wind shear/microburst detection system should give the best possible balance between a high probability of detection and a low false alarm rate.

In addition, it is desirable that the wind shear/microburst system be able to provide its information to a possible future wind shear/microburst forecasting system.

2.3 Technical Constraints

One technical constraint has been identified with respect to the compatibility with existing ground-based and aircraft-based equipment.

- Any wind shear/microburst detection system installed at, or near, an airport shall not interfere with the operation of existing ground-based Air Navigation Systems or airborne aircraft equipment.

Table 2-1 lists the equipment now in use, or planned for use, with the associated operating frequencies.

Table 2-1 Existing Frequency Assignments

Frequency Range	Equipment
9 - 14 kHz	Omega
90 - 110 kHz	Loran-C
190 - 1750 kHz	Automatic Direction Finder (ADF)
2850 - 3025 kHz	H.F. Air Ground Communications
3400 - 3500 kHz	H.F. Air Ground Communications
4650 - 4700 kHz	H.F. Air Ground Communications
5450 - 5680 kHz	H.F. Air Ground Communications
6525 - 6685 kHz	H.F. Air Ground Communications
8815 - 8965 kHz	H.F. Air Ground Communications
10005 - 10100 kHz	H.F. Air Ground Communications
11275 - 11400 kHz	H.F. Air Ground Communications
13260 - 13560 kHz	H.F. Air Ground Communications
17900 - 17970 kHz	H.F. Air Ground Communications
21924 - 22000 kHz	H.F. Air Ground Communications

Table 2-1 Existing Frequency Assignments (Continued)

Frequency Range	Equipment
75 MHz	ILS - Marker Beacon
108 - 118 MHz	ILS - Localizer, VOR
118 - 137 MHz	VHF Air Ground Communications
121.5 - 243 MHz	ELT
328.6 - 335.6 MHz	ILS - Glide Path
406 - 406.1 MHz	Possible new band for ELT
890 - 902 MHz	Airphone - Airborne Telephone
942 - 960 MHz	Airphone - Airborne Telephone
960 - 1215 MHz	DME, TACAN
1030 MHz, Rx 1090 MHz, Tx	SSR Transponder
1215 - 1240 MHz	Future Band for Navstar Satellite System
1250 - 1350 MHz	Ground Based Primary Radar
1300 - 1350 MHz	RAMP Primary Radars
1545 - 1559 MHz	Future Aeronautical Mobile Satellite (Earth to Space)
1559 - 1610 MHz	Future Band for Navstar Satellite System
1610 - 1626.5 MHz	Proposed for Radio Determination Satellite System (Earth to Space)

Table 2-1 Existing Frequency Assignments (Continued)

Frequency Range	Equipment
1646.5 - 1660.5 MHz	Future Aeronautical Mobile Satellite (Earth to Space)
2483.5 - 2500 MHz	Proposed for Radio Determination Satellite System (Earth to Space)
2700 - 2850 MHz	Ground Based Primary Radar
4200 - 4400 MHz	Radio Altimeter
5030 - 5090.7 MHz may extend to 5150 MHz	MLS
5350 - 5460 MHz	Airborne Weather Radar
8750 - 8850 MHz	Airborne Doppler Navigator
9300 - 9500 MHz	Airborne Weather Radar
13.25 - 13.4 GHz	Airborne Doppler Navigator
15.4 - 15.7 GHz	National MLS
15.7 - 16.6 GHz	Ground Based Airport Surface Detection Equipment
24.25 - 25.25 GHz	Ground Based Airport Surface Detection Equipment

2.4 Environmental Constraints

The Facility Engineering and Systems Development Branch of Transport Canada has produced a specification entitled "General Specification for Procurement of Electronic Equipment".(1) This specification sets forth the general requirements for electronic equipment or systems procured by the Transport Canada. These requirements are categorized as follows:

Electrical Design Requirements
Mechanical Design Requirements
Environmental and Service Condition Requirements
Configuration Control/Equipment Identification
Quality Assurance Requirements
Testing Requirements
Electromagnetic Compatibility (EMC) Requirements
Safety Requirements
Spares
Packing and Shipping Requirements

Any structures that form part of a wind shear/microburst detection system will be subject to zoning requirements within the boundaries of airports. These requirements are described in "Land Use in the Vicinity of Airports", produced by the Air Navigation Systems Requirements Branch of Transport Canada.(2)

The above requirements will apply to any wind shear/microburst detection system that is ultimately installed by Transport Canada. These requirements, for the most part, do not apply at this stage of the project. A notable exception is the Environmental Requirements. Transport Canada classifies equipment according to the severity of the environmental and service conditions that the equipment will operate under. These classifications are explained below.

2.4.1 Class 1 Surface Mobile

This classification is for equipment designed for portable use where mechanical shock and vibration are of prime concern. Table 2-2 specifies the environmental limits that shall apply to equipment in this class.

2.4.2 Class 2 Outdoor (Exposed)

This classification is for equipment that will be located outside and exposed to severe environmental conditions. An example of equipment in this class is a Radar Antenna Pedestal System with its associated antenna, drive motor, rotor joints, etc. Equipment in this classification shall operate in a continuous unattended mode under the environmental limits specified in Table 2-2.

2.4.3 Class 3 Fixed Sheltered (Unheated)

This classification is for equipment that will operate in unheated, but sheltered environment, where temperature and humidity are not controlled. An example of equipment in this class is a radar antenna under a radome. Equipment in this classification shall operate in a continuous unattended mode under the environmental limits specified in Table 2-3.

2.4.4 Class 4 Fixed Sheltered (Heated)

This classification is for equipment that will operate in sheltered and heated environments. Examples of equipment in this class are VORs and ILS Sites. Equipment in this classification shall operate in a continuous unattended mode under the environmental limits specified in Table 2-3.

2.4.5 Class 5 Fixed Sheltered (Heated and Cooled)

This classification is for equipment that will operate in sheltered and heated environments which are normally air-cooled and the humidity is relatively constant (e.g. operations and equipment rooms). Equipment in this classification shall operate within the environmental limits specified in Table 2-4.

2.4.6 Class 6 Fixed Sheltered (Conditioned)

This classification is for equipment that will operate in air conditioned and controlled environments where temperature and humidity fluctuations are minimized (e.g. computer rooms). Equipment in this classification shall operate within the environmental limits specified in Table 2-4.

Table 2-2 Class 1 and 2 Environmental Requirements

Environmental Category	Equipment Classification	
	1	2
AMBIENT TEMP. - Operating	-55°C to 55°C	-55°C to 55°C
- Non-operating	-55°C to 65°C	-55°C to 65°C
AMBIENT RELATIVE HUMIDITY	Up to 100%	Up to 100%
ALTITUDE - Operating	0 m to 3000 m ASL	0 m to 3000 m ASL
- Non-Operating	0 m to 15000 m ASL	0 m to 15000 m ASL
SAND AND DUST	Fine dust up to 150 microns	Fine dust up to 150 microns
MECHANICAL SHOCK	40 g peak, 18 msec duration	N/A
VIBRATION	2.5 g, up to 500 Hz	N/A
INDUCED TEMPERATURE RISE (Solar Radiation)	N/A	Minimum exposure of 4 hours at 1135 $w/m^2/h$
ADVERSE WEATHER - Operating	N/A	Wind 0 to 160 km/h gusting up to 175 km/h with 5.0 cm radial thickness of ice
- Non-operating	N/A	Wind 0 to 160 km/h gusting up to 240 km/h with 5.0 cm radial thickness of ice
SALT ATMOSPHERE	N/A	As encountered in coastal areas
DUTY CYCLE	N/A	Continuous unattended mode except for scheduled maintenance interruptions

Table 2-3 Class 3 and 4 Environmental Requirements

Environmental Category	Equipment Classification	
	3	4
AMBIENT TEMP. - Operating	-50°C to 55°C	-10°C to 50°C
- Non-operating	-55°C to 65°C	-40°C to 55°C
AMBIENT RELATIVE HUMIDITY	10% to 97%	5% to 90%
ALTITUDE - Operating	0 m to 3000 m ASL	0 m to 3000 m ASL
- Non-Operating	0 m to 15000 m ASL	0 m to 15000 m ASL
SAND AND DUST	Fine dust up to 150 microns	N/A

Table 2-4 Class 5 and 6 Environmental Requirements

Environmental Category	Equipment Classification	
	5	6
AMBIENT TEMP. - Operating	10°C to 40°C	15°C to 35°C
- Non-operating	-30°C to 55°C	-30°C to 55°C
AMBIENT RELATIVE HUMIDITY	40% to 80%	40% to 60%
ALTITUDE - Operating	0 m to 1500 m ASL	0 m to 1500 m ASL
- Non-Operating	0 m to 15000 m ASL	0 m to 15000 m ASL

3. TECHNICAL SPECIFICATIONS

The technical specifications are presented throughout the following five sections:

3.1 Meteorological Review
3.2 Wind Shear Parameters
3.3 Microburst Parameters
3.4 Review of Detection Technology
3.5 Derived Requirements

3.1 Meteorological Review

Before examining methods for detecting and predicting wind shear it is useful to review the meteorological descriptions and causes of wind shear. Reference is made to the ICAO Circular throughout this report as it serves as the basis for much of the following text.(1)

3.1.1 Definitions

A discussion of the meteorology of wind shear should clearly start with a description of how the quantity is defined and could be measured. Wind shear involves wind speeds and directions which change rapidly when the point of observation moves a short distance. The Glossary of Meteorology contains the following definition of wind shear.

Wind Shear - The local variation of the wind vector or any of its components in a given direction. The vertical shear can be expressed in terms of the height, $\delta V/\delta z$, or of pressure, $\delta V/\delta p$, as the vertical coordinate. If the wind is geostrophic, the vertical shear is given by the thermal-wind equation. The wind shear at a point is said to be cyclonic or anticyclonic according to whether the sense of rotation from the wind vector to the shear vector at the point is cyclonic or anticyclonic.(2)

In terms of vector notation, wind shear is the vector difference between two observed wind vectors divided by the distance that separates the two points of measurement.

This is expressed mathematically as follows:

$$\bar{s} = \frac{\bar{v}_2 - \bar{v}_1}{d} \qquad (1)$$

Where $\bar{s}$ is the wind shear vector over the distance d which separates the two vectors $\bar{v}_1$ and $\bar{v}_2$. This is illustrated in Figure 3-1 where $-\bar{v}_1$ has been obtained by reversing the direction of $\bar{v}_1$ and then adding the resulting vectors. The units commonly used in aviation are:

knots/100 ft

while in scientific work the units used are:

$$\frac{\text{m / sec}}{\text{m}} \equiv \text{sec}^{-1}$$

The two units may be interconnected using the fact that:

$$\frac{1 \text{ kt}}{100 \text{ ft}} = 0.017 \text{ sec}^{-1} \qquad (2)$$

Note that the distance d can be chosen in any direction. If d is chosen in the vertical direction, then we obtain the "vertical wind shear" and if d is chosen in the horizontal direction, we obtain the "horizontal wind shear". Except for the mechanically-driven small scale turbulence in the boundary layer, there is no reason to assume that wind shear is the same in different directions.

The following points must be considered in a discussion of wind shear as it relates to aircraft operation. Horizontal winds are generally much larger than vertical winds in the atmosphere. As a result, vertical wind shears are generally larger than horizontal wind shears. When aircraft change altitude, particularly during take off and landing, there may be an appreciable observed wind shear along the glide path. In many cases this is the result of a strong vertical wind shear component. Aircraft normally take off and land into the wind so that the head/tail component usually predominates over the cross track component of this vertical wind shear. The exceptions to this situation are briefly discussed below and include: mountain waves, isotropic boundary layer turbulence, wake vortices and thunderstorms.

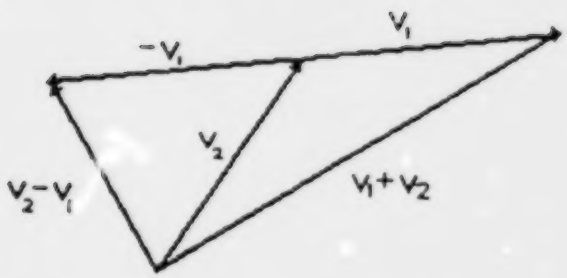

Figure 3-1 Geometrical construction for the sum and difference between two wind vectors $\overline{v}_1$ and $\overline{v}_2$.

Meteorologists normally measure winds through the use of balloons. Since a balloon responds only to the average wind of the layer in which it flies, and since it progresses from the surface upwards, it is likely to measure only vertical wind shear and smooth out sudden changes in horizontal wind. This may result in an underestimation of extremely local horizontal wind shear. It should be noted that an aircraft would do effectively the same thing by an amount related to aircraft size. Care is required in the interpretation of wind shear data and the effects of the measurement technique.

3.1.2 The Normal Atmosphere

Before proceeding to a discussion of the types of wind shear phenomena which cause problems for pilots, it is useful to describe the type and magnitude of wind shears which occur in the normal or undisturbed atmosphere. Meteorological texts have traditionally divided the lower atmosphere into three distinct layers. The first of these layers is the "surface boundary" layer where the air flow is dominated by the turbulence generated through friction with the ground. The second layer is the "Ekman" layer in which the role of the surface friction slowly decreases with increasing height until the third layer or "free atmosphere" is reached where the role of surface friction is minimal and the wind is determined by the large scale meteorology. The wind shear present in each of these three layers is briefly discussed below. Before proceeding, however, it is necessary to examine causal forces underlying air movement in the atmosphere.

The major process involved in forcing the motion of the atmosphere is differential heating. When air is heated both the pressure and the density change. This difference in pressure results in a pressure gradient and the tendency of air to move from a high pressure region to a lower pressure region constitutes the "pressure gradient force". Figure 3-2 illustrates a linear pressure gradient.

With reference to Figure 3-2, if we choose two separate locations then the net force on the element, F_x, is:

$$F_x = pA - \left(p + \frac{\delta p}{\delta x}\Delta x\right) A \qquad (3)$$

where p is the pressure, x is the distance, A is the area of the end of the illustrated element, and Δx is the length of the illustrated element.

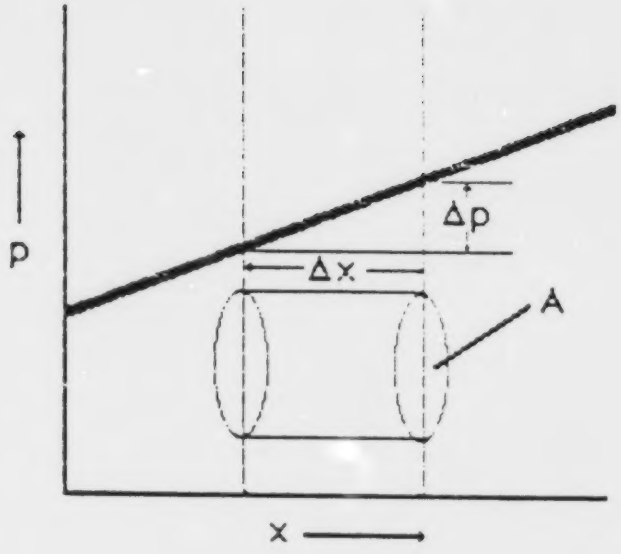

Where:
x is the distance
p is the pressure
A is the area of the end of the cylinder
Δx is the change in distance
Δp is the change in pressure

Figure 3-2 Graphic illustration of the parameters used in the derivation of the gradient wind equation.

However, $A\Delta x$ is the volume, V, of the element:

$$V = A\Delta x = \frac{M}{\rho} \tag{4}$$

where M is the mass of the air in the element and ρ is the density of the air in the element. Thus we have:

$$F_x = -\frac{M}{\rho}\frac{\delta p}{\delta x} \tag{5}$$

By analogy the equations for the net force on the element in the y and z directions, F_y and F_z can be obtained.

The other forces involved in the lower atmosphere are: friction due to the interaction with the surface roughness, F_f, and the Coriolis force, F_c, which is given by:

$$F_c = 2\ M\ \omega\ u\ \sin\lambda \tag{6}$$

where M is the mass, ω is the angular velocity of the earth, u is the wind speed, and λ is the latitude. The Coriolis force is perpendicular to both the wind speed and the axis of the angular rotation. Wind patterns dominated by the Coriolis force will tend to be deflected into a circle. Since the Coriolis force at the equator is reduced to zero, the importance of this force is much reduced in tropical regions compared to the mid-latitudes.

i) The Surface Boundary Layer. When the atmosphere shows a strong horizontal wind the lower layer, near the ground, is strongly mixed by turbulent processes. Under these conditions the atmosphere is neutrally stable and the average wind speed, as a function of height, can be determined from the solution of a boundary value problem where the surface layer is assumed to be at rest due to friction. The theoretical relationship between horizontal wind speed, u, and the height, z, is given by the Prandtl equation:

$$u = \frac{u^*}{\kappa} \ln \frac{z}{z_o} \qquad (7)$$

where u^* is the friction velocity, κ is a constant of value ~0.38 and z_o is the roughness length which is a measure of the degree of surface convolution.

The results of this equation are generally in accordance with observations and demonstrate modest wind shear except very close to the ground (i.e. the lowest 10 m). Although the results for unstable and stable conditions differ somewhat, there is no appreciable difference in terms of wind shear. Thus the normal result is that the head wind speed decreases with altitude on landing and increases with altitude on take off. It should be noted that wind direction does not change much in the lowest 100 m (Figure 3-3).

ii) The Ekman Layer. Above the surface boundary layer the effect of the surface friction is much reduced and the pressure gradient force is balanced against the Coriolis force. Since the Coriolis force is perpendicular to the wind velocity, the wind changes direction and increases in speed from the bottom of the Ekman layer (~100 m), where the pressure gradient, friction and Coriolis force are of similar magnitudes, up to the top of the Ekman layer (~500 m), where friction plays a negligible role, and the pressure gradient force is balanced by the Coriolis force. This produces the "geostrophic wind" determined by the large scale meteorology.

The Ekman spiral (Figure 3-4) shows that the wind increases in speed with height and changes direction by about 45 degrees between approximately 10 m and 500 m.

iii) The Geostrophic Layer. Above 500 m the pressure gradient force is in approximate equilibrium with the Coriolis force. Wind shears in the geostrophic layer are generally modest. The only exception is clear air turbulence, frequently occurring at jet stream boundaries, which is small scale and normally only results in passenger discomfort rather than structural damage to the aircraft. The exception to this rule is the wind shear resulting from the wind flow near a frontal system. This is illustrated in Figure 3-5. Mountain waves can also produce wind shear in this geostrophic layer.

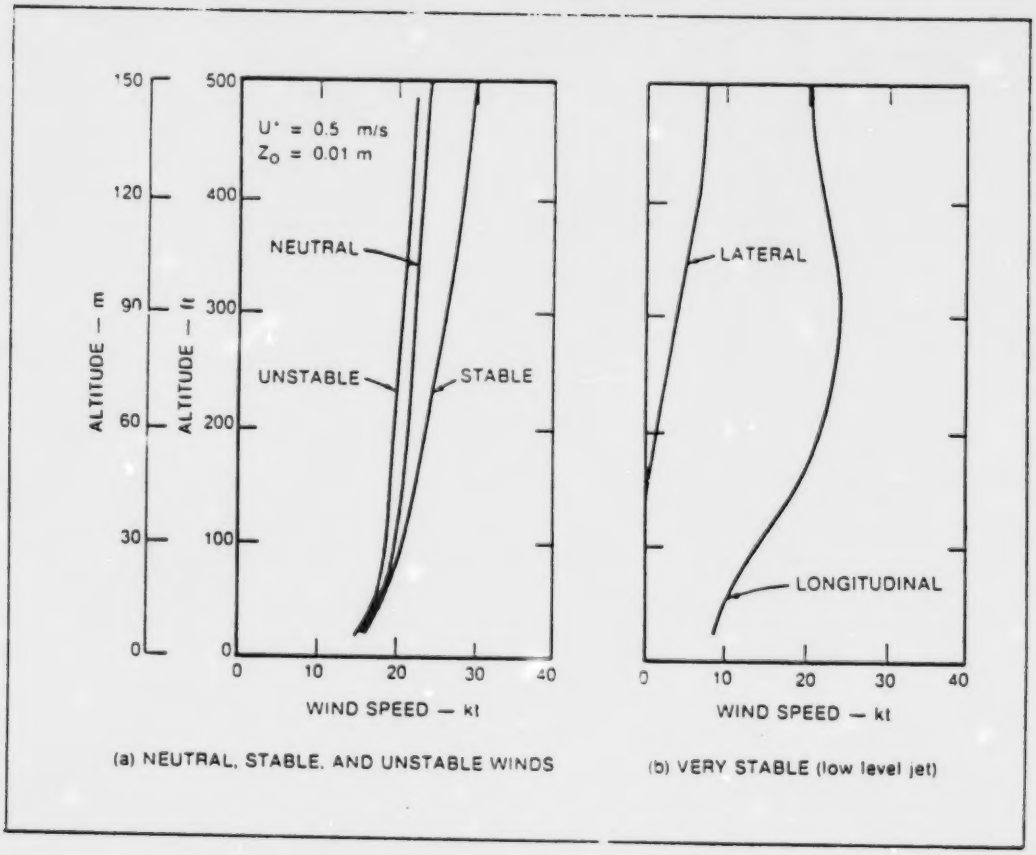

Figure 3-3 Theoretical wind profiles due to surface friction and geostrophic wind aloft - surface boundary layer. (from Ellis and Keenan, 1978)

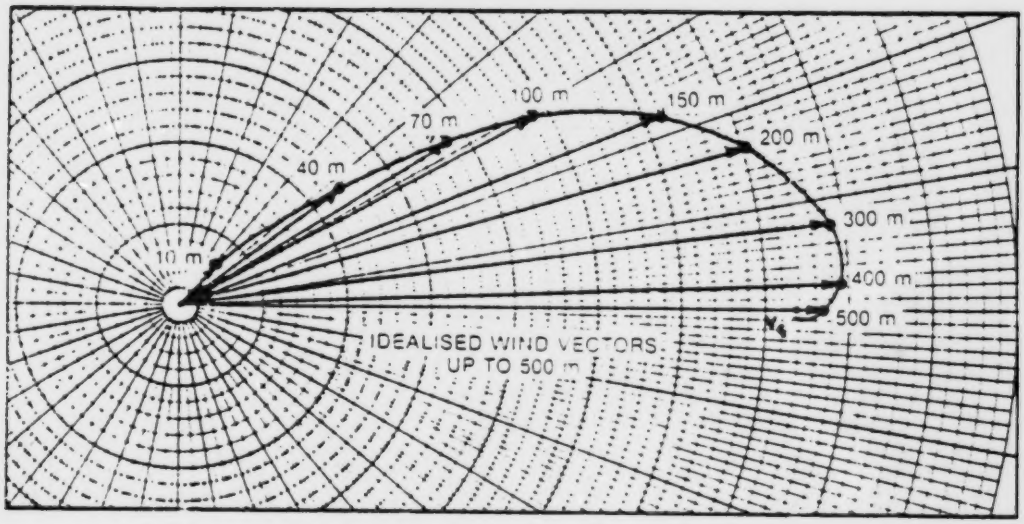

Figure 3-4 Theoretical change in wind speed and direction with height - Ekman layer wind profile.
(from ICAO Circular 186-AN/122, 1987)

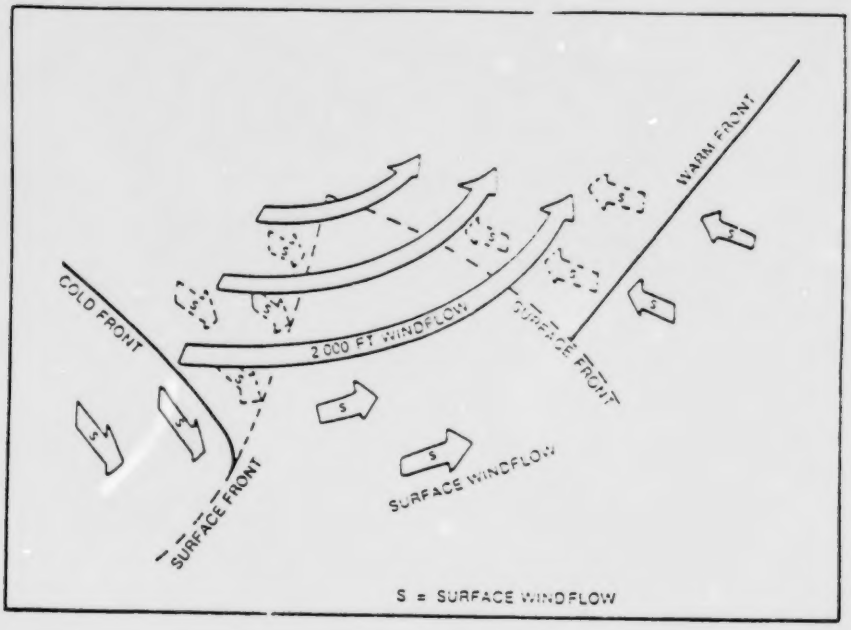

a) Three dimensional diagrammatic view of wind flow around warm/cold frontal system up to 2000 ft, northern hemisphere (vertical scale exaggerated).

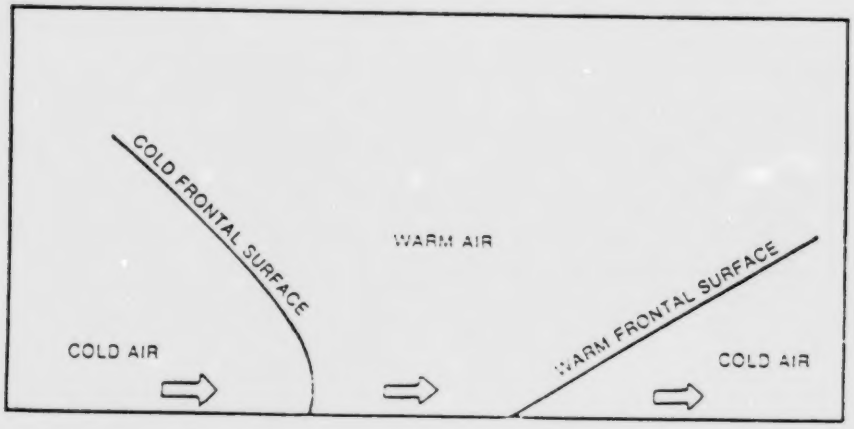

b) Cross-sectional diagrammatic view across warm/cold frontal system (vertical scale exaggerated).

Figure 3-5 Wind flow around surface frontal systems (from ICAO Circular 186-AN/122, 1987)

3.1.3 The Causes of Low Level Wind Shear

There are several possible causes for wind shears of magnitude greater than those indicated in the previous section. These causes are discussed below. Analysis of U.S. weather-related aviation accidents and incidents (see Glossary for formal definitions of accident and incident) are summarized in Table 3-1. Convective storms (i.e. thunderstorms and rain/snow showers) were found to be the cause of over sixty percent of all weather related accidents and incidents. Lansford noted that in the United States during the period 1982 to 1985, 65 percent of the 449 deaths resulting from airline accidents were caused by wind shear.(3) In Canada, the Canadian Aviation Safety Board records show that from 1976 to 1986, 105 accidents/incidents were attributed to wind shifts, turbulence, and wind shear.

i) Wind Flow Around Obstacles. Low level wind shear is most commonly due to the presence of obstacles adjacent to the airfield, such as trees and hangars, in the path of strong surface wind. In this situation there may be a sudden change in wind flow, usually from strong horizontal to almost calm, as the aircraft changes height or moves horizontally (Figure 3-6). At commercial airports these obstacles have either been removed or the problems are well known.

The same phenomenon may sometimes exist for airfields built in the lee of hills or mountain ranges. When the air is stable the flow of the air over the obstacle, which can be tens of kilometres away, may result in lee wave formation. These lee waves are common in several parts of the world, for example the Chinook wind in Alberta, South Island of New Zealand and in the lee of the Sierras in the United States of America. In the specific case of Christchurch, New Zealand, the mountain range is approximately 120 km distant. Mathews and Hicks carried out a climatological study of wind profiles at the Springbank airport, using a Doppler Sodar built at the University of Calgary.(4) In one case, the head wind to tail wind changes an aircraft would have experienced in penetrating the shear layer were as large as 45 m/s, comparable to that encountered in downbursts. Since the air is generally stable for the formation of these waves the wind shear may persist for some time and can be readily detected by acoustic sounders or balloon. This type of wind shear is not a major concern of this report.

ii) Wake Vortices. This phenomenon is similar in many ways to the wind flow around obstacles as it is also a stable air problem. As an aircraft flies, in stable air, it leaves in its wake a pair of counter-rotating tubes, or vortices, of air flow. A stable air mass is one in which small disturbances such as vortices do not grow. If the air is unstable the vortex will couple with the thermodynamic stability and produce a different (principally upward) motion. Horizontal winds may be present in stable air. If

Table 3-1 Distribution and Causes of U.S. Wind Shear Accidents and Incidents (1959 - 1983)

Weather System	Number of Wind Shear Events*
Convective Storms (Thunderstorms, Rain/Snow Showers)	33
Front	7
Strong Surface Winds	2
Unstable (Turbulent) Air	2
Strong Winds on Top of Temperature Inversion	1
Sea Breeze Front	0
Mountain Wave	0
Unknown	6
Total	51

*Event - accident or incident (See Glossary for formal definitions of accident and incident).

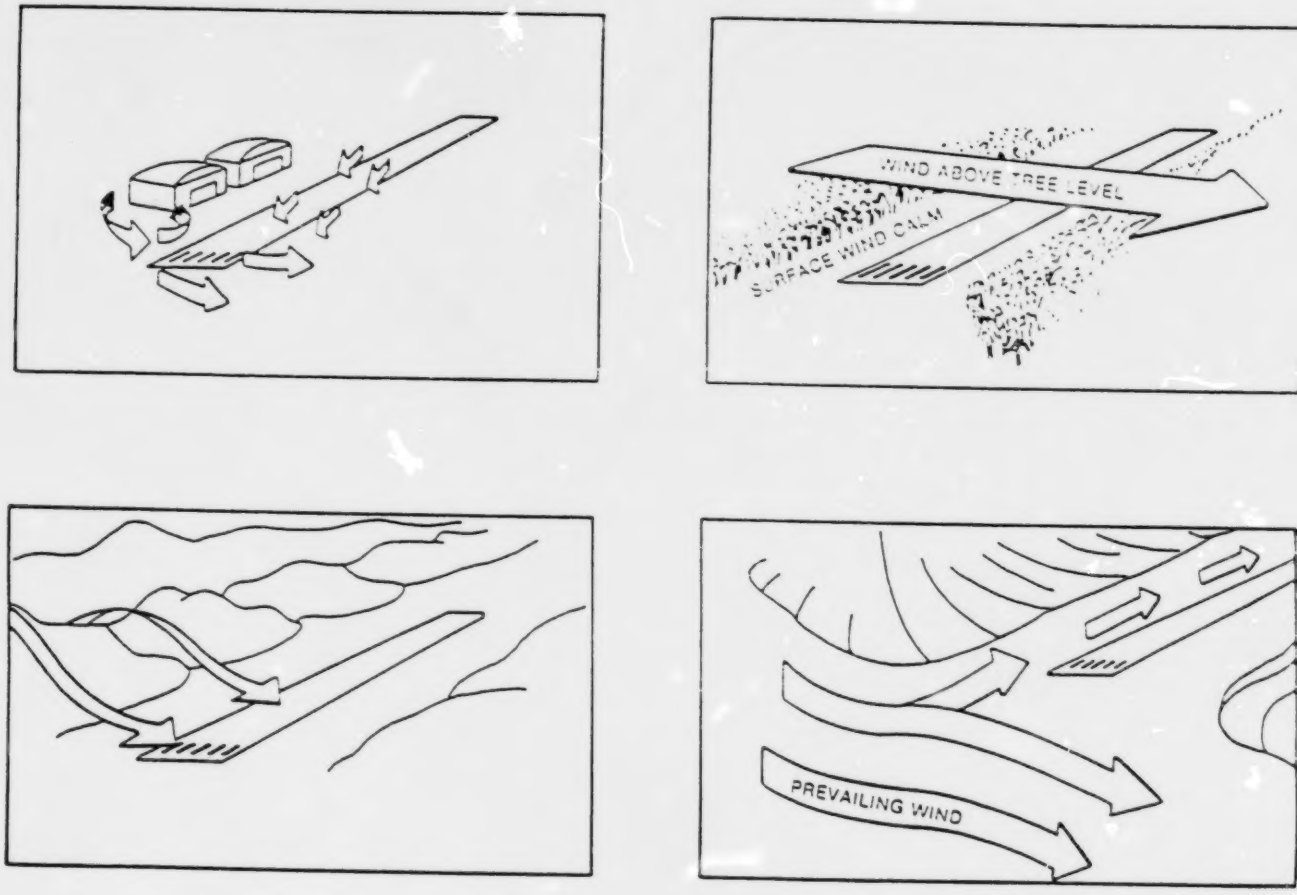

Figure 3-6 Obstacle wind flows: typical situations where fixed objects near runways can produce wind shear. (From ICAO Circular 186-AN/122, 1987)

there is a light wind across the glide path it may cause the vortices to move so that the next plane through the area may hit one of the vortices head-on (the other having drifted off to one side). The effect of wake vortices is extreme in the case of a small aircraft following a large aircraft. The resulting torque on the second aircraft may be considerable. This phenomenon occurs in clear air, and thus detection is not trivial, but the prediction of "wake vortex conditions" (stable air with light cross wind) is easily made by conventional meteorological means.

iii) Thunderstorms. There are basically two types of thunderstorms which occur in Canada; those which occur in lines generally associated with fronts, and the single isolated "air mass" thunderstorms. Throughout most of Canada the frontal type are much more common (this is substantiated through unpublished findings from McGill University and Alberta research centres). They are generally less severe than the air mass type but pose a greater threat to en route aviation since the avoidance of the line may involve a much longer detour than for the air mass type. Frontal thunderstorms are more likely to hit a given airfield than air mass thunderstorms due to their large horizontal extent perpendicular to their direction of travel.

Except for the occasional occurrences elsewhere, the air mass types are largely a summer prairie phenomenon in Canada, especially in the foothills of Alberta. They produce considerable amounts of lightning, hail, turbulence and wind shear. Their main virtue, from an aviation perspective, is their small horizontal extent and relatively rapid movement. By far the safest aviation practice is to keep well clear of them and to avoid landing when they are in the vicinity since they usually move away quickly. The main reason for their rapid movement is that these air masses are relatively tall structures which travel with the generally strong westward winds that prevail at high altitudes. Naturally, exceptions can be found to this general rule, particularly in the foothills of large mountains and/or early in the storm's life cycle.

As noted earlier, thunderstorms may create several hazards to aviation as listed below.

a) Tornadoes. These phenomena are triggered by severe thunderstorms and destroy everything in their path. Their small horizontal extent make interception of a tornado by an aircraft unlikely and the use of radar to avoid tornadoes is well established. The physics of tornadoes has been studied extensively, mainly because of the great damage and concomitant loss of life.

b) Turbulence. In the sixties there was evidence that the turbulence associated with thunderstorms was a major cause of accidents in the U.S.(5) This turbulence is mainly the result of strong up and downdraughts carrying horizontal momentum to different levels in the thunderstorm. The resultant wind shear gives rise to strong turbulence at the up and downdraught vertical boundaries.

c) Hail. Strong thunderstorms frequently give rise to the development of hail. Hail is the result of raindrops, produced by condensation of moist air in strong updraughts, being carried above their freezing level. These frozen raindrops then fall through more moist air and become coated with layers of water which subsequently freeze. The large particles that result can constitute an extreme hazard to aviation. As hail falls it often starts to melt, coating the ice center with a thin layer of water resulting in a radar target that generates a higher reflective radar signal than a dry hailstone or a pure water droplet. Nevertheless, most hail stones are readily detected because of their typically large diameter which gives a strong radar signal even when the hail is dry.

Although dual polarization and dual frequency radars can identify hail with more certainty than a conventional weather radar, these types of radars are expensive to build and operate and reliable hail detection algorithms are not yet ready for operational use. Algorithms based on echo intensity, height in the storm and storm volume occupied by the maximum intensity can provide adequate indication of the presence of hail. However, hail algorithms such as the one developed for the NEXRAD system must be adjusted for each location to account for the local climate.

d) Gust Fronts. The meteorological analysis of the measurements of wind patterns around thunderstorms dates back to at least as early as Bohun in 1671.(6) The first modern analysis was presented by the Thunderstorm Project in the United States in 1947.(7) More recent work using sophisticated technology has not significantly altered this analysis.

The triggering mechanism for both types of thunderstorm is a pool of warm and moist surface air giving rise to convective instability and strong updraughts. The rising columns of air produce growing, towering cumulus clouds. The structure of the storm at this stage is usually a loose collection of cells but may also be a single "super cell". When the mature stage of the storm is reached, a substantial rain fall is produced by the clouds and a downdraught is developed.

This downdraught of cool air is aided in its descent by radiative cooling, evaporative cooling, and the loading of the air parcel through drag due to the falling raindrops. Evaporative cooling is caused by the evaporation of cloud liquid water in the entrained high-level cool dry air. When the decaying storm phase is reached the heavy rain and strong localized downdraught is replaced by a weak downdraught and widespread light rain throughout the whole system. In dry atmospheric conditions the rain shaft producing the downdraught may totally evaporate before reaching the surface. This phenomenon is defined as virga.

When the strong downdraught, produced during the mature stage of the thunderstorm's evolution, hits the ground the air spreads out and produces a gust front. This cold air spreads out below the thunderstorm forcing the warm moist air entering the system to rise over the front, as illustrated in Figure 3-7. This gust front may extend as much as 20 km in front of the thunderstorm and produce sudden changes in wind speed and direction in the clear air. An aircraft flying into this gust front may experience a 180 degree change in wind direction and gusts of up to 50 kt. The detailed morphology of each individual thunderstorm gust front is quite varied, ranging from severe wind shear conditions to practically no wind shear, and the presence of low level "roll clouds" to simply a sudden change in the air temperature. The passage of the front may also be marked by the arrival of raindrops, dust clouds or turbulence. In this case the gust front may be characterized as a faint "arc cloud" on weather radar display and satellite imagery. If the gust front occurs in clear air it may not be detectable by either weather radar or satellite.

Many researchers have attempted to visualize the evolution over time of gust fronts based on extensive case studies. One of the best descriptions to date is that provided by Wakimoto (1982)(8) as illustrated in Figure 3-8.

Stage I shows the downdraught of dense, cold air associated with the heavy rainfall region. Stage II shows the subsequent situation where the strong downdraught has hit the ground and is spreading out at low levels carrying raindrops with it. Since surface friction slows the air flow layer nearest to the ground the maximum velocity may be found 100 m - 300 m above the surface, propagating into the warm air. As a result, both the wind speed and rate of gust front propagation can be significantly higher than the winds recorded by anemometer towers.

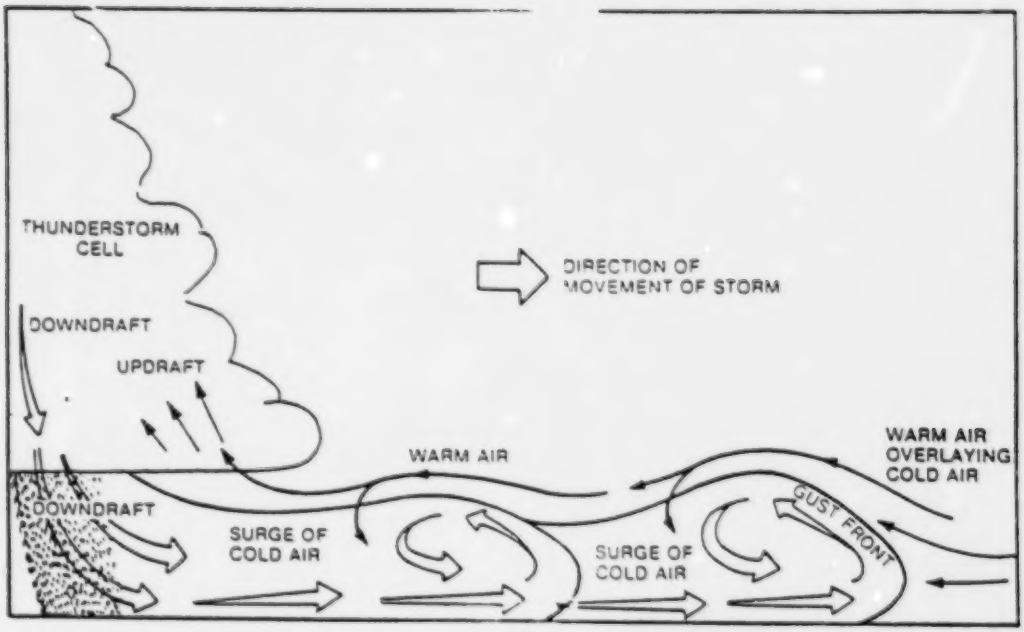

Figure 3-7 Major wind patterns in a typical gust front
(From ICAO Circular 186-AN/122, 1987)

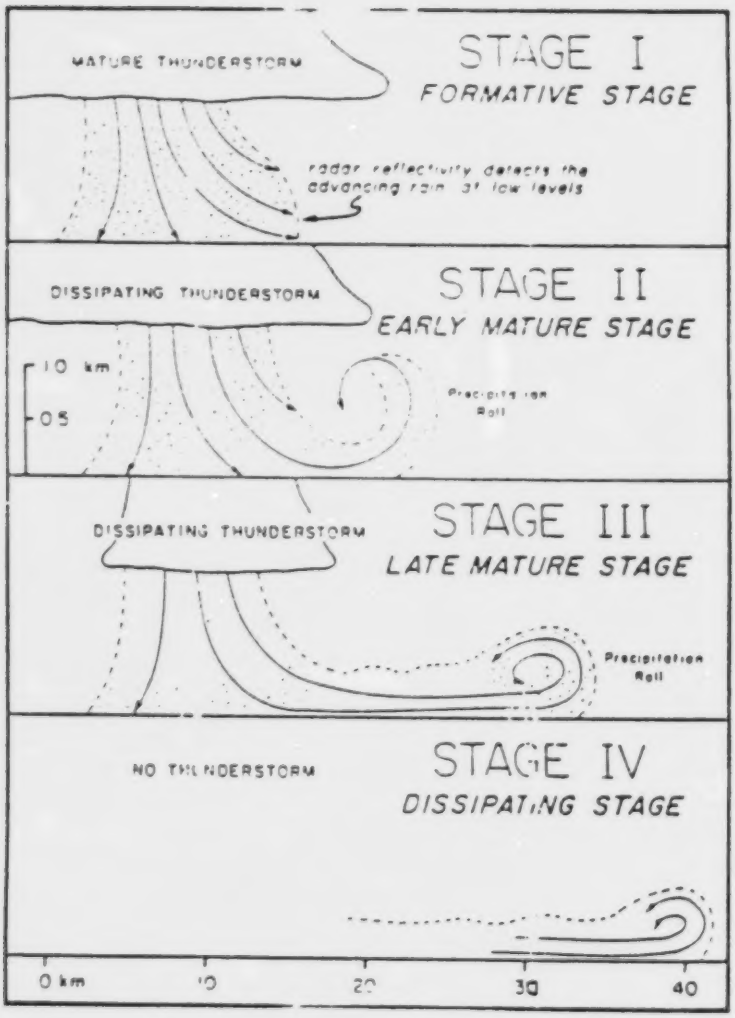

Figure 3-8 Gust front development over time (from Wakimoto, 1982)

During Stage III the roll vortex has been carried out beyond the immediate vicinity of the thunderstorm but is still carrying some precipitation with it.

In Stage IV the roll vortex, which is dissipating, is devoid of precipitation and is now located approximately 30 km from the now dissipated thunderstorm. These four stages occur, to varying degrees, in the majority of thunderstorms. The gust fronts which constitute severe hazards are those where the downdraught is sufficiently vigorous that the roll vortex extends well beyond the immediate vicinity of the thunderstorm while still possessing wind velocities which are sufficient to be hazardous. Recently the more severe gust front phenomena have been termed "downbursts" and "microbursts", mainly by Fujita (5) in his series of analyses of thunderstorm related accident reports.

e) Downbursts, Macrobursts, and Microbursts. A downburst is a strong downdraught which induces an outflow of damaging winds on or near the ground. A large downburst, in excess of 4 km in horizontal dimension, is called a macroburst, while a small downburst, less than 4 km in horizontal dimension, is called a microburst. These phenomena, which are of major concern in this study, are extreme versions of the gust front described previously with the microburst being the smallest, and sometimes most intense. From a meteorological perspective the prediction of the intensity or horizontal extent of downdraughts has not been possible; this is clearly an area of great importance. The factors contributing to the downdraught, as stated above, are radiative cooling, evaporative cooling, and loading by the heavy rain. If the thermodynamic variables were the prime parameters then all of the thunderstorms in a field of air mass thunderstorms would produce similar downbursts. This is clearly not the case since only a few thunderstorms produce these hazardous downbursts. There must therefore be something different about the downburst-producing thunderstorms when compared to the others. The early detection of this critical difference would constitute a major advance in aviation safety since it would enable an early warning of impending downbursts to be issued. To date there has been no progress in this area since funding levels have been minimal compared to the larger field experiments, conducted in the U.S., designed to detect microbursts once they have occurred.

The types of wind patterns observed and recorded at ground level during the occurrence of a particular microburst are shown in Figure 3-9. In this figure, the ordinate is wind speed in knots and the abscissa is time in minutes, increasing to the left as one would see in a chart recorder. The wind barbs show the mean wind speed and direction as a function of

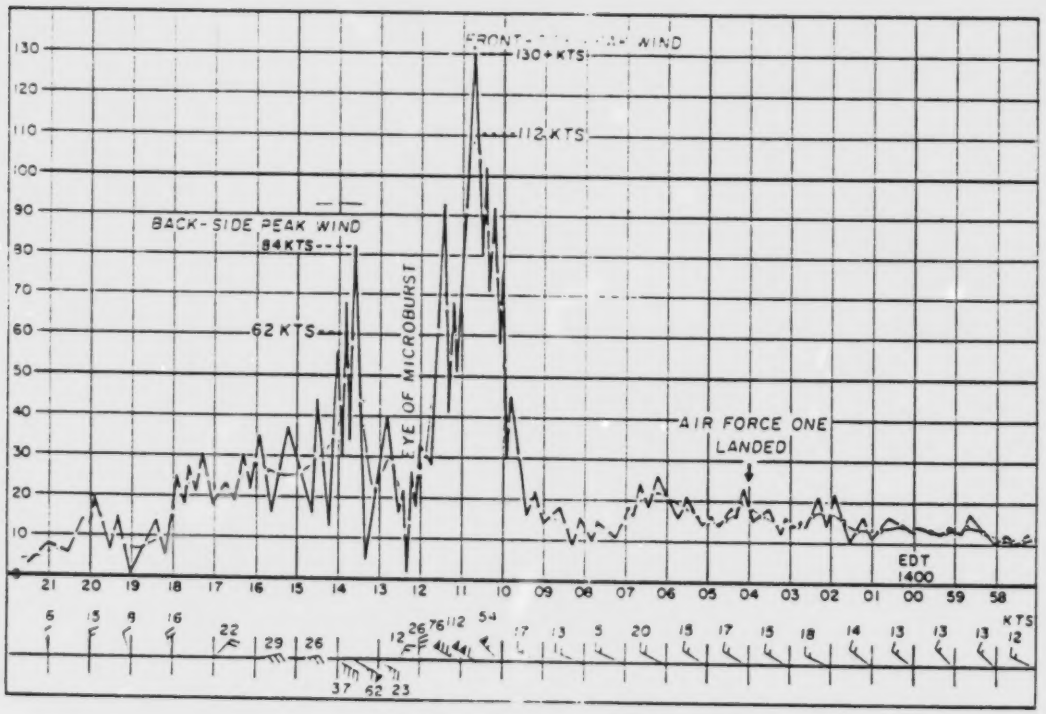

Figure 3-9 Surface winds associated with a particular microburst. The ordinate is wind speed (knots) and the abscissa is time (minutes), increasing to the left. The wind barbs show the mean wind speed and direction as a function of time. (from Fujita, 1985)

time and illustrate the dramatic shift in speed and direction of the winds around the eye of the microburst. As may be seen, there was a 180 degree change in wind direction and a change in wind speed from +130 kt to -84 kt over four minutes, corresponding to an approximate horizontal distance of one mile. Fujita's (1986)(9) detailed reconstruction of a microburst is illustrated in Figure 3-10. The essential features are similar to those shown in Figure 3-8 with the exception of three separate vortices, presumably due to pulsations in the downdraught speed. Fujita has analyzed TV pictures of a microburst and believes he can detect the detailed trajectory of the downburst as it emerges from the cloud burst.(5) One such analysis is shown in Figure 3-11 where the location of the cold air interface is plotted every ten seconds. The duration of the phenomenon, from the emergence of the downdraught from the cloud base to the impact of the downdraught with the surface, is 30 seconds and it is almost totally dissipated after a period of two minutes. This illustrates the extreme speed necessary to identify and issue a warning of these phenomena.

These analyses are confined to two dimensions and do not completely illustrate the air flows within the microburst structure. Just as is in the case of the wind changes discussed in the Ekman layer, the convergence of the air into the thunderstorm and upper part of the downdraught shows a spiral structure which then spreads out, in a laminar flow way, near the surface. This rather complex air flow is difficult to illustrate but an attempt is made in Figure 3-12. This spiral motion is important because it increases the detectability of the wind pattern by Doppler radar since the spiral motion produces a characteristic pattern in radial velocity.

The smaller microburst phenomena evidently have a small horizontal extent and may not even be detectable by surface anemometers while the larger downburst may produce sustained high winds resulting in severe damage at the surface. They are, however, almost certainly manifestations of the same processes which produce the gust fronts. The detection and warning of phenomena as small and transitory as microbursts presents a major challenge. Currently, it is not clear that the forecasting of these phenomena, even tens of seconds before they occur, is possible at aircraft height.

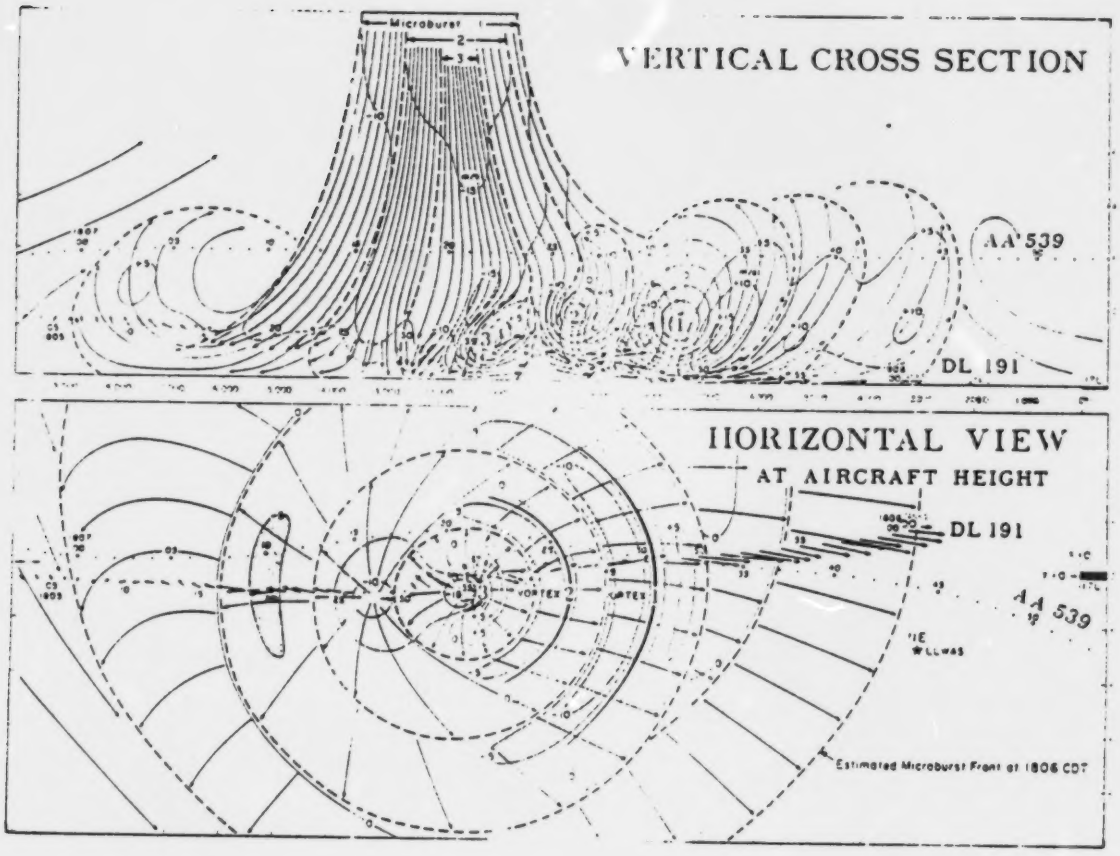

Figure 3-10 Microburst wind analysis - 3 dimensional visualization of the structure of a microburst (from Fujita and McCarthy, 1987)

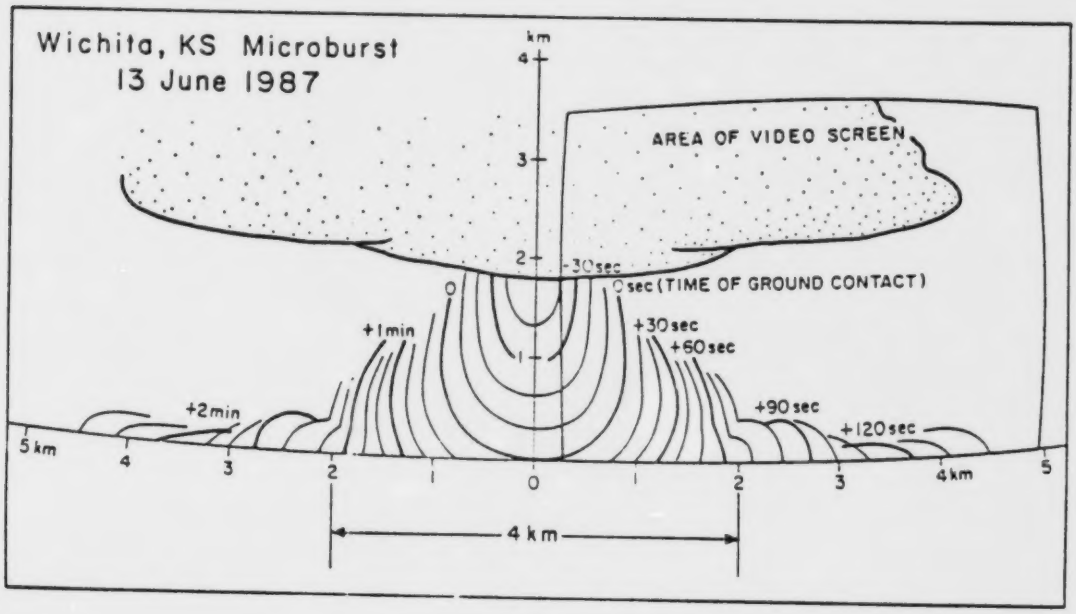

Figure 3-11 Time history of a microburst as deduced from TV image analysis (from Fujita and McCarthy, 1987)

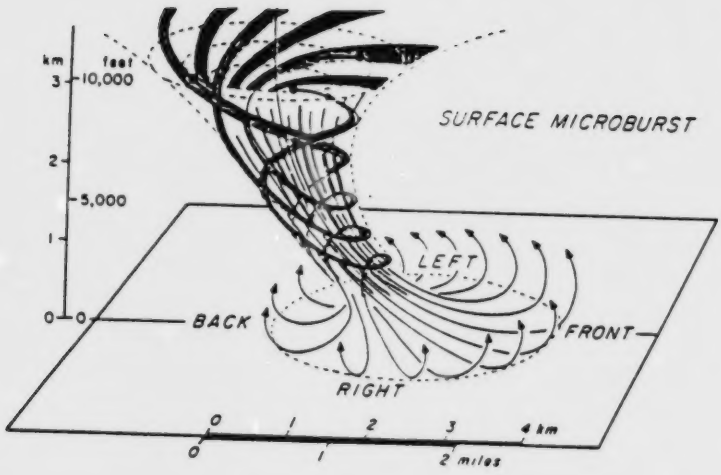

Figure 3-12 Simplified air flow diagram, showing the rotational nature of microburst air flow (from Fujita, 1985)

3.1.4 Climatology of Thunderstorms

In assessing the risk of an aircraft and a microburst "meeting" close to a Canadian airport an analysis would have to be done, for each airport, that considered both the probability of a microburst occurring near the airport and the number and frequency of aircraft movements near the airport. This type of analysis is clearly beyond the scope of this study.

In determining the feasibility of detecting wind shear/microburst phenomena it is important to know where they are most likely to occur. The reason that climatology of thunderstorms is reviewed is because storms are a cause of the majority of wind shear related accidents and incidents (see Table 3-1). However, innocuous-looking rain showers and towering cumulus with virga can also produce dangerous microbursts and these situations should also be considered.

Tables 3-2 and 3-3 represent the monthly and annual mean number of thunderstorm days at Canadian and American airports.(11) These data illustrate the fact that the Canadian east and west coasts have a relatively low thunderstorm occurrence. Central Canada locations report a number of thunderstorm days similar to many U.S locations.

Further interpretation of these data is difficult and must be done with care. The data in Table 3-2 is collected from a set of Atmospheric Canada publications called "Principal Station Data (PSD)". It is interesting to note that the AES definition of a thunderstorm day is "a day when thunder is heard, or when lightning or hail is seen but thunder is not heard because ambient noise is too loud".(12) Thunderstorms are more difficult to observe visually in Eastern Canada than in the prairies due to the frequent occurrence of low intervening cloud in the more humid east (McGill University thunderstorm photography experiments had to be transferred to Alberta in order to get useful results). This suggests that the number of thunderstorm days reported for the prairies would be larger than those reported for the east for a similar occurrence rate of thunderstorms.

As described earlier, the evaporation mechanism is a significant factor in the occurrence of a microburst. For example, the surface humidity, on thunderstorm days, is lower in Edmonton than in Montreal, which means that there is a stronger evaporative mechanism active in Edmonton than in Montreal. Unfortunately the PSD statistics do not allow for the isolation of humidity and cloudiness data on thunderstorm days. The evaporative mechanism factor may explain why Florida, which is very humid in the summer and has the most thunderstorm days in the U.S., appears to have very low aircraft accident statistics. Also, the wet microburst that occurs here is visually menacing causing pilots to instinctively avoid them.

Table 3-2 Monthly and Annual Mean Number of Days with Thunderstorms at Selected Canadian Airports
(From an internal Transport Canada report "Microbursts - A Review")

Airport	J	F	M	A	M	J	J	A	S	O	N	D	Annual
Victoria	0.0	0.0	0.1	0.1	0.5	0.4	0.5	0.5	0.4	0.1	0.2	0.1	2.9
Vancouver	0.1	0.0	0.2	0.5	0.5	0.6	0.7	0.7	0.4	0.3	0.2	0.1	4.3
Calgary	0.0	0.1	0.0	0.2	1.7	5.3	8.5	5.0	0.8	0.1	0.0	0.0	21.7
Edmonton	0.0	0.0	0.0	0.2	3.4	6.2	9.2	5.6	1.0	0.2	0.0	0.0	25.8
Regina	0.0	0.0	0.0	0.4	2.3	5.5	7.0	5.7	1.3	0.1	0.0	0.1	22.4
Saskatoon	0.0	0.0	0.1	0.4	1.6	3.8	7.1	4.6	0.9	0.1	0.0	0.0	18.6
Winnipeg	0.0	0.0	0.1	0.7	2.4	5.3	7.0	6.2	2.3	0.4	0.0	0.0	24.4
Thunder Bay	0.0	0.0	0.1	0.8	2.8	5.2	6.4	5.8	3.0	1.1	0.3	0.1	25.6
Sudbury	0.2	0.0	0.2	0.8	2.3	4.4	4.1	3.6	2.5	1.2	0.3	0.0	19.6
Toronto	0.1	0.1	0.5	2.1	3.0	4.1	5.3	4.8	2.7	1.0	0.6	0.1	24.4
Trenton	0.1	0.1	0.6	1.6	3.0	4.6	5.2	4.9	3.1	0.9	0.6	0.1	24.8
Ottawa	0.0	0.0	0.2	0.8	2.3	4.8	6.3	4.7	2.3	1.1	0.2	0.0	22.7
Dorval	0.1	0.0	0.3	0.8	2.2	4.4	6.3	5.3	2.2	0.8	0.2	0.1	22.7
St. Hubert	0.1	0.0	0.2	1.0	2.7	5.2	6.9	7.5	2.1	0.9	0.3	0.1	27.0
Quebec	0.1	0.0	0.2	0.4	1.8	3.9	5.5	4.2	1.7	0.6	0.1	0.0	18.5
Moncton	0.1	0.0	0.1	0.1	0.1	2.9	3.8	2.9	0.7	0.6	0.1	0.0	12.3
Fredericton	0.0	0.0	0.1	0.4	1.3	2.5	4.1	3.5	0.8	0.5	0.1	0.1	13.4
Charlottetown	0.1	0.0	0.0	0.1	0.5	1.8	2.1	1.9	0.6	0.2	0.1	0.0	7.4
Halifax	0.1	0.2	0.1	0.4	1.0	1.8	1.7	1.9	0.4	0.9	0.4	0.0	8.9
Gander	0.0	0.0	0.1	0.1	0.4	1.1	2.0	2.1	0.4	0.2	0.0	0.0	6.4

Table 3-3 Monthly and Annual Mean Number of Days with Thunderstorms at Selected American Airports
(From an internal Transport Canada report "Microbursts - A Review")

Airport	J	F	M	A	M	J	J	A	S	O	N	D	Annual
O'Hare	0.1	0.3	1.4	3.8	5.5	5.3	5.7	4.0	5.0	2.0	1.0	0.0	34.1
Laguardia	0.0	0.0	1.0	2.0	4.0	5.0	7.0	6.0	3.0	1.0	1.0	0.0	31.0
Kennedy	0.2	0.2	0.9	1.5	4.1	4.3	6.2	4.3	3.0	0.8	0.3	0.1	25.9
Los Angeles	0.4	0.2	0.2	0.5	0.0	0.0	0.3	0.3	0.2	0.0	0.3	0.2	2.6
Denver (Stapleton)	0.0	0.0	0.0	2.0	6.0	9.0	12.0	10.0	4.0	1.0	0.0	0.0	44.0
Atlanta (Hartsfield)	1.0	1.0	3.0	4.0	6.0	9.0	11.0	9.0	3.0	1.0	1.0	1.0	50.0
New Orleans (Moisant)	2.0	2.0	4.0	5.0	6.0	11.0	16.0	15.0	8.0	2.0	2.0	2.0	75.0
Dallas/ Fort Worth	2.0	3.0	4.0	6.0	8.0	7.0	5.0	5.0	4.0	3.0	2.0	2.0	51.0
San Francisco	0.2	0.2	0.0	0.4	0.2	0.0	0.2	0.4	0.1	0.0	0.0	0.1	1.8

Improved statistics concerning the frequency of different types of thunderstorms within a few kilometers of Canadian airports are required before any significant conclusions may be drawn from the climatological data. An analysis of available radar data showing the frequency and range of thunderstorms should be carried out for the several Canadian airports for which radar data exists. Consideration should be given to extending these analyses to include occurrences of towering cumulus with virga and rain showers.

It is known that many locations in the U.S., which experience a number of thunderstorm days per year comparable to central Canadian locations, have reported microbursts and aviation accidents.

3.2 Wind Shear Parameters

This section identifies those parameters required to model or characterize typical hazardous wind shear conditions.

3.2.1 Normal Strong Wind

The definition and meteorological causes of wind shear were discussed in Section 3.1 where "normal" atmospheric boundary layer conditions were described. Irrespective of the origin of the shear, the hazardous conditions are usually associated with strong winds a few hundred feet above the ground. This situation is illustrated in Figure 3-13 where the boundary layer wind shear pattern is shown. In this example a 60 kt wind, 1000 ft above the surface, results in a maximum vertical shear of more than 10 kt/100 ft very close to the ground. If the surface is rough, or the atmosphere unstable, then a similar flow will result in a layer of turbulence which may well have vertical wind shear, over a short distance, of a magnitude similar to that shown in Figure 3-13 and also horizontal wind shear of the same order as shown in Figure 3-14. A useful characteristic of turbulence is that the mean wind profile becomes more linear than the flow case as shown in Figure 3-13. The combination of a gradient of more like 7 kt/100 ft with an additional few kt/100 ft for the turbulence can be expected.

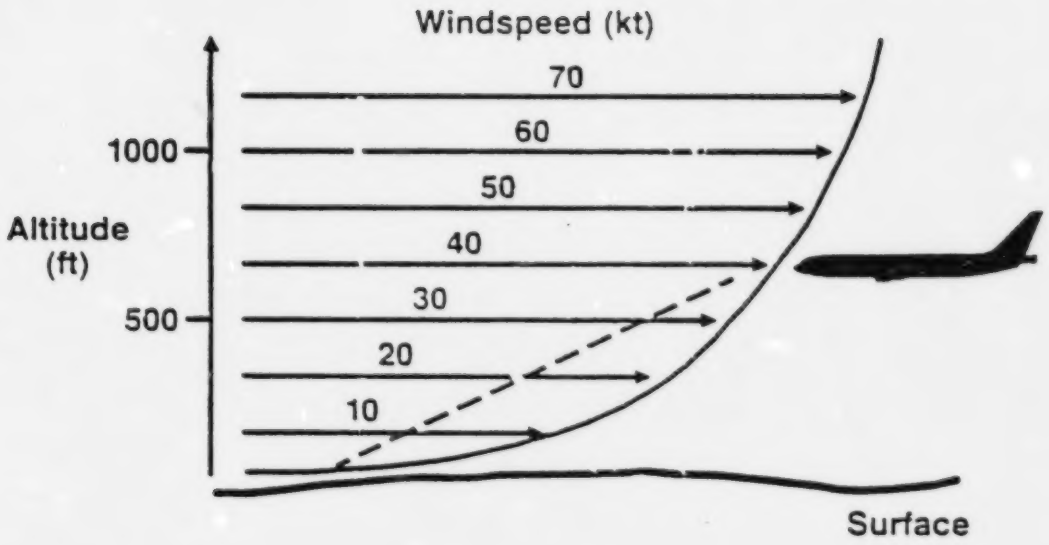

Figure 3-13 Boundary layer wind shear
(from Fujita and McCarthy, 1987)

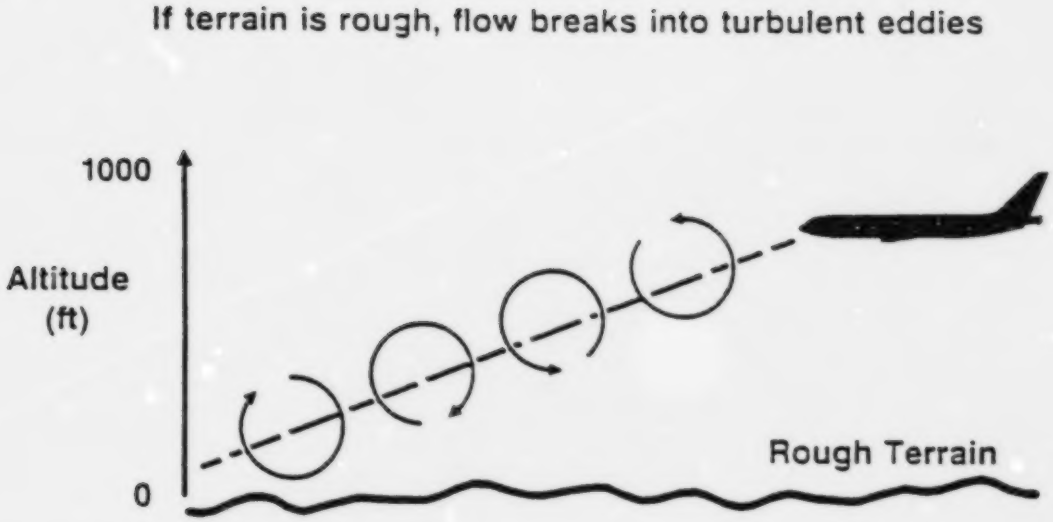

Figure 3-14 Gust front eddies due to rough terrain - simplified view (from Fujita and McCarthy, 1987)

3.2.2 Obstacle Wind Shear

The wind shear from surface obstacles such as the lee waves, as described in Section 3.1, is of a magnitude similar to that produced by normal strong winds. At a single front, wind reversals of 25 kt over a few hundred feet can occur, resulting in wind shears of the order of 10 kt/100 ft.

3.2.3 Gust Fronts, Downbursts, Macrobursts, and Microbursts

The overall speed differences for gust fronts, downbursts, macrobursts, and microbursts are at least comparable with the above values but the changes may occur over much shorter distances giving rise to very large shears within a few hundred feet of the ground. Figure 3-15 represents a sketch of a possible microburst in a dry environment. In coastal regions or Eastern Canada the storm would produce more rain than Figure 3-15 indicates and the main driving mechanism would be loading from heavy precipitation rather than evaporative cooling. Although the wind speeds would be on the order indicated for microbursts (see Table 3-4), the changes could occur over distances of approximately 1000 ft.

3.2.4 Severity of Shear

In general, the range of wind shear intensities which are of concern to aircraft operations are as follows:

Light	0 - 4 kt/100 ft
Moderate	5 - 8 kt/100 ft
Strong	9 - 12 kt/100 ft
Severe	above 12 kt/100 ft

This interim classification system was recommended by the Fifth Air Navigation Conference (Montreal, 1967). Since then it has become evident that this simple approach to the classification of wind shear intensity is not entirely satisfactory. A number of proposals have been made to improve the interim classification but none have been accepted. The current tendency appears to be to avoid the issue of wind shear altogether by basing future warning systems on the computation of the expected aerodynamic response of individual aircraft types to standard wind shear models.(1)

It is not clear that the magnitude of the shear is the most important criterion affecting safety. For example, a wind shear of 1/10 kt between between two points separated by a distance of one foot would constitute a "strong wind shear" as defined above, although the effect of such a wind shear on an aircraft would almost certainly be negligible. This wind shear would have the same numerical value as a potentially disastrous wind shear of 100 kt over 1000 ft. Clearly only those wind shears on a scale comparable to that of the aircraft constitute major hazards. It may be that the reason some aircraft are more

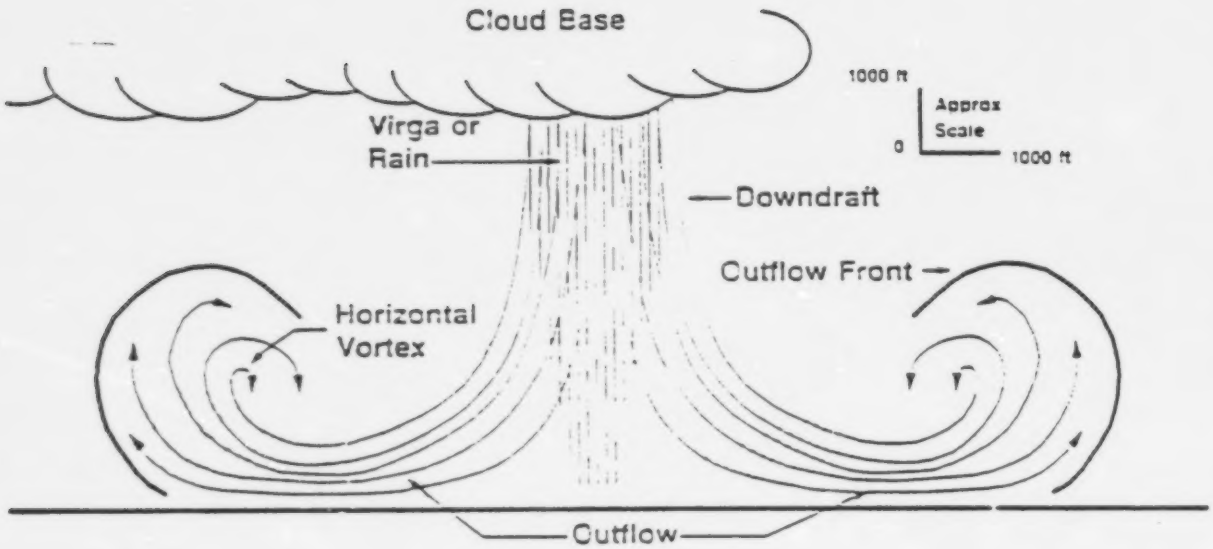

Figure 3-15 Microburst wind analysis
(from Fujita and McCarthy, 1987)

sensitive to wind shear than others has to do with both the response time of the aircraft and how the aircraft itself matches the horizontal extent of the meteorologically produced wind shear at the speed at which the aircraft is flying.

3.3 Microburst Parameters

Table 3-4 shows typical results obtained from examination of traces such as those shown in Figure 3-16. There are a whole range of phenomena called gust fronts, downbursts, microbursts, and macrobursts with overlapping characteristics. In addition, the microburst phenomena is small in horizontal extent and transitory in occurrence so that the data in Table 3-4 should be used with care. It is important to understand that an extremely variable phenomena is being described and that it is not possible to derive precise design specifications from the range of data currently available. Fujita expresses this variability well in The Downburst: "Not all microbursts are alike; some are accompanied by heavy rain, while others form beneath small virga. The parent clouds which induce microbursts are not always thunderstorms. Quite often, isolated rain showers spawn relatively strong microbursts which endanger aircraft operations at low altitude."(5) This is very important when considering the Canadian requirement. Do microbursts occur in Canada? Will they be the same as those that occur in the U.S.? The parameters presented in Table 3-4 are derived from recordings of occurrences of the phenomena in the U.S.

It is evident, from the discussion in Section 3.2 above, that all thunderstorms generate downdraughts during the mature, heavy rainfall stage in their life cycle. It is also obvious that not all thunderstorms represent a hazard to aviation at a significant distance from the rainfall core. In this sense the scientific situation is clear; given sufficient horizontal clearance (20 or 30 km for example) wind shear hazards from thunderstorms disappear. Conversely, penetration of the air space below any thunderstorm cloud and rain envelope, at low altitude, is extremely hazardous and should not be attempted except in an emergency. The hazard to aviation consists of unexpected wind shear patterns adjacent to, but not directly under, thunderstorms. If thunderstorms were always hazardous at 20 km then it would be normal practice to avoid them. The thunderstorm's wind shear or "microburst" hazard then depends on the production of significant wind shears at least a few kilometers horizontally from the thunderstorm. Not all of the literature agrees with this. Many of Fujita's reports show aircraft only a few kilometers from thunderstorm cores.

This section attempts to identify those microburst parameters which might be useful in aiding the detection of wind shear by remote sensing in order to issue early warnings. The wind velocity difference is the critical parameter to establish. However, with the exception of surface anemometry, the wind must be inferred indirectly to produce the wind shear warning. It therefore becomes necessary to examine other

Table 3-4 Typical Microburst Parameters

Diurnal Characteristics	Closely related to the diurnal characteristics of the local convective activity (e.g. air mass thunderstorms are more likely in the afternoon).
Duration	1 to 8 minutes with an average of 3 minutes
Size	
Core Diameter	1 to 2 km
Outflow Diameter	up to 4 km
Height of max. winds	50 - 100 m above the ground's surface.
Downdraught	Extends to within 1 km of the ground's surface.
Wind Speed	
Horizontal Peak	20 - 40 m/s
Horizontal Average	10 - 15 m/s
Horizontal Shear	20 m/s over 5 km
Vertical Peak	5 - 15 m/s
Vertical Shear	10 m/s over 1 km
Air Temperature	Microburst air can be warmer or up to - 5 degrees C or cooler than the environmental air.
Pressure	Microburst air can be up to + 2 millibars Hg higher in pressure than the environmental air.
Dew-Point Temperature	Microburst air can have a warmer dew point or up to a - 5 degree C cooler dew point than the environmental air.
Rainfall	0 mm/hr (dry microburst) $\geq$ 50 mm/hr (wet microburst)
Dust and bugs	Thought to be present in unknown concentration in dry microbursts.

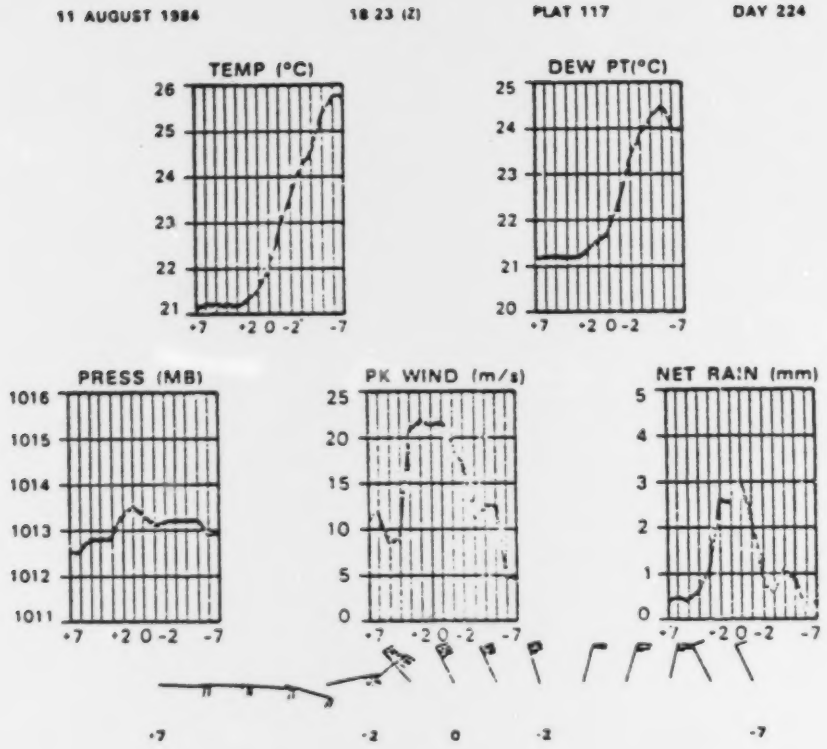

Figure 3-16 Actual meteorological parameter measurement for a documented microburst occurrence

parameters of the downburst which might allow detection. Typical microburst parameters are shown in Table 3-4. Figure 3-16 illustrates a typical example of the variation in meteorological parameters that can occur.

3.3.1 Diurnal Characteristics

Microbursts are spawned by convective clouds so their diurnal variations are closely related to the convective activity pattern of a given area. This relation to convective activity was demonstrated in the NIMROD and JAWS studies. The NIMROD network was situated just west of Chicago, Illinois while the JAWS network was situated just north of Denver, Colorado. In both experiments, there were distinct occurrence peaks for wet and dry microbursts. The occurrence peaks for wet and dry microbursts were different at each location.(5) During the NIMROD experiment the wet and dry peaks occurred from 5 p.m. to midnight and 10 a.m. to 11 a.m. respectively. During the JAWS experiment the peaks occurred between 2 p.m. to 3 p.m. and 2 p.m. to 4 p.m.

3.3.2 Duration

The duration of microbursts is variable. In 50 microbursts detected by the 27 Portable Automated Mesonet (PAM) stations of the NIMROD network it was found that microbursts were as short as 1.5 minutes and as long as 7.0 minutes in duration with an average duration of approximately 3.0 minutes. In 186 microbursts detected by the 27 PAM stations of the JAWS network it was found that microbursts were as short as 1.0 minute and as long as 8.0 minutes with an average duration of approximately 2.9 minutes.(5)

The small high intensity downdraughts of interest here are inevitably transitory. Their duration is dependent upon wind speeds and size. The larger, less intense microbursts last much longer than small intense events, but would still pass by a fixed surface observer rapidly.

3.3.3 Size

Downbursts occur at all size scales; they are arbitrarily subdivided into macrobursts and microbursts according to their horizontal scale of damaging winds. Microbursts are small downbursts with outburst winds extending between 40 m (131 feet) and 4 km (2.5 miles).(5)

3.3.4 Wind Speed

There are two wind components to be considered: the horizontal wind component which translates into head wind, tail wind and cross wind components for an aircraft, and the vertical wind component which will affect an aircraft's rate of climb with respect to the ground.

3.3.5 Air Temperature

The air temperature in microbursts can be either warmer or colder than their environment. This is in contrast to macrobursts, which are typically colder than their environment. The downflow cools due to evaporation or sublimation of the rain or hail particles falling inside the descending air current. However, these rain or hail particles do not always evaporate fast enough to keep the downflow cool and saturated. A warm downflow can descend to the ground based on its accumulated momentum.

Table 3-4 states that the microburst air can be up to 5 degrees C cooler than the environmental air. While this is true for the majority of microbursts, statistical analysis of the NIMROD and JAWS microbursts, reveals that approximately 40% of the microbursts are warmer than their environment.(5)

3.3.6 Pressure

Since there is a strong downdraught at the centre of the microburst we expect there will be a pressure maximum at the centre. This pressure maximum tends to be surrounded by rings of low and high pressure. Figure 3-17 shows pressure profiles taken across a microburst. Note the difference in profile, depending upon the relative position of the microburst centre.

Contrary to expectations, however, the surface pressure for an individual microburst can increase or decrease by as much as 2 to 3 mb during high winds. This is due to the conversion of total pressure into velocity pressure, which can result in a decrease in atmospheric pressure with the increase in outflow speed.(5)

3.3.7 Dew-Point Temperature

The NIMROD and JAWS experiments showed that dew-point temperature in microbursts can be either higher or lower than dew-point temperature in the surrounding air. A higher dew-point temperature would be expected in a precipitation-cooled downflow. Fujita suggests that a lower dew-point temperature could be caused by the addition of dry air into the microburst outflow during its rapid descent.(5)

3.3.8 Rainfall

Microbursts are caused, at least in part, by heavy rainfall. In the early stages of the thunderstorm's life cycle the microburst itself contains many raindrops. A distinction must be made at this point between "dry area" microbursts and "humid area" microbursts. In dry areas, a part of the driving mechanism is evaporative cooling. Therefore, the associated rainfall at the surface, and far from the thunderstorm cloud envelope, may be minimal. This pattern of

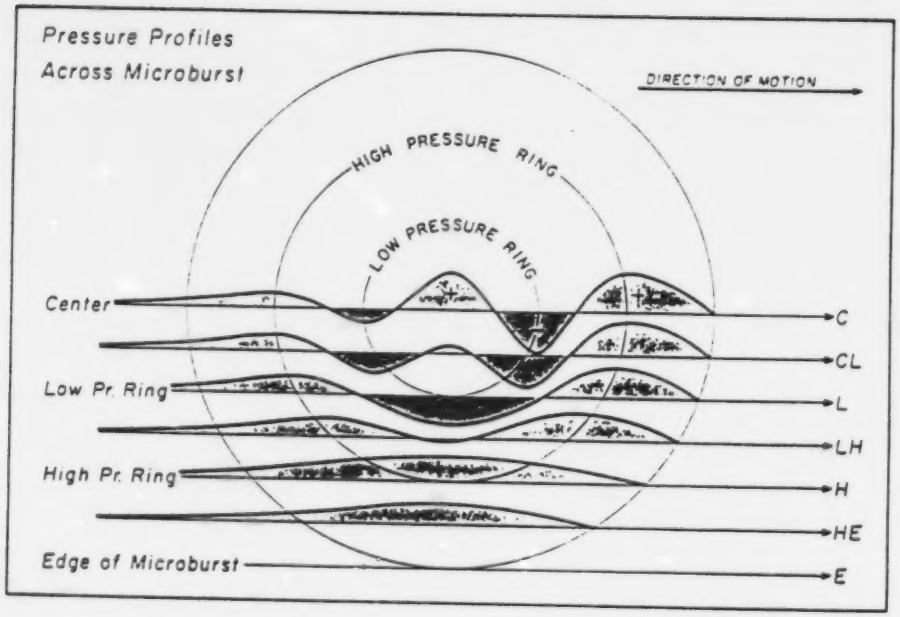

Figure 3-17 Pressure profiles across various portions of a microburst. C—the centre, CL—between the centre and the low pressure ring, L—low pressure ring ,etc. (from Fujita, 1985)

precipitation is characteristic of the dry area microbursts. It is not clear that these dry area microbursts do not contain raindrops since radar detectability was regularly reported from these phenomena in the JAWS experiment (13) probably due to the survival of a few large raindrops. In more humid areas, such as Eastern Canada, the evaporative cooling mechanism is much weaker and the presence of at least some rainfall during any significant wind shear phenomenon seems assured. The heavy rainfall increases the vertical wind speed by direct mechanical drag on the air. In humid areas this mechanism presumably predominates over evaporation. The spectrum of the raindrop's physical size, for those raindrops likely to be found in both humid and dry microburst outflows, is totally unknown although evaporation removes small drops first, leaving the larger drops behind. In view of the radar's high sensitivity to large, as opposed to small drops, this may assist in the radar detection of wind shear. Naturally, if the extent of the wind shear is to be estimated, Doppler radars would be required.

3.3.9 Dust and Bugs

Fujita's work on TV images of dry microbursts suggests that they may be visualized by the dust, debris and bugs stirred up by the strong winds at the surface although it may not be completely clear that the optically detected materials are not raindrops. There are no known data on the concentrations and particle sizes of microburst dust. The occurrence of dust is presumably more frequent in dry areas than in humid areas. This suggests that detection by lidar of the dry cases may be complimentary to the detection of wet cases by radar.

3.4 Review of Detection Technology

Before reviewing the detection technology the characteristics of the phenomena being detected must be considered. The meteorological analyses outlined in the previous sections suggest that the microburst, as a source of low level wind shear, has the following characteristics:

a) It will be associated with thunderstorm downdraughts, downdraughts from convective rain showers, high-based thunderstorms or towering cumulus virga.

b) It can extend horizontally as much as 20 km from the thunderstorm core.

c) It is of short duration (1-8 minutes).

d) It rapidly propagates away from the thunderstorm.

e) The centre of the wind velocity is 100 m or more above the surface.

f) The wind aloft leads the surface wind in both time and space.

g) The microburst air mass is usually colder and possibly drier than the air it displaces. (This varies depending upon whether the microburst is wet or dry, etc.)

h) The microburst air mass may contain raindrops, dust, or bugs.

Thunderstorm activity, the primary cause of microbursts, is readily detectable by weather radar. In Canada weather radars routinely delineate between thunderstorms and showers involving heavy rain. There is a high correlation between the existence of strong radar reflectivity at high altitude in storms and the occurrence of hail, lightning and presumably microbursts. Furthermore, systems to predict the evolution and likely movement of thunderstorms have been operational for years. For example, over the last 12 years the Montreal based McGill University Radar Weather Observatory has been providing automatic three hour predictions for the Dorval, Mirabel, Ottawa, and St. Hubert airports.

The rapid movement which is characteristic of microbursts creates a situation where it is insufficient to just monitor wind shear conditions along the glide paths. In order to provide advance warnings of wind shear conditions it is necessary to ensure the detectors scan either side of the glide path in order to detect any incoming vortex. Systems such as McGill University's system could be used to issue warnings indicating the presence of thunderstorms within 20 km of glide paths. The accuracy of these warnings would be very high with respect to the existence of severe convection, but the prediction of microbursts would not be possible.

Once acceptable detection technology has been identified it must be integrated into a system that will quickly and automatically recognize the wind shear condition and issue a warning. If human operator interpretation of data is required it would be necessary to have operators in place 24 hours a day, seven days a week for five or six months of the year. Since there are so few annual thunderstorm days in any Canadian location (see Section 3.1.4), years could pass before there is a wind shear occurrence. Since the duration of the phenomenon is only minutes, a human operator would have to be constantly alert; otherwise, it is very likely that if a wind shear occurred it would not be detected.

As stated above, the obvious solution to this aspect of the problem is an automated system which will quickly and accurately identify the wind shear phenomenon. Because microbursts vary in size, shape, and intensity, traditional pattern recognition software techniques do not always apply. This has resulted in the development of some very sophisticated algorithms by the Lincoln Labs in the U.S. to accommodate the peculiarities of microbursts. These microburst detection algorithms are forming the basis of the Terminal Doppler Weather Radar (TDWR) processing software and should be further investigated with respect to their applicability to Transport Canada's requirement.

Several technologies and systems have been either developed or adapted to facilitate the detection and prediction of wind shear phenomena. Any system designed to detect and provide advance warning of wind shear/microburst phenomena will have three major components: the basic front end sensor, a real time analysis processor, and an element to provide warning. It is feasible that expert systems will eventually be incorporated to provide automatic warnings to pilots and controllers. Due to the short duration of microbursts a wind shear/microburst detection system must meet the critical specification of real time operation. This section of the study focuses primarily on the sensor technologies; it is quite possible that more than one type of sensor will have to be utilized to solve the problem. Some technologies and methods are listed below and will be explained in detail in the following sections.

3.4.1 Visual Observation
3.4.2 Anemometers, Weather Vanes, and Microbarographs
3.4.3 Wind Profilers
3.4.4 Airborne Sensors
3.4.5 Doppler Radar
3.4.6 Rawinsondes
3.4.7 Acoustic Radars (Sodars)
3.4.8 Satellite Instrumentation
3.4.9 Lidars

3.4.1 Visual Observation

This technique involves direct observation of the meteorological phenomena associated with wind shear. The gust front/microburst vortex may be visually apparent due to the clouds, raindrops or dust associated with the turbulent winds. The characteristic appearance of virga, a rainshaft which may evaporate before it reaches the surface, is being addressed in pilot wind shear avoidance training. Pilots are generally at least as well placed as those on the surface to observe these phenomena. The visual observation technique is clearly limited to daylight hours.

3.4.2 Anemometers, Weather Vanes, and Microbarographs

Arrays of anemometers, with associated weather vanes, have been used as wind shear detection devices. The differences in wind speed and direction between the sensors in the array are monitored, on a continuous basis, in order to detect the surface effects of a microburst. While the anemometers do show some effects in the presence of a microburst, it is not clear that this enables an accurate forecast since the surface winds are significantly less than the winds aloft and are likely to occur later in time. The data from such systems installed at U.S. airports have proved to be of value in the analysis of microburst phenomena.

One such system is the U.S. Low Level Wind Shear Alert System (LLWAS). The basic system consists of five anemometric sensors located in a 3 km radius ring around the periphery of an airport with an additional sensor at the airport centre. Each sensor is mounted 6 to 30 m above the ground's surface. The spacing between the peripheral sensors and their height above ground level is usually determined by local topography. They report wind speed and direction back to a central computer via a land line or a VHF/UHF radio link. If a wind vector difference of typically 15 knots exists between the central sensor and any of the peripheral sensors, the air traffic control tower will alert pilots in the vicinity of a potential wind shear situation. At present, approximately 100 of the larger airports in the U.S. have installed operational LLWAS and this should increase to include an additional 110 airports by the end of 1992. Unfortunately, there are several problems with the LLWAS system:

a) The network is too spread out to detect a typical microburst. For example, a microburst 1 to 3 km in diameter can easily remain undetected over the 3 km network radius.

b) The network does not extend far enough to totally cover the complete aircraft approach and departure regions.

c) The system has no predictive capability since it can only indicate when a microburst is in the process of occurring.

d) The system can only assist in the detection of microbursts if they extend fully to the ground surface. Bedard, a researcher from NOAA, has shown in his recent studies conducted at Boulder, Colorado, that some microburst wind shears remain aloft. Mid-air microbursts (Figure 3-18) do not actually reach the ground surface and thus cannot be detected by the LLWAS. Even with a conventional microburst that reaches the surface the detected surface winds may be considerably lighter than the winds aloft and will occur later in time.

e) No information is detected regarding the vertical structure of the microburst.

As a result of these specific problems, an enhanced LLWAS system, known as ALWAS (Advanced LLWAS), has been developed. This enhancement includes the use of additional sensors (a total of 12 at Denver's Stapleton International Airport), modified computer algorithms to allow improved determination of wind direction inflows and outflows, improved man-machine display interfaces, and the incorporation of microbarographs (self recording barometers) into the sensor array.

The addition of these microbarographs can be used to measure the pressure gradient. The pressure gradient can be used in calculating the wind speed which in turn can be used to infer wind shear. It has been found

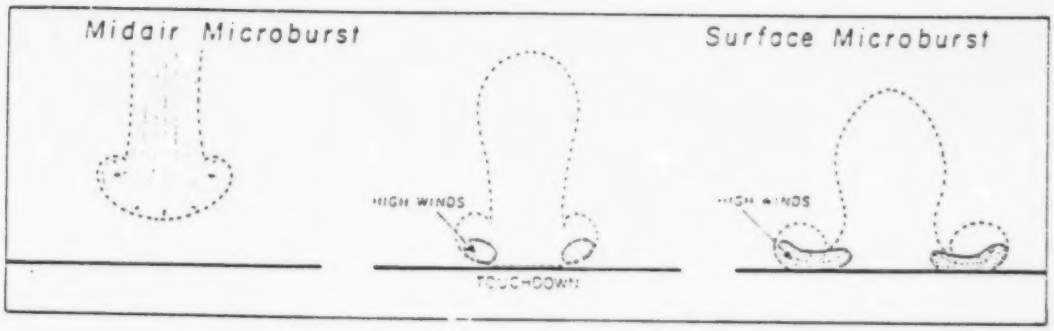

Figure 3-18 Stages of a descending microburst
(from Fujita, 1985)

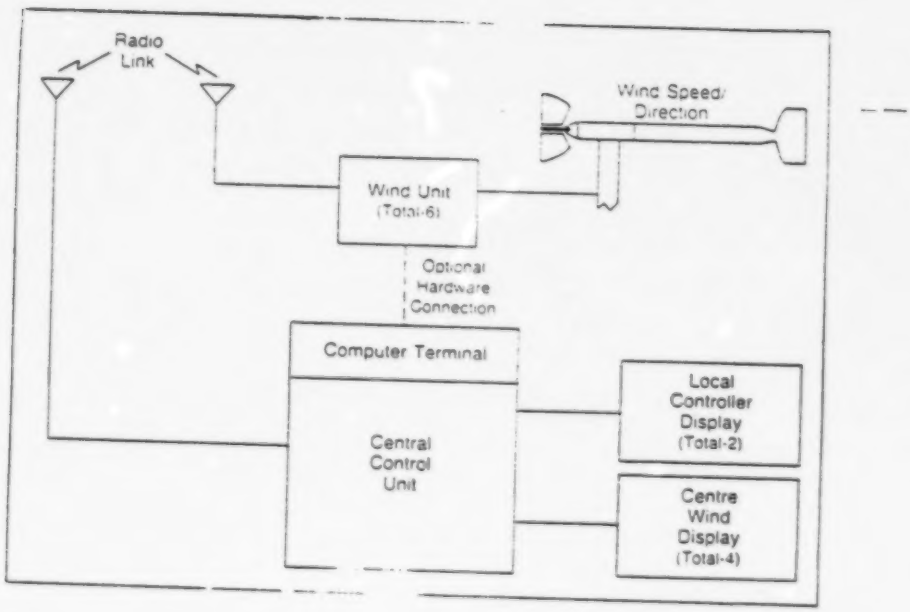

Figure 3-19 LOLA (Low Level Alert System)
(from Baker et al. 1986)

that a significant pressure change can occur as much as two minutes before the descending microburst downdraught reaches ground level. A current system, known as LOLA for Low Level Alert (Figure 3-19), is manufactured by Climatronics Corporation in the U.S. and has been approved by the FAA as a method for wind shear detection and alert.(14)

In the past year a similar system known as the Automated Weather Observing System (AWOS), has been certified by the FAA.(15,16) The AWOS1 system reports wind speed and direction, temperature, dew point and pressure, and is updated approximately every minute. The meteorological information is translated by computer to synthesized voice and then broadcast over an HF communications link. AWOS2 and AWOS3 systems also exist and, in addition to those parameters listed above, they monitor precipitation, visibility, and cloud height. These systems are now being manufactured in Canada by Pelorus Aviation Supplies Canada Ltd. of Calgary, under license to Handar Inc. of Sunnyvale, California. The first such system to be installed in Canada was recently commissioned in Dawson City in the Yukon. Unfortunately, these systems only relay information concerning present meteorological conditions. Software algorithms are currently being developed which may assist in the detection of wind shear.

3.4.3 Wind Profilers

These systems consist of large phased array antennas (12 x 12 m) consisting of either coaxial-collinear or Yagi elements that transmit on either the UHF (400 MHz) or VHF (50 MHz) frequencies. They are capable of measuring both horizontal and vertical winds within the coverage pattern. The antenna system, under computer control, can create three beam positions: one vertical and two oblique which are 15 degrees off-zenith in the north and east directions. Selectable power, pulse width, and pulse repetition frequency produce a system that can profile winds to a height of approximately 16 km with a vertical resolution of 250 m.

Horizontal winds can be measured to a velocity of 90 m/s and vertical winds to a velocity of 23 m/s with an estimated accuracy of 1 to 2 m/s. These systems can provide complete wind profiles every six minutes with wind speed and direction for each height resolution cell. This is accomplished by computer processing of the Doppler frequency shifts of the backscattered energy from atmospheric turbulence present due to humidity and temperature variations. These systems can be totally unattended with the data being communicated by landline modems or through automated satellite transmissions.

Presently, 30 systems are being networked by the Sperry Corporation (Figure 3-20) with Andrew Antennas responsible for the antenna manufacturing. This initial network (Figure 3-21) appears to be an experimental trial before an entire grid of wind profiling systems is implemented in the U.S. A similar system is manufactured by Tycho Technology, a subsidiary of the Finnish Vaisala Corporation.

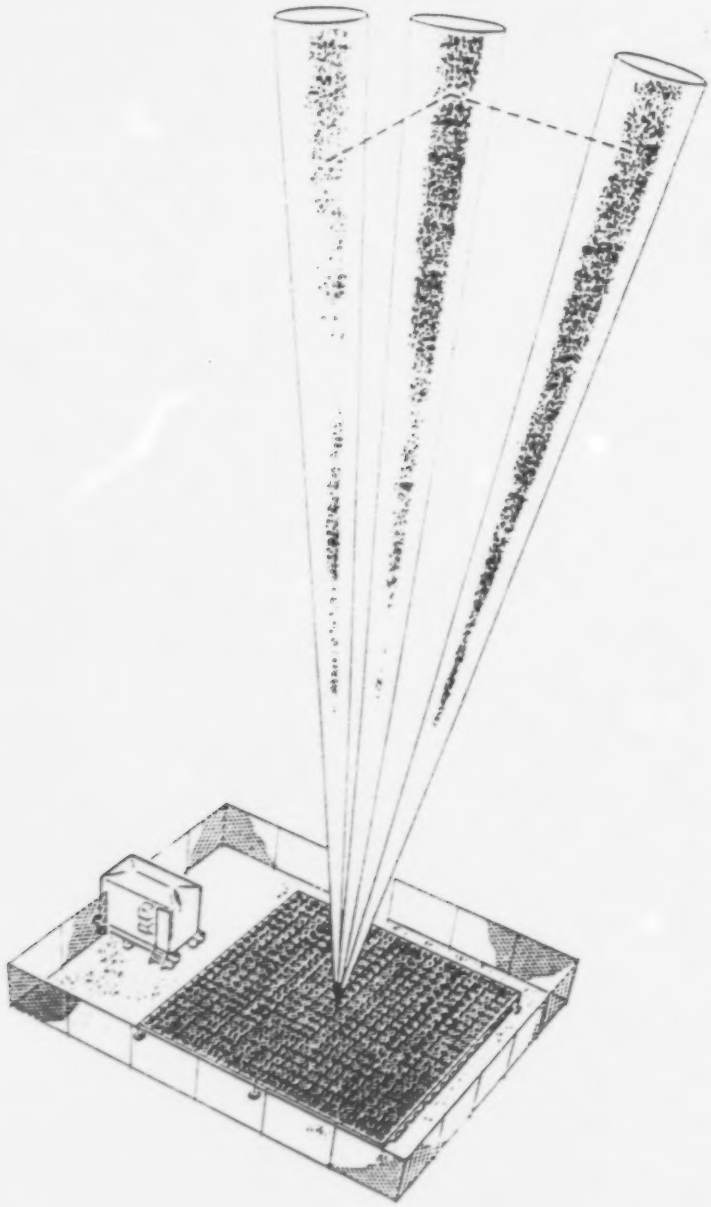

Figure 3-20 Wind profiler system
(from Sperry Corporation marketing information)

Figure 3-21 American wind profiler network grid sites

Another similar system uses a collection of 196 four-element Yagi antennas.(17) Each Yagi antenna is under computer control, either transmitting at the VHF frequency of 50 MHz or the UHF frequency of 400 MHz. The beam pattern of the antenna array can be directed vertically or at various angles from the zenith (Figure 3-22) enabling a three dimensional profile of wind movement to be determined. Information is gathered from both the echo reflectivity intensity and its Doppler shift.(18) This system can monitor atmospheric conditions from 500 m up to 90 km. It is commonly known as CAPSONDE (Figure 3-23) and is manufactured by the Radian Corporation in the U.S. at a cost of between $200,000 to $400,000 U.S. depending on transmit power requirements.

Even though the technology of wind profiling has advanced considerably, it does not appear to be appropriately suited for the detection of wind shear since certain disadvantages are apparent:

a) These systems are not effective at low elevations; winds at heights of 500 m and below cannot be reliably profiled.

b) An overall update rate of six minutes is inadequate for microburst detection when microbursts can have a much shorter duration.

c) The beam cannot be easily pointed along the glide path as the antenna arrays are usually quite large. To fully cover the entire glide-path trajectory several vertical pointing antennas would be required.

d) These systems are usually expensive ($200,000 to $600,000 U.S.).

3.4.4 Airborne Sensors

All airborne wind shear detection systems are classified as being "reactive"; they indicate the aircraft has entered a wind shear situation. Presently, most systems detect the presence of the wind shear phenomena and alert the aircrew accordingly, albeit only a few seconds before the pilot would normally realize that he has encountered the wind shear. However, these additional few seconds are usually critical to successfully avoid the wind shear situation or to respond with the correct emergency procedure. Some systems have been developed to include escape guidance procedures where the pilot will be informed, through conventional avionics instrumentation, of the best way to successfully exit the wind shear situation.

The three companies that are presently involved in the development of these airborne detection, alert and guidance systems for wind shear are:

a) Sperry Honeywell
b) Safe Flight Instrument Corporation
c) Sundstrand Data Control

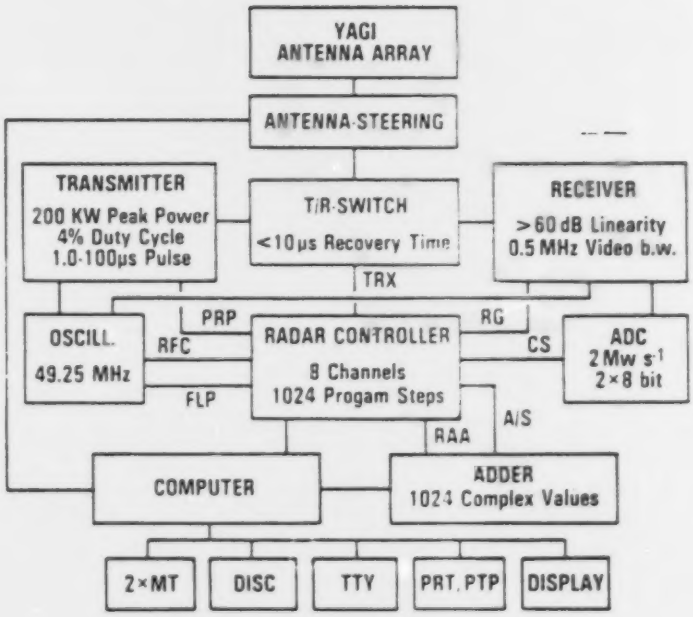

Figure 3-22 Continuous atmospheric profiler radar system (CAPSONDE)
(from Radian Corporation marketing information)

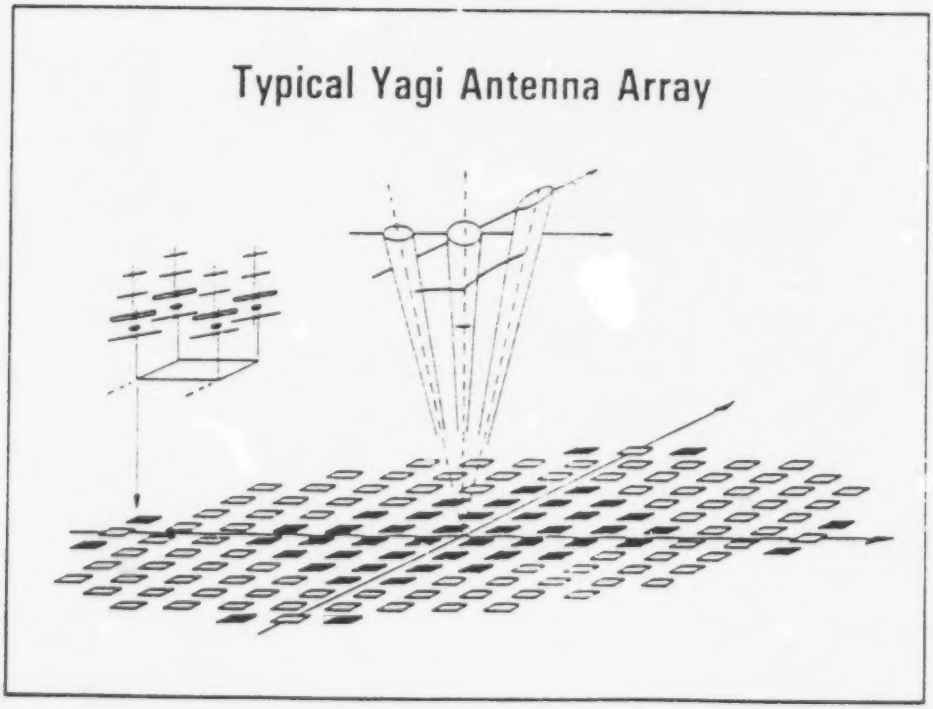

Figure 3-23 Continuous atmospheric profiler radar system (CAPSONDE) typical Yagi antenna array (from Radian Corporation marketing information)

The Sperry Honeywell system uses existing onboard sensors that transfer their information to the performance management system.(19) This system provides two levels of detection. The first level of detection, a cautionary warning, is activated when the aircraft experiences a considerable updraught or excessive head wind. The pilot is notified by the activation of a flashing yellow annunciator. This warning is only operational during the final approach phase. The second level of detection occurs when the aircraft is experiencing a downdraught and an increasing tail wind. The indicator is a flashing red annunciator associated with an aural message of "wind shear, wind shear". These detection and alerting systems, referred to as Phase I systems, have been commissioned, and are fully operational, by Piedmont Airlines on their 737-200 aircraft. A Phase II system provides flight guidance to safely exit a wind shear situation by presenting appropriate pitch altitude commands and directions to successfully execute a go-around procedure. Sperry Honeywell is working with McDonnell Douglas to integrate a wind shear detection, alert and guidance system into the aircraft's electronic flight instrument system.

Safe Flight Instrument Corporation has developed a wind shear detection, alert and escape guidance system that also utilizes existing sensors and its own computer system (Figure 3-24).(20,21) The computer software resolves the information into the two orthogonal components of a wind shear: the horizontal wind shear and the downdraught or vertical component. If an established threshold is exceeded, an aural alert is generated indicating the likelihood of the existence of a wind shear condition. The recovery guidance commands are based primarily on controlling the aircraft's angle of attack and increasing the thrust.(22,23) Safe Flight is working closely with both Boeing and McDonnell Douglas.

The Sundstrand system is based around an enhanced ground proximity warning system (GPWS). This system also makes use of existing sensors, so the system can easily be incorporated without any additional hardware requirements.(24) This system has already been certified for the B-737, B-747 and B-757. Similar indicators and aural alerts are used to inform the pilot of the hazardous wind shear situation (Figure 3-25).

Other advanced systems utilizing airborne Doppler radar and Lidar are in the development and evaluation phases.(25) However, these systems are being designed to be able to scan ahead of the aircraft to distances of 500 to 800 m, allowing additional reaction time for the crew to respond.

An advanced holographic, heads-up guidance system has been newly developed by Flight Dynamics. This system has received FAA certification and is being flight tested aboard Federal Express 727s. It offers wind shear detection, warning and exit guidance.(26)

It is evident that there has been considerable work performed in the development of airborne wind shear detection, alert and escape guidance systems. As a result of this effort the following instrument deviations have been proposed as being sufficient to identify a wind shear situation:

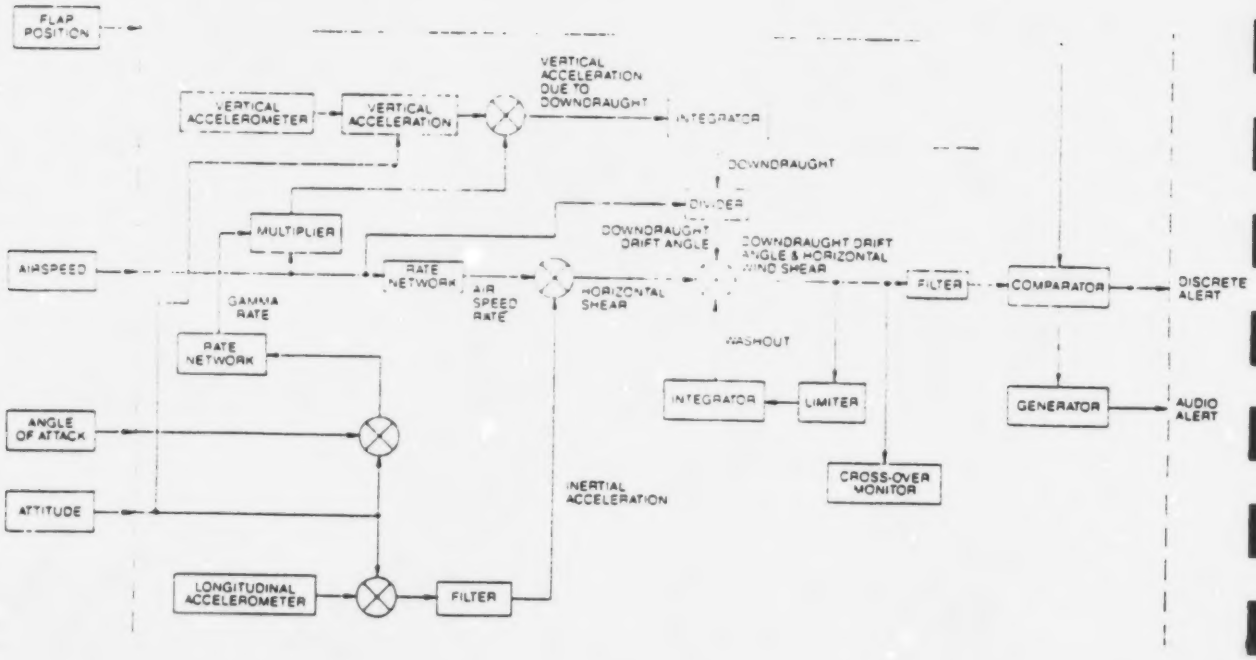

Figure 3-24 Functional block diagram of Safe Flight's airborne wind shear detection system (from Green, 1986)

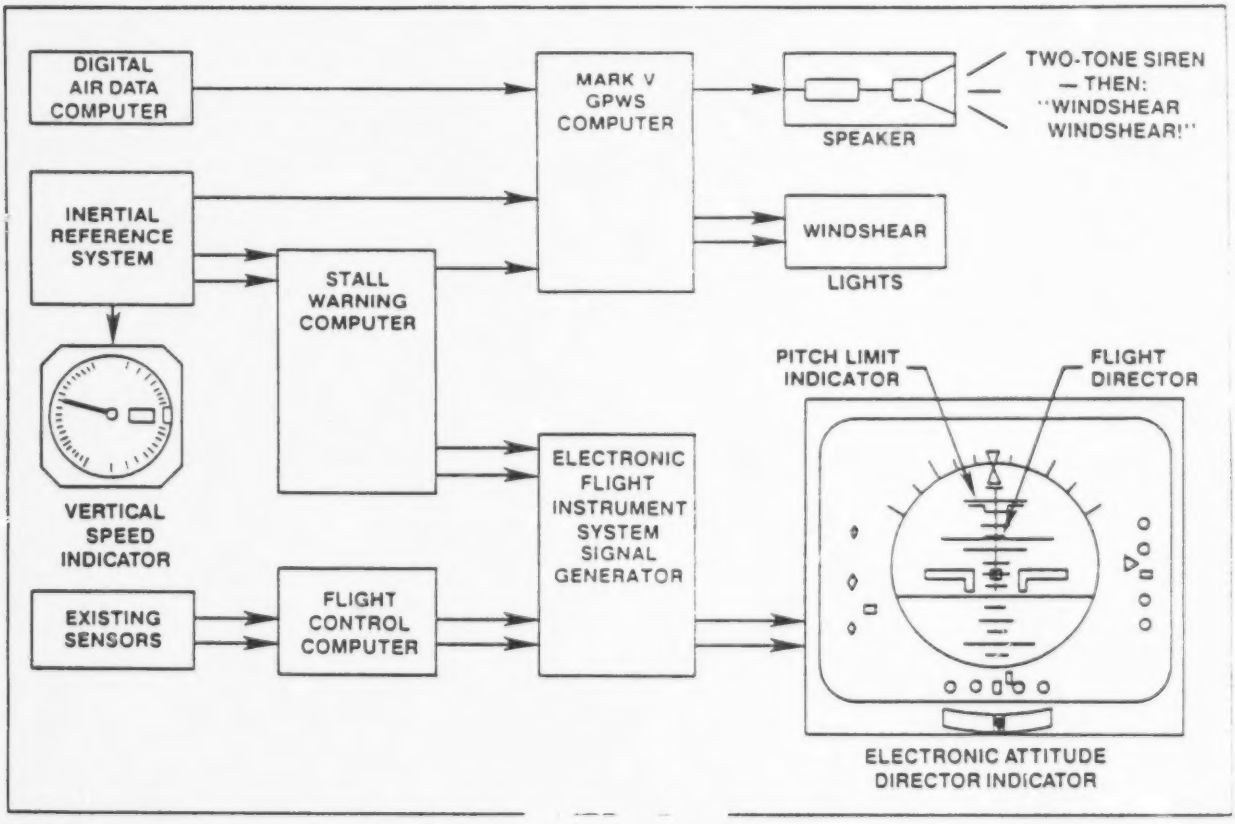

Figure 3-25 Sundstrand's airborne wind shear detection system (from Rahr, 1987)

- airspeed deviations of the order of 15 knots
- pitch excursions of the order of 5 degrees
- vertical speed excursions of the order of 150 mpm

Despite this proposal, no standard specifications for instrument deviations have been established to indicate the presence of a wind shear condition.

The situation with respect to recovery guidance systems is further complicated by the fact that there will probably be different escape procedures for different aircraft and some aircraft will be difficult, if not impossible, to retrofit.(27) It appears that the overall consensus of the airline industry and the regulatory organizations is that airborne forward-looking detectors are essential protection against wind shear. Nevertheless, airborne detectors do not appear to be the complete solution to the problem and should be used in association with predictive ground-based detection systems.

3.4.5 Doppler Radar

Conventional radar can detect gust fronts. It is not clear whether this detection is due to particles suspended in the air (raindrops, dust or bugs) or due to changes in the refractive index due to differences in temperature and/or humidity. Doppler radar is very similar to conventional radar in that it can measure the distance parameter by the time it takes the transmitted signal to bounce off an object and return. However, unlike conventional radar, Doppler radar can also measure the relative velocity of the object by determining the frequency or doppler shift of the reflected signal. Objects that are moving away from the radar site lower the frequency of the reflected signal (negative Doppler frequency) while those moving towards the radar site increase the frequency (positive Doppler frequency). When a Doppler radar is monitoring wind motion it is probably measuring the velocities of particles in the air such as water droplets, blown dust, insects, etc. In the case of clear air turbulence, the Doppler radar technique can monitor changes in the refractive index of the air mass caused by temperature or humidity variations.

Another recent discovery that reinforces the use of Doppler radar to detect gust fronts is the fact that radar reflectivity or echo intensity actually decreases before a microburst develops.(28) This occurs because, before the downdraught descends, the surrounding storm clouds become depleted of water due to rain and evaporation, thus reducing the major radar backscatter reflector. With conventional radar the returns diminish, suggesting the microburst area is not as severe as it really appears.

In recent years, several programs have been initiated in the U.S. to investigate the wind shear phenomena using Doppler radars as the main sensors.(5)

NIMROD - Northern Illinois Meteorological Research on Downburst. This study was conducted from May 19 to July 1, 1978 at Chicago's O'Hare International Airport. It utilized three Doppler radars in a triangle configuration of 56 x 57 x 60 km with the radars at the vertices enabling complete three dimensional wind speed and direction profiling.

JAWS - Joint Airport Weather Studies. This study was conducted from May 15 to August 9, 1982 at Denver's Stapleton Airport. It also used three Doppler radars but configured in a much smaller triangle of dimensions 15 x 18 x 28 km.

CINDE - Convection Initiation and Downburst Experiment. This 1987 study further examined the physical principles that produce boundary layer features leading to convective initiation and to examine precursor and forcing features aloft leading to microbursts and downbursts. Radars and facilities were shared with the Terminal Doppler Weather Radar (TDWR) Program located north and east of Stapleton International Airport.

CLAWS - Classify, Locate and Avoid Wind Shear. This study was conducted from July 2 to August 15, 1984 with a single Doppler radar at Denver's Stapleton Airport.

COHMEX - Cooperative Huntsville Meteorological Experiment. This study was comprised of three individual projects; two that incorporated the use of Doppler radars. These two were entitled FLOWS, for Federal Aviation Administration - Lincoln Laboratory Operational Weather Studies, and MIST, for Microburst and Severe Thunderstorm experiments. They were primarily conducted from June 15 to July 31, 1986 in the Huntsville, Alabama region. The FLOWS project utilized two Doppler radars while the MIST experiment used three in the triangular configuration.

It must be noted that these Doppler radars were all custom designed, highly specialized sensors that were developed by the Lincoln Laboratory or the National Centre for Atmospheric Research (NCAR). These radar systems are not commercially available.

As a result, two major programs for the development of Doppler weather radars are in progress. The NEXRAD (Next Generation Weather Radar) program is a development sponsored primarily by the U.S. National Weather Service, a branch of the National Oceanic and Atmospheric Administration Office in Boulder, Colorado. The system's primary parameters are that it transmits on a S band frequency of 3 GHz (10 cm), can observe out to a range of 460 km, and extend up to a height of approximately 18 km. The radar performs a complete scan in azimuth, then increments up a step in elevation and performs a complete new azimuth scan, taking five to six minutes to conduct a complete 360 degree azimuth, 20 degree elevation coverage pattern. Unisys has just recently won a competitive bid to develop the first 10 NEXRAD systems. This contract has options for up to 185 additional systems which will be installed across the U.S. in a national coverage grid.(29)

NEXRAD is an expensive system that has been primarily designed as a meteorological forecasting system, not as a wind shear detection system. The equipment will most likely be situated too far from the airport to assist in microburst observation. Also, large antennas are needed to generate the required one degree beamwidth for long range operation at the 10 cm wavelength. The result is a very large antenna which is incapable of rapid scanning; its update rate of every 5 minutes is not adequate to detect the shorter duration microbursts. As well, the selected frequency of 3 GHz poses some interference and frequency allocations problems with present airport spectrum assignments. Since the surface of the earth is curved and the horizontally spreading downbursts produce their wind shear only a few hundred feet above the ground, long range operation of a dedicated microburst detection radar is not feasible. This suggests that high power and large antenna diameter may not be required for microburst detection. Therefore, there exists the possibility that a small, relatively low power Doppler radar could be developed which would allow fast scanning to give timely downburst warning at a fraction of the cost of the NEXRAD type system.

The FAA has initiated the development of a Terminal Doppler Weather Radar (TDWR). It is basically the same configuration as the NEXRAD system except it has a C-band 6 GHz (5 cm) transmitter receiver and has a shorter range coverage of 110 km. The system can perform sector scans from 90 to 120 degrees, enabling it to observe and dwell longer on critical approach and departure regions from the runways. Because it is using the large 9 m NEXRAD antenna and an increased transmission frequency, the TDWR system's angular resolution has been enhanced to be less than one degree. Extensive Doppler signal processing using FFT techniques assists in the real time data analysis. The FAA will commence installation of these TDWR systems in 1992 and will be installed in approximately 110 of the medium-to-large sized airports in the U.S.

Each system will probably cost in the range of $4.5 Million per installation. However, a smaller, low power Doppler radar designed specifically for the detection of microbursts would be considerably less expensive.

Problems do occur with pulsed Doppler radar systems. A common error that can occur in the measurement of winds of relative high velocity is frequency aliasing or velocity foldback. The result of this error is that a high velocity wind can be interpreted as a slow velocity wind moving in the opposite direction. This may occur because the pulse repetition rate (PRF) of the radar is not sufficient to observe these high velocity winds. To avoid this problem a PRF rate must be selected that is high enough to observe the weather conditions but not so high as to jeopardize the range coverage. Another major problem results from the excessive reflections from ground clutter. Because the system is required to detect microburst outflow very close to the ground, interference from buildings, towers, vegetation etc. will be extreme.

Extensive signal processing is required to eliminate or filter out this ground clutter interference while still retaining the information pertaining to the wind velocity movement.

An alternative to pulse Doppler radar is frequency modulated continuous wave (FM-CW) Doppler radar.(30) Because of the CW transmission, this radar can transmit at lower power, full duty-cycle as compared with a pulsed Doppler system. More average power can be delivered to the microburst activity, facilitating higher sensitivity and enhanced wind detection resolution. Due to this higher resolution, the cancellation of ground clutter is easier and more effective. Radian Corporation, a Texas based company, has a FM-CW Doppler radar under development for NOAA and the U.S. Army, which could possibly be used for the detection of wind shear.

3.4.6 Rawinsondes

Radio wind sounding systems consist of a balloon with a radiosonde sensor tethered beneath it.(31) The radiosonde transducers measure the atmospheric parameters of pressure, temperature and humidity at a high sampling rate of approximately eight samples every ten seconds. The radiosonde then transmits the data to a ground station via a UHF communication link either at 403 MHz or 1680 MHz. The balloon is tracked by the means of modern navaids (Omega) techniques (Figure 3-26). The radiosonde contains a small VLF Omega receiver that continuously reports its location to the ground station. The location of the ground station has already been predetermined by surveying or through a similar Omega receiver which allows the relative location of the balloon to be continuously monitored. The change in the location of the balloon is used to derive wind speed and direction, while the balloon altitude is derived from the pressure sensor data.

The sounding system can monitor to heights of 30 km. The measured data is processed at the ground station and then transmitted in standard meteorological formats. A typical display presentation of the atmospheric parameters is shown in Figure 3-27.

The two main companies that produce radiosondes and sounding systems are Vaisala Inc. of Finland and VIZ Test Equipment, a company which has a Canadian division located in Guelph, Ontario.

Even though these sounding systems are used to assist in forecasting weather formations, they are not ideally suited to detect wind shear phenomena. Wind shear resulting from a microburst is very transitory; the chance of a balloon being released at the right time is obviously small. Where the balloon observation technique has obvious merit is in the identification of stable wind shears such as lee waves or wind shear resulting from the flow of air over obstacles. These latter wind shear phenomena are not the primary focus of this report as they do not constitute a major hazard to aviation.

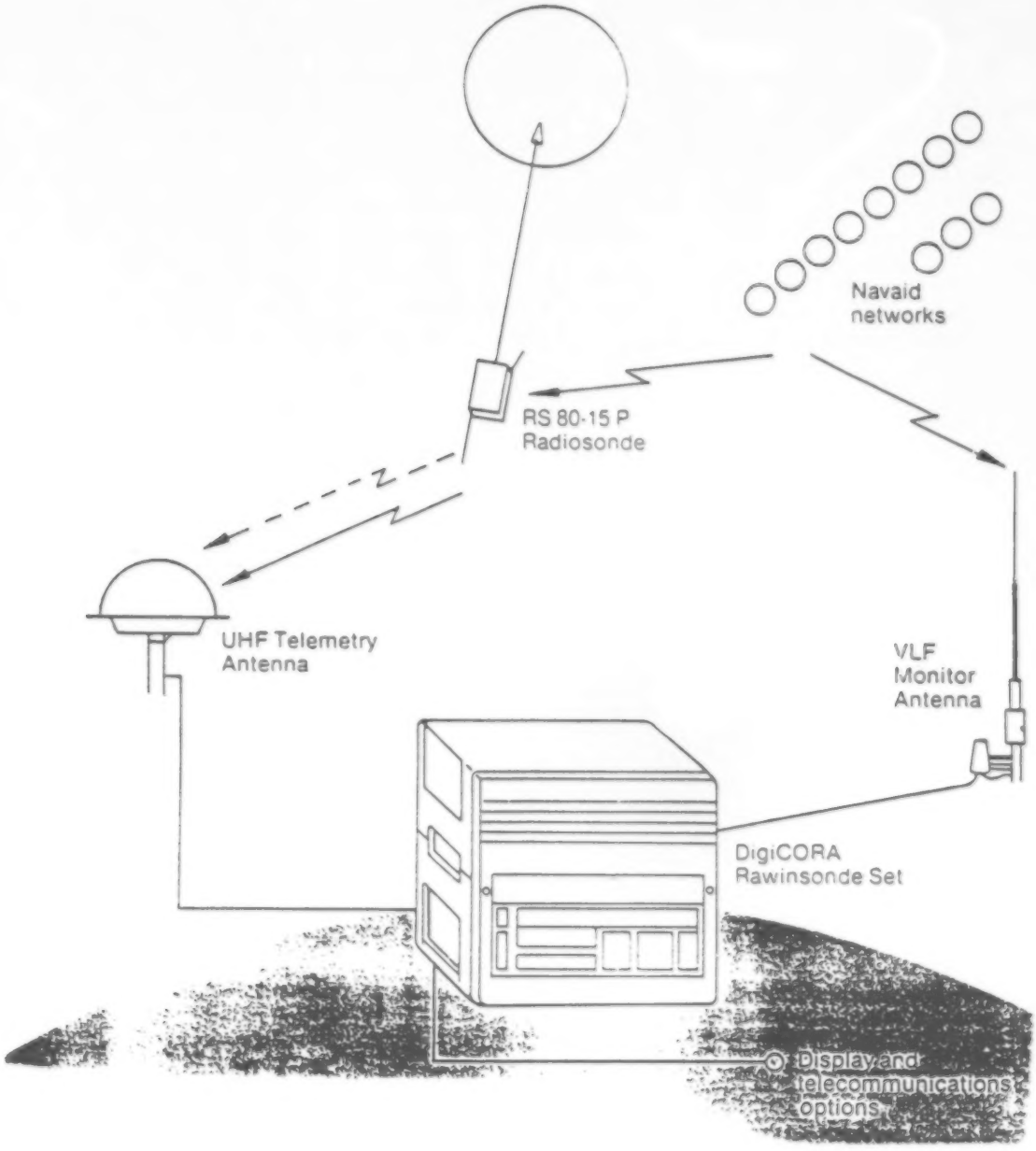

Figure 3-26 Rawinsonde operation principle
(from Vaisala Inc. marketing information)

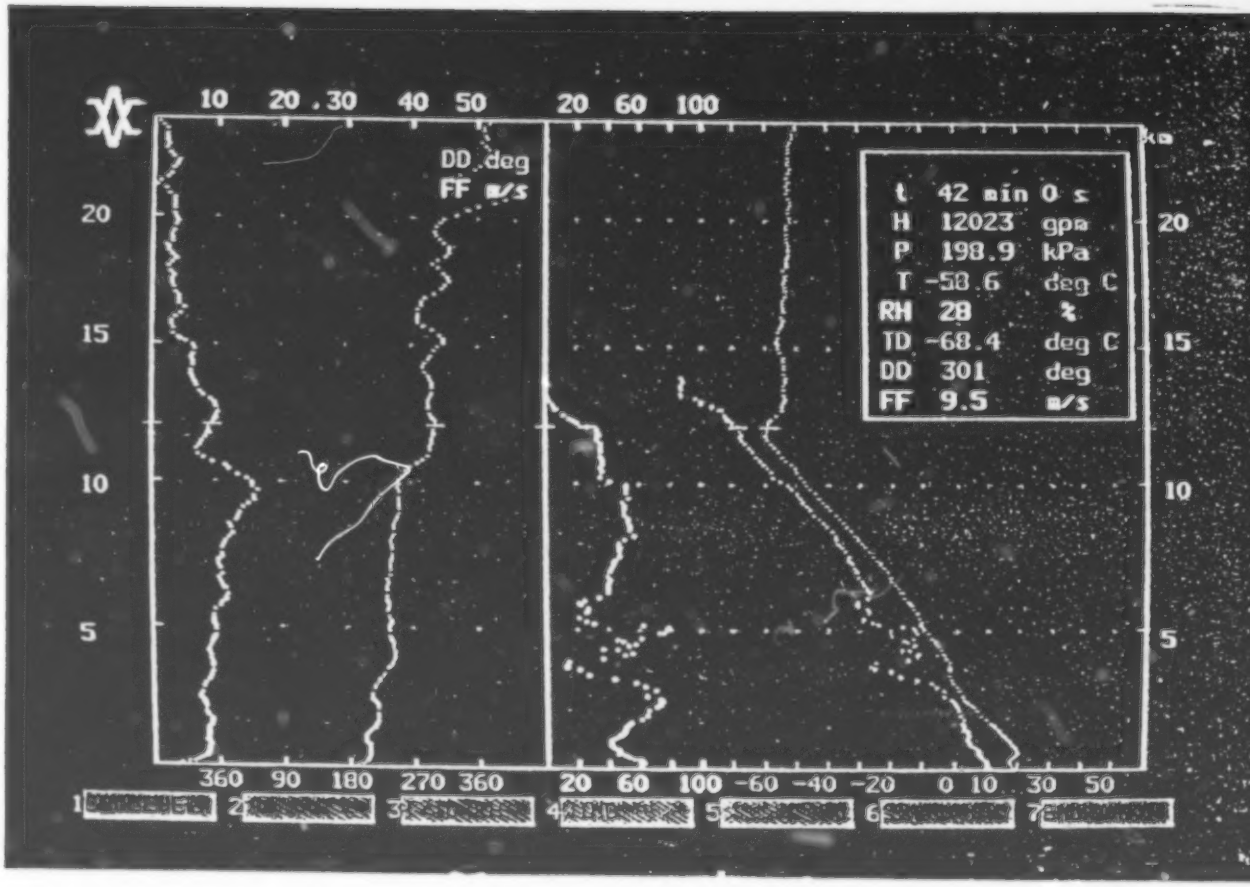

Figure 3-27 Meteorological presentation from rawinsonde data (from Vaisala Inc. marketing information)

3.4.7 Acoustic Radar (SODAR - SOund Detection And Ranging)

Sodars utilize acoustic sounding to measure wind speed and direction as well as vertical velocity. The technique is essentially similar to the Doppler radar except that the detection principle is based on soundwaves as opposed to electromagnetic waves. The return signal echoes off the differences in temperature, pressure, humidity and turbulence normally present in the atmosphere. Sodars usually operate in the 1000 to 5000 Hz frequency range and have measuring heights of between 600 to 900 m with a resolution of 15 to 30 m. Several systems have been commissioned worldwide to the point where there are some 100 facilities operational including those at Zurich, Frankfurt, Copenhagen, Stockholm and Seoul.

The standard Sodar configuration consists of three antennas; one pointing directly vertical with the other two obliquely positioned in the horizontal plane squinting 30 degrees off the zenith (Figure 3-28). An alternate configuration is presented in Figure 3-29. This ensures wind profiling in the three vector coordinates. The size of the antenna is frequency dependent, with a typical Sodar transmitting at a 2000 Hz frequency having an antenna dish of approximately 1.5 m in diameter. Each antenna is surrounded with a large funnel to shield the antenna from neighboring ground noise.(32,33) The antenna dishes and funnel structures can be heated to prevent the accumulation of ice during adverse weather conditions. The data is collected from the three antenna sensors and processed to resolve the information into an overall wind vector at each height resolution cell.

One of the main problems with the Sodar technology has been the long data integration times of ten minutes which now appears to have been decreased to three minutes with a running average updated every minute. A typical wind profile is illustrated in Figure 3-30.

The Sodar technology has advanced considerably in the past years. Sodar can now provide reliable measurements during a variety of meteorological situations. It has been shown that accurate measurements of up to a height of 180 m can be determined in rainfall rates of 50 mm/hr or winds of 30 m/s at a range of 10 m. These measurements are accurate to within 0.5 m/s in speed and three degrees in direction.(34)

Several advantages exist when using the Sodar technology. Because of the low speed of the acoustic pulse transmission, it is possible to process the information in real time with specially generated software packages that run on basic PC machines. The data Doppler shift is calculated with software Fourier transform techniques facilitating system modifications that are not available with custom hardware designs. Initial investment costs would be approximately $200,000 to $500,000 per system with maintenance costs at a minimum. The antennas are reasonably small and do not consume much space and, if desired, can be portable (positioned on the trailer of a flatbed truck) (Figure 3-31).

Figure 3-28 Doppler Sodar configuration
(from Fage and Huguet, 1985)

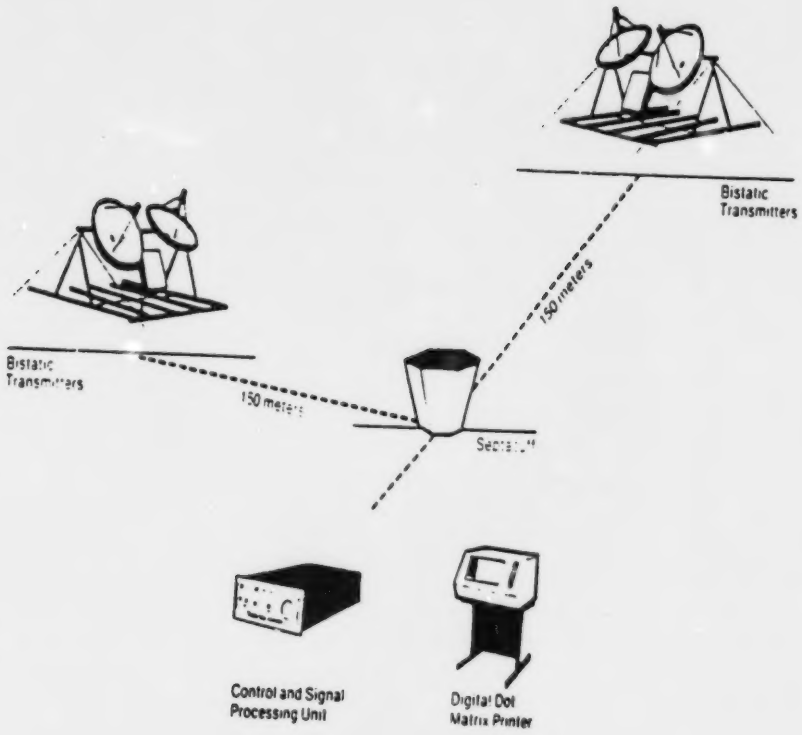

Figure 3-29 Alternate Sodar configuration
(from Griffith et al.)

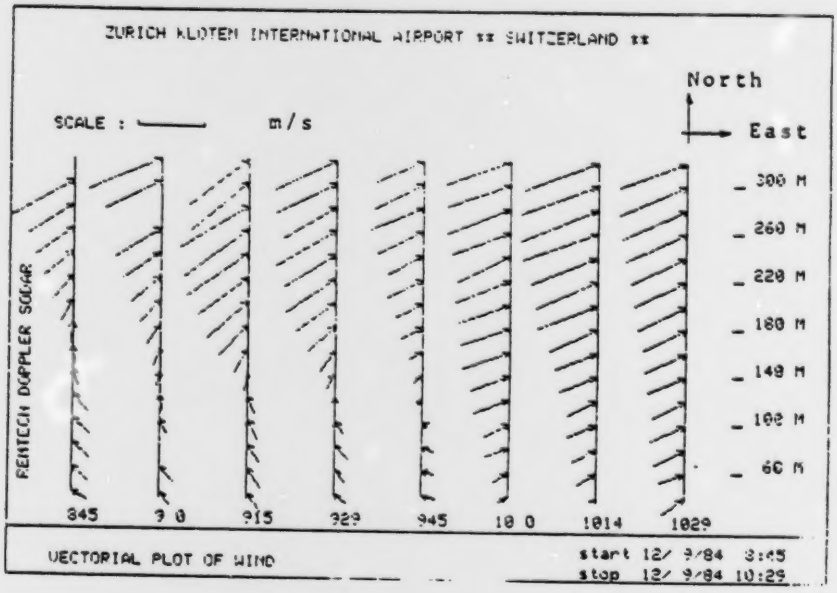

Figure 3-30 Sodar data presentation (from Fage and Huguet, 1985)

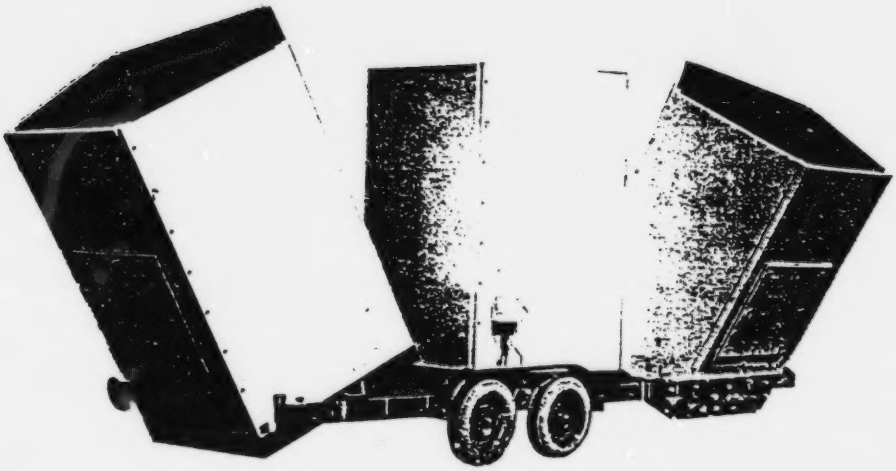

Figure 3-31 AeroVironment Inc. Sodar
(from AeroVironment Inc. marketing information)

Several companies now manufacture Sodar systems. Two prominent ones in the U.S. are Radian, who have an operational system located at the Austin, Texas airport, and AeroVironment who have just installed a system at Kampoo Airport in Seoul, Korea. A major offshore supplier is Societe Remtech of France. A limitation of conventional Sodar systems is that they can only monitor wind movement directly above the antenna position. To overcome this limitation Remtech has undertaken the development of a system that measures the wind speed and direction along the glide path.(35) These systems have been identified as the "mega" Sodars and have the configuration as depicted in Figure 3-32. The antenna is placed at the end of the runway with its beam directed up the three degree glide path. The antenna is not the standard Sodar configuration, as there is only a single antenna array consisting of smaller cellular components. This enables the beam pattern to be electronically steered which results in a three dimensional coverage capability. The system can be configured to transmit at a frequency of 1600 Hz with a 6 m antenna or 800 Hz with a 12 m antenna. An improved data update rate can be achieved by coding the transmitted acoustic pulse. The transmitted acoustic pulse can be coded with up to six different combinations resulting in six independent measurements. The Megasodar is designed to cover a range of approximately 3,000 m, with accurate measurements up to 150 m. It is expected to have an accuracy of about 0.1 m/s for radial winds measured along the glide path. This system appears to be limited to the detection of wind shears that occur within the 3 km range of the sensor and are inadequate for longer range coverage.

A major difficulty with the Sodar is its comparative sensitivity to environmental noise, including raindrops and presumably aircraft, in comparison with the weakly scattered signal. A rapidly scanning Sodar appears to be out of the question due to the noise generated by the scanner and to the severe signal/noise sampling problem. It is also unlikely that a Sodar could be pointed along the three degree aircraft glidepath because of additional noise interference due to wind and ground clutter. The problem of ground clutter interference is intensified since the antenna side lobes would be intersecting the ground. It appears that the most useful application of Sodar is for the detection of low level stable jets and obstacle flows rather than the transitory microburst phenomena of major concern here.

3.4.8 Satellite Instrumentation

NOAA plans and manages the Geosynchronous Operational Environmental Satellite (GOES) system. GOES satellites provide meteorological data from two instruments the Imager and the Sounder. On GOES-Next, the new generation of GOES satellites, the Imager will provide one visible and four IR channels for imaging of clouds, the earth's surface and water vapor fields. The Imager visible channel will be capable of approximately one km spatial resolution. The Sounder will provide 19 sounding channels for sounding to determine atmospheric thermal and vapor structure. The Sounder spatial resolution will be, at best, 8 km.

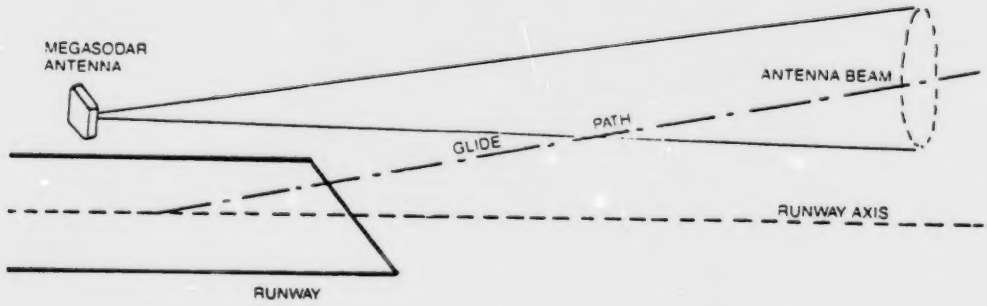

Figure 3-32 Megasodar glidepath system
(from Donzier and Fage, 1986)

As stated above the sounder can measure the atmosphere's temperature and humidity values.(36) Laser technology is used for both measurements. To monitor humidity levels two lasers, tuned to different frequencies, are utilized. One is tuned to a frequency that is absorbed by water molecules, the other slightly off this frequency. The difference in reflected brightness (intensity) of the two beams indicates the amount of water vapor in the air. A similar system is used to measure the air temperature. In this situation one laser is tuned to a frequency that is suitably absorbed by oxygen. Since the temperature can be directly related to oxygen density, the temperature of the air can be extracted from the difference in the brightness of the two reflected beams.

The data provided from the GOES system are quite suitable for meteorological forecasting but they do not appear to be applicable for the detection of the short-lived microburst. The reason for this is that even the most frequent satellite imagery produced by the GOES satellite is only produced on a half hour basis. As a result, current satellite imagery is not useful in the routine identification of gust fronts but is useful for the delineation and tracking of thunderstorms.

3.4.9 Lidars (LIght Detection and Ranging)

The detection of wind shear by Doppler radar may prove difficult if the microburst air contains no precipitation-sized particles. An alternative, but related, technology is the use of Doppler Lidars. Since the early 1970's a series of coherent CW and pulsed Doppler Lidar systems have been developed. The most likely candidate for microburst wind shear detection is the pulsed system using a carbon dioxide laser with a wavelength of 10.6 μm and a peak power of 5 kw. The 5 to 8 μm wavelength is readily absorbed by water vapor and therefore should be avoided. NASA has extensively tested a carbon dioxide Lidar with a pulse length of 300 m and a beam width of 30 cm. The useful range of a Lidar can be calculated using the same equations that would be used for the range calculation for a radar with the exception that the particles that a Lidar responds to are the much smaller aerosol or dust particles. Calculations suggest, and experimental work confirms, a useful range of up to 20 km. The range is affected by both the concentration and size distribution of aerosol particles and by the amount of water vapour along the line of sight. Aerosol and dust particles having radii between 1 and 5 μm are the primary scatterers at the carbon dioxide wavelength. There is little doubt that even a dry microburst, which contains very little rain, will stir up a considerable amount of dust and other particles as it impacts with the ground.

Lidars have also been used experimentally to successfully detect the more difficult to observe wake vortices.(37)

Laser sources emit short, high intensity light pulses which when they hit aerosol particles (dust, pollen, pollutants, water droplets, etc.) generate a small amount of back scattered light. This back scattered

light, whose frequency has been modified by the Doppler velocity of the particle is picked up by the receiver telescope. The incident and reflected beams are mixed resulting in a frequency modulation of the Doppler velocity shift. A typical Lidar system is illustrated in Figure 3-33.

Various laser sources can be utilized, but the carbon dioxide laser appears to be the most prevalent in the application of wind motion measurement. These systems can operate either in the CW or pulsed modes. The optical radiation usually has a very narrow spectral width and thus has a high degree of coherence enabling quite accurate relative motion measurements.

As early as 1974, the FAA, in conjunction with NASA's Marshall Space Flight Center and the Raytheon Company, had experimented with Doppler Lidar systems at JFK International Airport.(38) Raytheon has remained active in the field and has developed a sophisticated pulse Doppler laser radar. CW Doppler lasers, commonly referred to as LDAs (Laser Doppler Anemometers) have been developed by several companies including Optech (39), Crouzet SA of France (40), the DFVLR Institute of Optoelectronics of Germany (41), and the Royal Signals and Radar Establishment of the United Kingdom. These systems vary in configuration and use ranging from airborne installations to mobile shelters with applications ranging from true air speed measurements to gas concentration measurements. Presently NOAA has installed, at Boulder Colorado, a carbon dioxide pulsed Doppler laser that has a range of between 12 to 20 km transmitting every five seconds.(42)

Such systems can be scanned in a manner similar to a radar so that the air along and immediately adjacent to the glide path can be examined almost continuously. In the event there is heavy rain, the Lidar beam will be totally obscured. There is, therefore, the possibility of a combined scattering Doppler radar and Lidar, the radar being appropriate for wet microbursts and the laser being appropriate for dry microbursts.

Lidar systems do have several disadvantages: their capability to operate is severely limited by rainy and cloudy conditions; the equipment is relatively sensitive and hard to maintain; their range resolution is not adequate; the laser tubes usually have a limited lifespan; and the systems can be costly, ranging from $300,000 to $500,000 U.S., usually requiring experienced personnel to interpret the data.

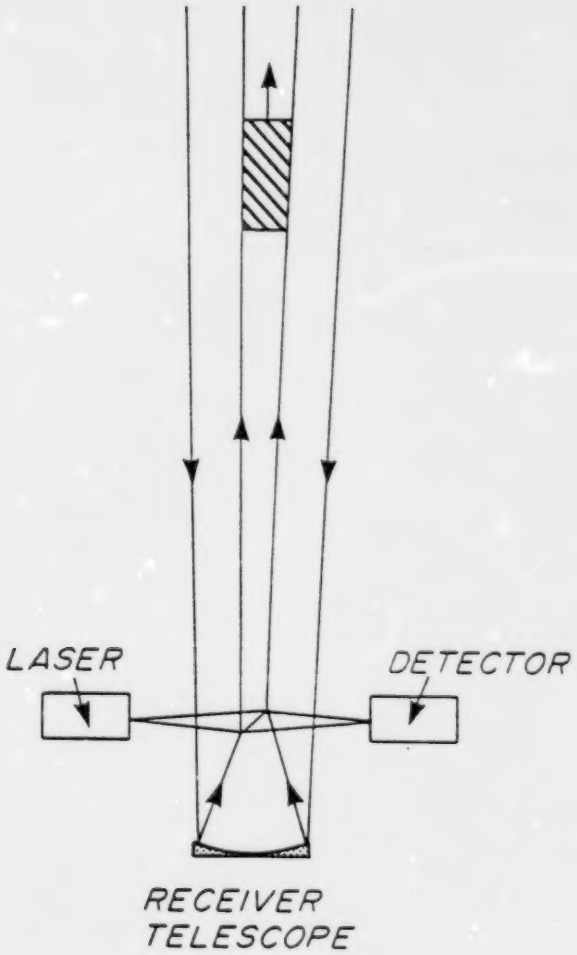

Figure 3-33 General configuration of a Lidar system (Carswell, 1983)

3.5 Derived Requirements

The following sections briefly explain the sensor requirements or specifications necessary to determine the detection of wind shear phenomena, assuming one uses the microburst parameters in Table 3-4 as detection criteria. These sections describe the technologies as they exist today. These technologies have been primarily developed for other applications but because of the serious nature of the wind shear phenomenon they have been adapted to assist in the detection of wind shear. The final section presents a generic specification for microburst detection and is not characteristic of any one technology.

3.5.1 LLWAS Specifications

The remote sensor arrays are comprised of the following elements.

Anemometers

Parameter	Wind speed
Type	Three cup or four blade propeller configuration that utilizes the magnetic Hall-Effect principle to convey speed data
Range	0 to 130 kts
Accuracy	+/- 1.5 kts
Resolution	1 kt

Weather Vane

Parameter	Wind direction
Type	Precision potentiometer with a voltage output proportional to wind direction
Threshold	Operational in light winds of 1.5 kts
Range 360 degrees	
Accuracy	+/- 5 degrees maximum
Resolution	1 degree

Sensor Interrogation

Rate	Once every 10 seconds by computer control
Method	Dedicated land line or UHF/VHF link
Power	Standard 120 V, 60 Hz service with 48 hour battery backup
Protection	Lightning rod with suitable grounding system

Optional Pressure Sensors

Parameter	Static Pressure
Range	-30 m to 3000 m 800 mmHg to 445 mmHg
Accuracy	+/- 0.2 millibars
Resolution	0.1 millibars

3.5.2 Wind Profiler Specifications

Either antenna configuration, the four-element Yagi or the coaxial-collinear phased array, can be utilized for the detection of wind shear.

Parameter	
Horizontal Wind	+/- 90 m/s
Vertical Wind	+/- 23 m/s
Accuracy	1 to 2 m/s
Vertical Resolution	120 to 250 m
Vertical Coverage	
Lowest Level	500 to 750 m
Highest Level	16 to 60 km
Frequency	50 MHz VHF 400 MHz UHF
Pulse Length (minimum)	0.5 to 1.6 microseconds
Pulse Repetition Rate	Dependent on height coverage desired
Transmitted Power	Dependent on height coverage desired

	UHF	VHF
Antenna Aperture		
Coaxial array	12x12 m	50x50 m
Yagi element		56x56 m
Update Rate	Every 6 minutes	

3.5.3 Sodar Specifications

These specifications are divided into two sections: normal Sodar contemporary configuration and Megasodar. This division exists because of the considerable differences between the two acoustic sounding technologies.

Contemporary Systems

Parameter	
Horizontal Wind	0 to 40 m/s
Vertical Wind	0 to 40 m/s
Accuracy	
Speed	0.5 m/s
Direction	3 degrees
Vertical Resolution	15 to 30 m
Vertical Coverage	
Clear Weather Conditions	
Lowest Height	30 m
Highest Height	600 to 900 m
50 mm/hr rainfall rate	
Highest Height	180 m
Frequency	1000 to 5000 Hz
Pulse Length	10 to 500 msec
Pulse Repetition Rate	1 to 60 sec
Transmitted Power	75 W to 1.3 kw
Antenna Aperture (on 3 axes)	1.5 m
Update Rate	
Data Averaging	1 to 60 minutes
Processing Technique	FFT Doppler processing

Megasodar System

Parameter	
Glide Path Wind Direction	0 to 40 m/s
Vertical Wind	0 to 40 m/s
Accuracy	
Glide Path	0.5 km/hr
Vertical and Transverse	10 km/hr
Range (Glide Path)	3 km
Frequency	800 Hz or 1600 Hz Optional frequency agility on 6 frequencies
Antenna (Single)	
Aperture	
@ 800 Hz	12 m
@ 1600 Hz	6 m
Electronically Steerable	

3.5.4 Doppler Radar Specifications

The following sections will describe the specifications of the NEXRAD, TDWR programs and the McGill University Weather Radars, as well as information relating to other pulse Doppler radars and FM-CW systems.

NEXRAD

Frequency	3 GHz S-band (10 cm)
Pulse Repetition Rate	300 to 1200 Hz
Pulse Width	1.1 to 1.7 microseconds and 4 microseconds
Antenna	
Size	9 m
Beamwidth	1 degree
Azimuth	360 degrees
Elevation	20 degrees
Rotation	3.2 rpm (19.2 degrees per second)
Enclosure	Radome
Power	0.7 Mw peak

Reflectivity Range	
Coverage	460 km
Resolution	1 km
Velocity Parameter	
Limits	
Coverage	to 230 km
Resolution	every 250 m
Accuracy	1 m/s
Scan Rate	5 to 6 minutes

TDWR

This pulse Doppler radar is a variant of the NEXRAD radar except for the following differences.

Frequency	6 GHz C-band (5 cm)
Range (Reflectivity and Velocity)	110 km
Antenna	
Scan	90 to 120 degrees, selectable sectors
Beamwidth	0.5 degrees

McGill Weather Radar (A)

Frequency	3 GHz S-band (10 cm)
Pulse Repetition Rate	300 Hz
Pulse Width	1 or 2 microseconds
Antenna	
Size	3 m
Beamwidth	2.5 degrees
Azimuth	360 degrees
Elevation	34 degrees
Rotation	6 rpm
Enclosure	Radome
Power	750 kw
Reflectivity Range	
Coverage	480 km or 240 km
Resolution	2 km or 1 km
Velocity Parameters	None at present

Scan Rate	5 minutes

McGill Weather Radar (B)

Frequency	9.6 GHz X-band
Pulse Repetition Rate	300 Hz
Pulse Width	1 microsecond
Antenna	
Size	2 m
Beamwidth	1 degree
Azimuth	360 degrees
Elevation	34 degrees
Rotation	6 rpm
Enclosure	None
Power	75 kw
Reflectivity Range	
Coverage	480 km or 240 km
Resolution	2 km or 1 km
Velocity Parameters	None at present
Scan Rate	5 minutes

Doppler Radar, General (Radian Corporation)

Frequency	2.7 to 2.9 GHz S-band C-band option
Power	375 kw
Antenna	
Size	4.5 m
Beamwidth	S-band 2 degrees C-band 1 degree
Pulse Repetition Rate	Programmable
Pulse Width	Programmable

FM-CW Radar

Frequency	2.9 GHz
Power	400 W

Range	
Coverage	2 km
Resolution	56 m - 36 discrete range cells
Velocity Parameter	33 velocity cells per range cell
Azimuth	
Coverage	360 degrees
Resolution	< 1 degree
Antenna	
Configuration	Bistatic, separate transmit and receive antennas obliquely mounted

AES Radar (King City)

Frequency	5625 MHz
Pulse Repetition Rate	250 to 1200 Hz
Pulse width	0.5 to 2 μsec
Antenna	
Size	6.1 m
Beamwidth	0.65 degree
Elevation	-0.5 to +90.5 degrees
Rotation	0.5 rpm for Doppler 6.0 rpm standard
Power	260 kw peak
Reflectivity Range	
Coverage	450 km
Resolution	1 km and 2 km
Velocity	
Coverage	196 km
Resolution	0.25 km

3.5.5 Rawinsonde Specifications

The following specifications pertain to the capabilities of the radiosonde monitoring system and the balloon tracking system.

Pressure	
Range	1060 mb to 3 mb
Accuracy	+/- 0.5 mb
Resolution	0.1 mb

Humidity	
Range	0 to 100% Relative Humidity (RH)
Accuracy	+/- 2% RH
Resolution	1% RH
Temperature	
Range	-90 degrees C to 60 degrees C
Accuracy	+/- 0.2 degrees C
Resolution	0.1 degrees C
Wind	
Speed	0 to 99 m/s
Direction	360 degrees
Wind Vector Accuracy	0.5 m/s

3.5.6 Airborne Sensor Specifications

The various systems described all have thresholds relating to wind shear detection that are equipment and aircraft specific. Because airborne sensors should be used in association with ground based equipment, it is not relevant at this time to fully detail the operations of these systems. One may wish to review the references supplied by the specific manufacturers for a greater understanding of these airborne sensors.

3.5.7 Lidar Specifications

The following are typical specifications of a pulse Doppler laser system developed by Raytheon Corporation.

Power	10 kw
Wavelength	10.6 micrometers
Pulse Width	1 to 10 microseconds nominal 4 microseconds
Repetition Rate	200 pps
Optics	
Aperture	5 cm
Range	12 to 20 km
Resolution	150 m
Detection	Coherent

3.5.8 Generic Specifications

The following describes a system specification, in accordance with Transport Canada's requirements, for the detection of wind shear phenomena. The specific range and azimuth coverage were selected according to the MLS pattern surveillance which is discussed further in Section 4.2. The range resolution parameter was selected to ensure adequate sampling of the wind speeds close to the earth's surface. Actual radar pulse width requirements are determined in Section 5.3.2. This specification will be used as the basis to assess the capabilities of the various technologies that appear to be suitable to perform the detection requirement. In the situation where more than one technology must be integrated to accomplish the wind shear detection task, these specifications will form the functional requirements that a custom system must satisfy.

Range	
Coverage	
Horizontal	15 km
Vertical	4 km
Resolution	50 m
Azimuth	
Coverage	+/- 40 degrees with respect to runway heading
Resolution	1 degree
Elevation	
Coverage	15 degrees
Resolution	1 degree
Weather Parameters	
Temperature	
Range	-40 to 50 degrees C
Resolution	0.2 degrees C
Pressure	
Range	106.7 to 59.3 kPa
Resolution	0.01 kPa
Humidity	
Range	0 to 100% RH
Resolution	1% RH
Wind Velocity	
Horizontal	40 m/s
Vertical	15 m/s
Resolution	2 m/s

Wind Direction	
Azimuth	360 degrees
Resolution	1 degree

4. TECHNOLOGY EVALUATION

4.1 Introduction

The technologies for the detection and analysis of the wind shear /microbursts described in Section 3.4 will be evaluated with respect to the user requirements and specifications. These specifications have been documented fully in Section 2 and are summarized below:

i) Financial Constraints

- $1,000,000 Canadian, per airport.

ii) Operational Requirements

- Area of coverage to include a 15 km radius from the airport centre to an altitude of 1 km.
- The location (i.e. range and azimuth bearing) of the wind shear /microburst must be determined.
- Real time detection capability to provide adequate warning to pilots and Air Traffic Controllers of the occurrence of the wind shear condition.
- System must provide positive or negative detection status.
- High probability of detection with a low false alarm rate.
- Data is easily accessible.

iii) Technical Constraints

- Operational frequencies compatible with existing or committed frequency allocations.

iv) Environmental Constraints

- Determined by the equipment classification whose environmental requirements are as specified in Tables 2-2, 2-3, and 2-4.

v) Physical Constraints

- Physical structure requirements as described in the document "Land Use in the Vicinity of Airports".

Specific weather parameter ranges and resolutions have been presented as probable criteria to monitor in order to facilitate the detection of the wind shear/microburst phenomena. These have been documented in Section 3.5.8 and are repeated as follows:

Temperature	
Range	-40 to +50 °C
Resolution	0.2 °C
Pressure	
Range	106.7 kPa to 59.3 kPa (800 mmHg to 445 mmHg)
Resolution	0.01 kPa
Humidity	
Range	0 to 100% RH
Resolution	1% RH
Wind Velocity	
Horizontal	40 m/s
Vertical	15 m/s
Resolution	2 m/s
Wind Direction	
Azimuth	360 degrees
Resolution	1 degree

These requirements and specifications are thoroughly reviewed in the evaluation of the various detection technologies. It is apparent that no single technology is capable of satisfying all of the requirements and that the solution to the microburst detection problem will be a combination of suitable systems.

4.2 General Discussions

The prime area of concern was initially considered to be that of the approach glide path region. As a result, the detection surveillance region was taken to be that of the new MLS signal coverage to accommodate all future approach patterns. This area is depicted in Figure 4-1 and the original coverage parameters of Section 3.5.8 were derived from this description. This would have enabled some form of detection system to be located near the ends of the runways to generate the appropriate detection coverage. It has been resolved, since this original determination, that the area coverage should consist of a cylindrical volume located at the airport centre with a radius of 15 km and elevation of 1 km. This was determined because of the possibility during take-off procedures of a wind shear/microburst condition occurring along the path of the runway, within the airport facilities district. This precludes the positioning of any sensor near the end of the runways. To ensure adequate coverage on the desired area, the positioning of the sensors could have various configurations. Figures 4-2 and 4-3 illustrate two

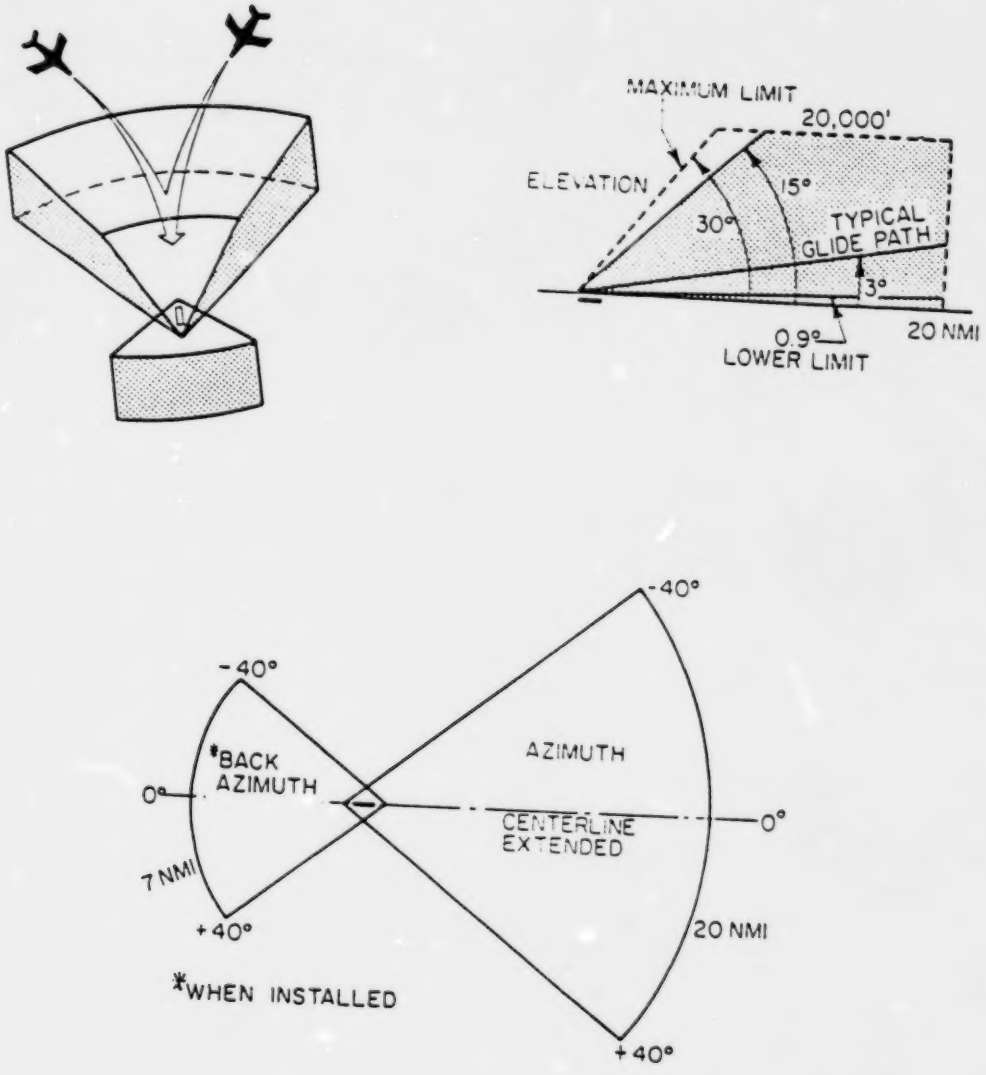

Figure 4-1 MLS signal coverage
(from FAA "Getting Ready for MLS", October 1982)

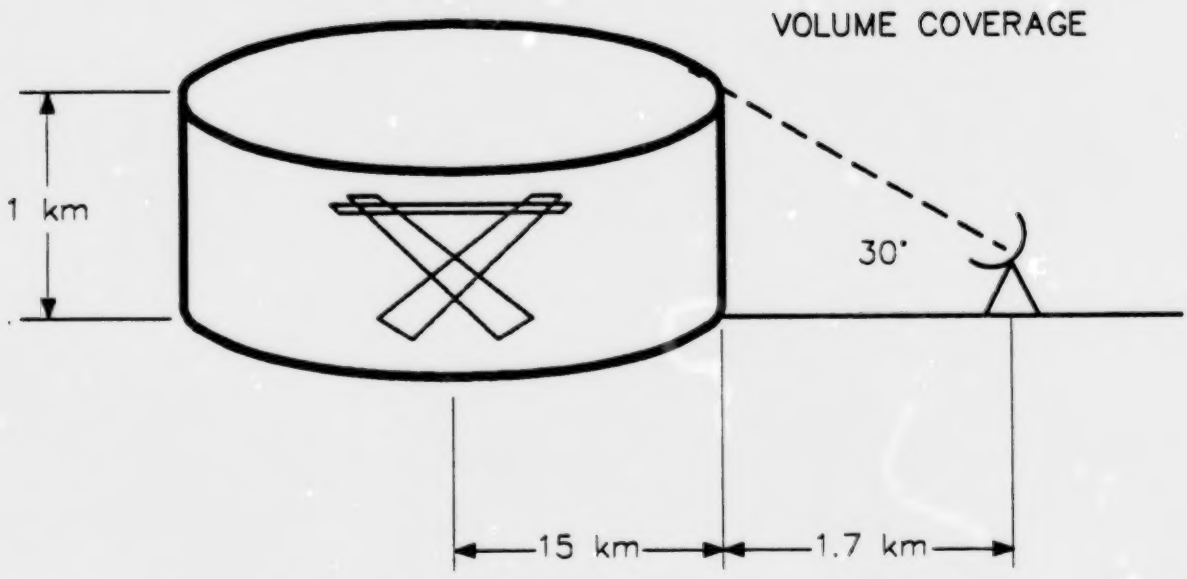

Figure 4-2 External sensor coverage

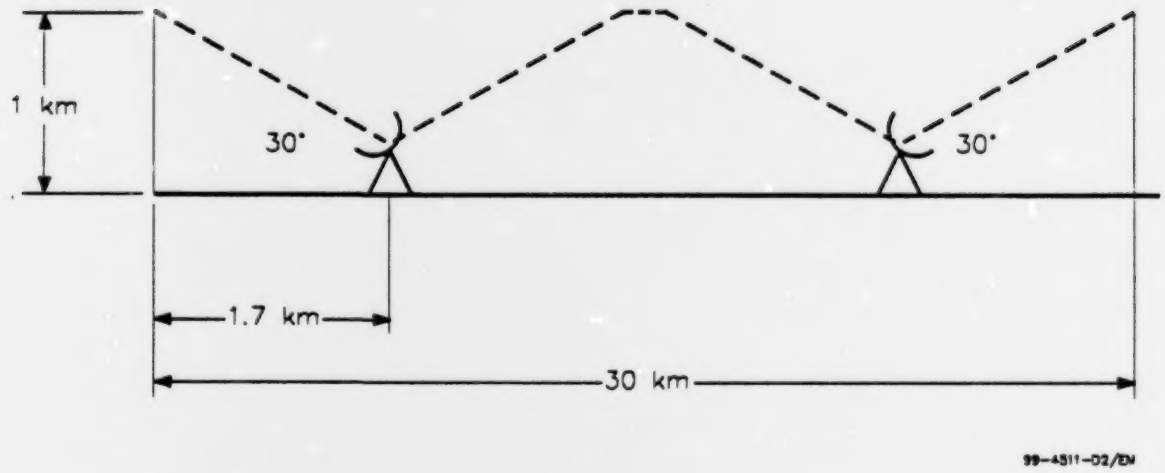

Figure 4-3 Internal sensor coverage

possibilities, assuming the sensor antenna has an elevation pattern back angle of 30 degrees. In Figure 4-2 the sensor is located external to the desirable region requiring a range coverage capability of approximately 32 km. Figure 4-3 illustrates a configuration where two sensors are located within the coverage region, but sufficiently far apart to ensure that each other's elevation pattern overlays the cone of silence above each sensor. They are also positioned at a sufficient distance from the region boundary to ensure elevation coverage to at least 1 km. This results in the sensors requiring a range coverage of approximately 13 km, half as much as the single sensor requirement. Assuming a runway length of 3200 m and a 2.5 degree glide path (Figure 4-4), at the 15 km range point the aircraft would have an altitude of 600 m (1950 ft). This 15 km range should be reviewed in terms of its adequacy in order to determine if sufficient altitude is available for an aircraft to recover if it encounters a wind shear/microburst condition.

4.3 Review and Analysis

The nine potential detection technologies referenced in Section 3.4 will be reviewed and analyzed with respect to the user requirements and specifications.

The technologies have been reviewed by means of a table format. Each table illustrates where the technologies are compliant with the user requirements by means of a check mark (✓). Where the technologies are not compliant, or descriptive data is relevant, factual information is recorded. An asterisk (*) beside the entry indicates non-compliance with the requirements. Some of the technologies such as the airborne sensors, rawinsondes and satellite instrumentation were deemed to be inappropriate for this detection purpose. Compliance tables have not been provided for these technologies.

4.3.1 Visual Observation

Certain characteristics of microbursts are visible to the naked eye, for example virga, dust clouds, wet gust fronts, etc. Pilots are presently being educated to recognize microbursts using these indicators. However, as a general method for the detection of wind shear conditions, visual observation as a sole means technique can be eliminated due to the following constraints:

i) Requires dedicated personnel knowledgeable in meteorological analysis.

ii) Observations are limited to daylight hours.

iii) The microburst phenomena is quite diverse in its appearance and often there is no visual indication of its presence.

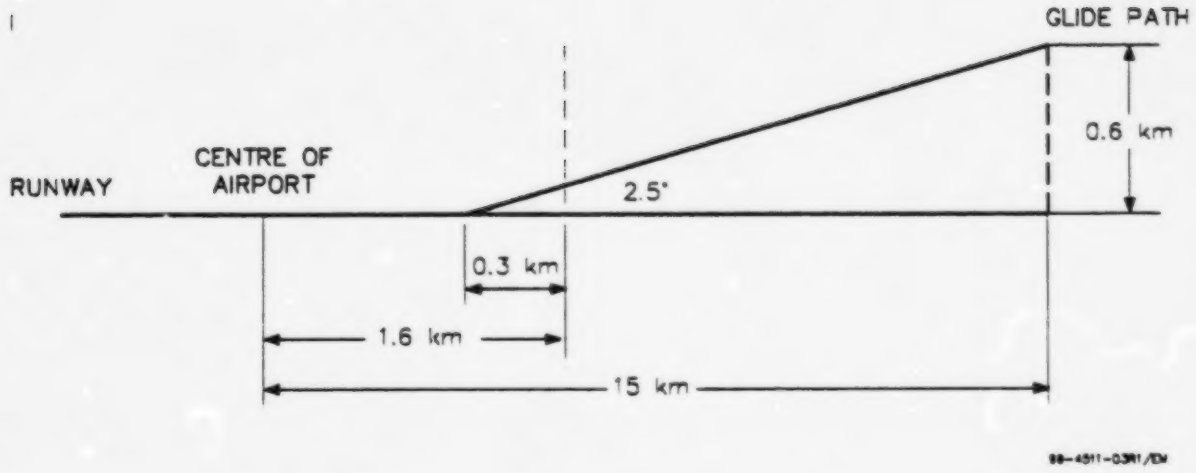

Figure 4-4 Glidepath elevation at 15 km range

4.3.2 Anemometers, Weather Vanes and Microbarographs

In reviewing the Low Level Wind Shear Alert Systems (LLWAS) two primary systems were identified in Section 3.4.2; the LOLA (Low Level Wind Shear Alert System) and AWOS (Automated Weather Observing System). Each system's capabilities are summarized with respect to the relevant user requirements and specifications in Table 4-1. The LOLA system is the only one that has the capability to perform low level wind shear detection. Its algorithm calculates the vector difference between any remote wind velocity sensor and a centrally located sensor. If this value exceeds an operator-selected sensitivity parameter an alarm is initiated. This algorithm is presently being upgraded to include the expansion from five remote stations to ten. The new algorithm will base the wind shear alarm on airport area average wind velocity and not only the wind velocity measured at the central location. The system software is being converted to the more modular "C" language from Basic to facilitate portability and future changes. Future development plans for the AWOS system include a proposed wind shear detection algorithm. In general, one should view these LLWAS systems as an incomplete solution to the wind shear detection problem. As indicated in Section 3.4.2, several problems exist, of which the two most significant are:

i) Lack of overall area coverage. A typical microburst of 1 to 3 km could go undetected, especially in the glidepath approach and departure regions.

ii) Failure of the system to measure winds aloft. Winds aloft are usually considerably stronger than surface winds during a microburst and occur before the microburst can be detected at the surface.

Nevertheless, the information that can be obtained from an LLWAS system can be used in association with a more capable detection system. The environmental measurements would augment any further data collected and facilitate the overall detection process.

4.3.3 Wind Profilers

The three wind profiler systems that were reviewed include the systems developed by NOAA and the Unisys Corporation, the Vaisala Corporation system and the Radian Corporation. Although all have evolved from the same basic technology and operate using same principles, the Radian Corporation's Capsonde System utilizes more sophisticated transmission techniques and signal processing methods. Table 4-2 summarizes the different capabilities of these three systems with respect to the user requirements and specifications. All three systems have two major problems; their coverage area is limited to that directly above the array location, and the minimum range is too large to obtain measurements near the surface. It is conceivable, especially if one utilized the portable Capsonde model, to cover the desired airport region. But, from a

Table 4-1 LLWAS Capabilities Review

	LOLA (Basic)	LOLA (Optional)	AWOS-1
Wind Speed Horizontal	50 m/s maximum	50 m/s maximum	76 m/s maximum
Wind Direction	✓	✓	✓
Temperature	-	✓	✓
Pressure	-	✓	✓
Wind Shear Detection Algorithm	✓	✓	-
Data Transmission			
Landline	✓	✓	✓
VHF Transceiver	150 to 175 MHz 8 Watts	150 to 175 MHz 8 Watts	118 to 136 MHz 10 Watts
Real Time Operation	10 sec	10 sec	60 sec
Operational Validity Checks	every 10 min	every 10 min	-
Coverage	positional	positional	positional
Environmental			
Class 2			
Temperature	-50°C	-50°C	-51°C
Icing	susceptible - external heating available	susceptible - external heating available	will continue to operate
Class 3			
Temperature	-30°C to +60°C	-30°C to +60°C	-51°C to +55°C
Relative Humidity	to 95%	to 95%	✓
Dust	remains operable	remains operable	no information
Class 5			
Temperature	client's	client's	no information
Non-operating	building environment	building environment	to operate
Cost (excluding land acquisition costs)	$225,000	$310,000	$37,700 per station

* denotes non-compliance

Table 4-2 Wind Profiler Capabilities Review

	Unisys	Vaisala	Capsonde
Wind Speed			
Horizontal (Max)	90 m/s	90 m/s	60 m/s
Vertical (Max)	23 m/s	23 m/s	variable
Wind Direction	3D mapping above array 18° squint	3D mapping above array 15° squint	3D mapping above array 30° continuous
Vertical Height			
Maximum	✓	✓	✓
Minimum	500 m*	500 m*	750 m*
Data Transmission			
Landline	✓	✓	✓
Other	GOES Satellite 401 MHz	GOES Satellite 401 MHz	HF link
Real Time Operation	6 min*	6 min*	10 min*
Operational Frequency	✓	✓	45 to 58 MHz
Operational Validity Checks	BITE only	BITE only	BITE only
Coverage	limited to above the array*	limited to above the array*	30° cone with respect to vertical*
Environmental			
Class 2 (Temperature)	-40°C	-40°C	-40°C
Class 5	✓	✓	✓
Cost	$500,000	$800,000	$500,000

* denotes non-compliance

financial perspective, this option would be too expensive. It is not recommended that wind profilers be utilized for wind shear/microburst detection at airports.

4.3.4 Airborne Sensors

Considerable development in airborne detection, alert and guidance recovery systems for wind shear has occurred. As indicated in Section 3.4.4 these systems are classified as "reactive", giving the pilot an additional few seconds to respond to the wind shear situation with corrective escape procedures. Airborne sensors will become more effective with the use of airborne forward-looking Doppler radar and Lidar systems that are able to scan up to 500 to 800 m ahead of the aircraft resulting in a much earlier indication of wind shear conditions. This is valuable information for the pilot but it is not readily available to the ground controller except possibly through radio communications or later through the PIREP process. Neither provides sufficient advance warning to enable the ground controller to adequately notify aircraft in the neighbouring airspace that a wind shear condition exists.

It might be beneficial if the companies that are developing these systems (Safe Flight, Sundstrand, Sperry Honeywell, and Flight Dynamics) were to incorporate some method to automatically communicate, to the ground controller, information about the detected wind shear. Airborne sensor systems are not recommended as a primary solution to the wind shear detection problem because they currently only supply information to the pilot, suitable on-board instrumentation is not available, and they provide insufficient warning time prior to the onset of wind shear. Nevertheless, this information is valuable. If the information could be distributed it would offer additional data that could be used as an operational confidence check for ground based detection systems. This could be quite advantageous in the evaluation of the performance of predictive wind shear algorithms.

4.3.5 Doppler Radar

Doppler radar appears to be the technology best suited to solving the microburst detection problem. It can measure relative wind velocity by means of the Doppler shift process and also can detect refractive index changes due to temperature and humidity variations. Various parameters will have to be investigated during the conceptual design phase to optimally satisfy the user requirements. These will include the following:

i) Frequency Allocation
ii) Power Requirements
iii) PRF Selection
iv) Pulse Width
v) Scan Rate and Pattern

In review of the major Doppler radar weather systems (NEXRAD, TDWR) it is obvious that these systems are not ideally suited for the microburst detection requirement. The antenna structures are too large, limiting the scan rate capability which will effect the necessity of real time operation. The capabilities of these systems are in most aspects excessive to the user requirements and specifications. Table 4-3 summarizes these capabilities with respect to the general technical requirements. It should be noted that considerable information can be obtained from the radar echo intensity or reflectivity relating to convective storm activities. This information could be used in conjunction with the Doppler velocity data to enhance the microburst detection capability. A radar with both Doppler and reflectivity measurement capabilities may be an appropriate solution.

4.3.6 Rawinsondes

The use of balloons with a tethered radiosonde sensor for the detection of wind shear is not a practical solution. If the immediate atmospheric conditions must be known, as in the case of a space shuttle launch, the release and tracking of an equipped balloon is a suitable approach. Also, information available from balloon soundings could indicate atmospheric conditions that are likely to support microburst development. Such data could be used to place a microburst detection system "on alert". However, where aircraft are landing and departing within minutes of each other, it is impractical to constantly release balloons. Also, these balloons would present a hazard in the critical approach and departure air routes even though the balloons are not of considerable size. Since the microburst phenomena is of relatively short duration (3 minutes on average) and small in size (2 to 4 km) the chances of releasing a balloon at the correct time and in the appropriate area is highly unlikely.

4.3.7 Sodars

The two major problems with Sodars have been their susceptibility to ambient noise, either ground or airplane generated, and their severe signal attenuation in heavy rain or strong winds. Enhanced antenna design, frequency transmission coding, and automatic noise thresholding have helped to minimize the effects of acoustic noise resulting in a reliable, more effective technology to assist in microburst detection. The three major companies involved in Sodar development are Remtech, Radian and Aerovironment. The user requirements pertaining to these systems are summarized in Table 4-4. The Sodars have no scanning capability; they simply map the atmospheric turbulence above the antenna location. This will not provide the desired area of coverage. As depicted in Figure 4-5, a microburst phenomena could easily progress across the airport vicinity and go undetected by the Sodars. Note that this figure also illustrates an integrated LLWAS system associated with the four Sodar systems located at the end of each runway. Even though

Table 4-3 Doppler Radar Capabilities Review

	NEXRAD	TDWR
Range		
Minimum	250 m	400 m
Maximum	230 km	110 km
Velocity		
Maximum Unambiguous Radial Velocity	± 40 m/s	± 40 m/s
Mean Radial Velocity Resolution		0.3 m/s
Coverage		
Azimuth	360°	360° or 90° to 120° sectors
Elevation	20°	-1° to 60°
Cost	$3.5 Million*	$4.5 Million*
Real Time Operation	5 to 6 minutes*	dependant on scan pattern*

* denotes non-compliance

Table 4-4 Sodar Capabilities Review

	Remtech	Radian	Aerovironment
Wind Speed			
Horizontal (Max)	30 m/s*	✓	25 m/s*
Vertical (Max)	✓	✓	3.7 m/s*
Wind Direction	3D mapping above antenna 18° angle	3D mapping above bistatic quadrant	3D mapping above antenna 30° angle
Vertical Height			
Minimum	30 m	10 m	45 m
Maximum	1500 m	2000 m	1500 m
Real Time Operation	1 min	1 min	2 min
Operational Frequency	✓	✓	✓
Operational Validity Checks	BITE only	BITE only	BITE only
Coverage	18° cone with respect to vertical*	150 m bistatic antenna quadrant*	30° cone with respect to vertical*
Environmental			
Class 2 (Temperature)	-30°C to 50°C	can be configured in any environment (heaters optional)	-30°C to 50°C
Class 5 (Temperature)	15°C to 25°C	0°C to 40°C	15°C to 30°C
Cost	$225,000	$100,000	$80,000 antenna $25,000 Wind Shear Warning S/W

* denotes non-compliance

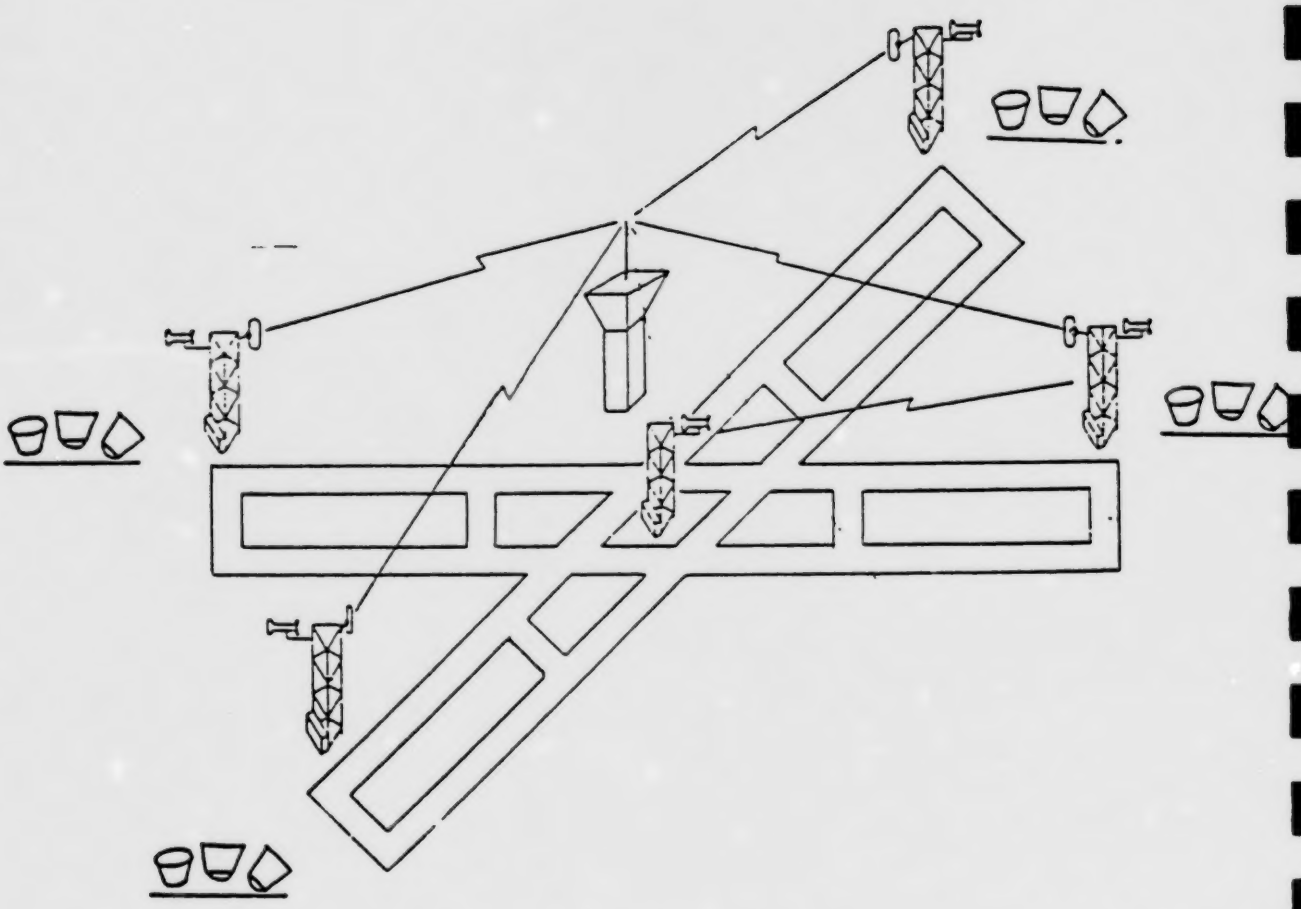

Figure 4-5 Integrated Sodar and LLWAS detection systems
(from REMTECH marketing literature)

the Sodar technology has proven to be suitable for the detection of the microburst situation, several systems would have to be used to provide the required coverage. This would be too expensive.

4.3.8 Satellite Instrumentation

The instrumentation on the GOES system is limited in its use for assisting in the detection of microburst conditions. Its maximum update of half an hour is insufficient for the short-lived microburst phenomena. Also, the laser technology, used to determine the atmosphere's temperature and humidity, suffers from extreme atmospheric absorption. During periods of heavy cloud cover detection penetration to the earth's surface would be impossible. For these important reasons the present capabilities of satellite instrumentation has been disregarded as a possible solution to the microburst detection problem.

4.3.9 Lidars

The laser detection and ranging systems have developed significantly over the past years, but even with this advancement most of the systems can still be classified as research tools in the developmental prototype stages. The systems reviewed from Raytheon and Lincoln Labs fall into this category, while those available from Optech are custom built to meet specific user requirements. Table 4-5 summarizes the capabilities of these three Lidar systems. The major advantage of using a Lidar system is its short wavelength and its system coherency. As a result it is very sensitive to aerosol particles and changes in refractive index due to temperature and humidity variations. Lidars then become ideal for the detection of dry microbursts. However, they also have several disadvantages. Due to the short wavelength, the Lidar transmission is very susceptible to atmospheric absorption. This attenuation is due primarily to the absorption by water. As illustrated in Table 5-6, the shorter the wavelength, the more extreme the attenuation. Note the different columns of attenuation relating to the various laser sources. It is readily apparent why the carbon dioxide laser is the best choice for use in a detection system. Other problems that exist with Lidar systems are: they are relatively expensive, hard to maintain, the life expectancy of the laser tubes is limited and the processed output is usually not presented in a "user friendly" display requiring experienced personnel to interpret the data.

As mentioned previously, Lidar systems appear to be quite suitable for dry microburst detection. In the Canadian environment, however, it is assumed that wet microbursts, associated with convective thunderstorm activities, will be the predominant category. Given this assumption, it is hard to justify the inclusion of the Lidar technique within an integrated microburst detection and alert system.

Table 4-5 Lidar Capabilities Review

	Raytheon	Lincoln Labs	Optech
Wind Speed Horizontal (Max) Vertical (Max)	✓ ✓	✓ ✓	Requires Doppler Processing*
Wind Direction	360°	360°	Requires Scanning Assembly
Range Minimum Maximum	300 m* 12 km*	10 m 5 km*	0.5 m 1 km*
Real Time Operation	seconds PRF dependant	seconds PRF dependant	seconds PRF dependant
Operational Frequency	✓	✓	✓
Operational Validity Checks	targets of opportunity	BITE and targets of opportunity	BITE only
Coverage	360° azimuth elevation selectable	360° azimuth elevation selectable	equipment specific
Environmental	All require cooling to stabilize transmitters and detectors.*		
Cost	Costs are specific to client's specifications.*		

* denotes non-compliance

Table 4-6 Atmospheric Propagation
(from Electro/81, Professional Program Session Record, April 1981)

	Ruby	YAG	CO_2	mm	S
dB/km	λ 0.7 μm	λ 1.06 μm	λ 10.6 μm	λ 0.3 cm	λ 1 cm
0.2	Extremely Clear	Extremely Clear			
0.6	Standard Clear (V=25 km)	Standard Clear			2.5 mm/h
0.8		Clear			Fog (V=30 m)
1.0	Clear (V=15 km)			Advection Fog (V=120 m)	
2.0	Light Haze (V=5 km)		Rain 2.5 mm/h	Rain 2.5 mm/h	
3.0	Medium Haze (V=5 km)		Radiation Fog (V=0.5 km) / Rain 4 mm/h	Rain 4 mm/h	12.5 mm/h
5.0	Haze (V=3 km)		Snow 0.2 mm/h		25 mm/h

V = Visibility

4.4 Recommendation for an Appropriate Technology

To satisfy the user requirements and specifications it is recommended that a combination LLWAS/Doppler Radar system be developed to solve the microburst detection problem. The LLWAS will monitor all the required meteorological parameters, especially the important atmospheric pressure value. The Doppler radar will consist of a lightweight, variable scan rate and pattern coverage, inexpensive system satisfying the technical user requirements. The Doppler radar system would perform alternate azimuth elevation scans at a high rotation rate to enable detection of the descended, short-lived microburst. The radial velocity due to the movement of water droplets, dust or bug particles or aerosols will be determined for each range resolution cell. This radial component will then be resolved into both the vertical and horizontal vectors. The wind shear value between adjacent range cells or across several neighbouring range cells can then be calculated. If this value exceeds a set threshold, a warning is generated. A block diagram of the proposed wind shear detection system is illustrated in Figure 6-1.

5. CONCEPTUAL DESIGN FOR A WIND SHEAR DETECTION SYSTEM

5.1 System Overview

The recommended system consists of an integrated LLWAS and Doppler radar. The LLWAS will be utilized to acquire the meteorological data (wind speed and direction, temperature, pressure and relative humidity) near the surface of the airport while the Doppler radar will be performing a volume scan above the airport surface to determine wind speed and direction.

5.2 LLWAS Subsystem Description

The LLWAS Subsystem will consist of up to ten remote stations and one centrally located station. The ten remote stations will be located around the perimeter of the airport and within the airport boundaries. Station placement will be dependent upon local topography. Each station will consist of a 10 to 30 metre weather tower securely attached to a concrete base. Each tower will be equipped with the following sensors or protection devices:

- wind speed sensor
- wind direction monitor
- temperature sensors
- pressure transducer
- relative humidity sensor
- obstruction lights
- lightning rod
- VHF antenna

5.2.1 Sensors and Associated Protection Devices

i) Wind Velocity Monitor. These transducers are responsible for determining wind speed and direction. The wind speed is sensed by means of a three-cup anemometer or a four-blade propeller. Either system functions by means of a Hall-Effect device (magnetic pick-up induced in a stationary coil by rotating magnets) that produces an AC sine wave whose frequency is directly proportional to the wind speed. The wind direction is determined with a weather vane attached to a precision potentiometer that generates an analog voltage proportional to the wind azimuth angle. The following specifications apply to the wind velocity monitor:

Wind Speed	0 - 50 m/s with an accuracy of ± 0.07 m/s
Survivability	0 - 90 m/s
Threshold	1 m/s

Wind Direction	360° mechanical 355° electrical with 5° deadband
Accuracy	± 2°
Threshold	1 m/s

Each sensor is equipped with a de-icing heater to prevent freeze-up. The heater is controlled by a built-in thermostat where the operational temperature value can be selected.

ii) Temperature, Pressure and Relative Humidity Transducers. These sensors will be housed in a weatherproof environmental enclosure located at the base of the tower above the snow line. Temperature is measured using a precision thermister. Atmospheric pressure is measured by a digital barometer and dew point temperature is measured by means of a lithium chloride cell. The measurement range of the barometer ensures adequate coverage at the major airports throughout Canada. These major Canadian airports are listed in Table 5-1 with their respective elevations above sea level.

The following specifications apply to these sensors:

Temperature	-40° C to +50° C with an accuracy of ± 1° C
Resolution	0.2° C
Pressure	106.7 kPa to 59.3 kPa with an accuracy of ± 0.05 kPa
Resolution	4 Pa
Dew Point Temperature	-30° C to +50° C
Resolution	1° C

iii) Lightning Protection. The weather tower is protected by a lightning rod that is connected to a grounding rod which should extend at least 10 feet below the ground's surface. All tower mounted equipment is protected from power line transients and surges and all sensor and communication cables have their input/output signals protected with surge arrestors.

iv) Obstruction Lighting. The top of the weather tower is marked with dual lamps that are connected in parallel. The station installation should meet the requirements for obstruction marking and lighting.

v) VHF Antenna. The VHF antenna supports transmissions over the operating frequency range of 150 MHz to 175 MHz if a VHF transceiver is required at the weather station.

Table 5-1 Elevation Above Sea Level (ASL) of Major Canadian Airports (from Canadian Flight Supplement)

Canadian Airport	Elevation Above Sea Level (ASL)
St. John's	140 m (461')
Gander	151 m (496')
Halifax	145 m (477')
Moncton	71 m (233')
Quebec City	74 m (243')
Dorval	36 m (117')
Mirabel	82 m (270')
Ottawa	114 m (374')
Pearson	173 m (569')
Thunder Bay	199 m (653')
Winnipeg	239 m (783')
Saskatoon	504 m (1653')
Calgary	1084 m (3557')
Edmonton	723 m (2373')
Vancouver	2.8 m (9')
Victoria	19 m (63')

The above numbers represent the highest point on the usable landing surface expressed to the nearest foot above sea level.

5.2.2 Data Collection and Processing Unit

The centre field and remote weather stations utilize a data collection and processing unit surrounded by a weatherproof enclosure which is mounted near the base of the tower. It acquires and conditions sensor data, reduces and processes the meteorological information and communicates with the base station. The major subsystems within the data collection and processing unit include:

i) Processor Module. The microprocessor subassembly performs the principle functions of sensor interrogation, data conditioning, data digitization, data reduction and data processing. Up to 13 sensor channels can be monitored while generating the appropriate sensor excitation requirements of precision voltage and current references. The raw sensor data is first conditioned before being digitized by an A/D converter. The data must be checked to ensure that it is accurate and complete during the data reduction phase. The subsequent data processing includes such calculations as average values, minimum and maximum excursions, and rates of change. The processor sub-assembly generates and controls all the appropriate interface commands required to communicate with the data communications module. A real time crystal-controlled clock serves as the reference to generate the sensor sampling rate, basic memory and system clock, and I/O control signals. The design should be based on CMOS technology in order to minimize power usage.

ii) Data Communications Module. The remote station data can be transmitted to the base station by one of two methods. If landline interconnections are available, the data is transmitted using a modem unit. This modem operates asynchronously, in full duplex mode, with a selectable transmission rate (e.g. 110 to 9600 Baud). If the landline interface is not feasible, a VHF transceiver unit is utilized. This transceiver operates over a frequency range of 150 to 175 MHz with a RF power output of up to 8 Watts. Each remote station is polled once every 10 seconds.

iii) Power Supply. The power supply generates all the necessary voltages to operate the data collection and processing unit. It normally operates from 120 VAC, 60 Hz, 3 wire single-phase service. If a power outage does occur, battery backup will maintain normal operations for at least 48 hours. The AC power input cables are fully protected by surge arrestors.

iv) Sensor Cabling. All sensor connections consist of weatherproof shielded cabling with environmentally sealed connections.

5.2.3 Central Processing Unit

The central processing unit is located within the terminal/tower area. It consists of a personal computer equipped with a hard disk and a tape drive unit, a keyboard, and a monochrome display. Wind shear detection calculations are performed between the 10 second remote station polling intervals. This wind shear detection algorithm is based on the comparison of the average airport wind vector to the vector monitored at each remote station. A vector difference of 9 knots is the current threshold for a wind shear detection alert, however, this value can be selected by an operator if increased sensitivity or improved false alarm control is required. An audible and visual alarm is generated if the wind shear threshold parameter is exceeded. The system should indicate the status of each of the remote stations on an operator's display. This presentation will require modification to incorporate the additional information that is received from the Doppler radar sensor. As well, the wind shear detection algorithm that presently utilizes surface wind information will have additional data from the radar system to process.

To meet the requirement of a system operational confidence check, the LLWAS should perform an automatic test every 10 minutes. If any remote station fails to communicate its information within the 10 second interval it would be flagged as being defective and the possible use of any incorrect data is inhibited.

5.3 Doppler Radar Subsystem Description

5.3.1 General Discussion

In Section 4, two sensor configurations were described to meet the range-elevation requirement. The external single external sensor configuration is proposed for the following reasons:

a) Data from two sensors would require correlation processing (coordinate conversion) before the information could be used.

b) One sensor could very easily interfere with the other, especially if close in frequency. Signal processing could be added to eliminate this problem but this would increase the cost.

c) The hardware for the single external sensor configuration is likely to be less costly.

It is recommended that a radar system be developed with the capacity to generate information relating to Doppler velocity values. Reflectivity intensity information, available with standard radar processing techniques, could be made available as an option to enhance the system's overall detection capabilities. To obtain the Doppler velocity measurements, the radar transmitter must be coherent to enable the use of suitable signal processing techniques (e.g. FFT analysis). The analysis

of power requirements will aid in determining the specification of the eventual transmitter technology. Use of higher frequencies will tend to minimize the size of system components such as the antenna dish, waveguide runs, and antenna pedestal. However, with an increase in frequency, there is a corresponding increase in atmospheric attenuation and the power output from the transmitter decreases substantially. These relationships will need to be addressed during the conceptual design.

It has yet to be determined what transmitted power levels are required to ensure a high level of detection probability. No reliable theoretical means are available to determine this power requirement from first principles. A prototype developmental system that can be subjected to some practical testing is one method to further quantify this requirement.

5.3.2 Parameter Selection

Various radar system parameters must be discussed with respect to the user requirements. These include:

i) Transmission Frequency
ii) PRF Rate
iii) Range-Velocity Ambiguity Interrelationships
iv) Pulse Width
v) Transmission Power Levels
vi) Dry Microburst Considerations
vii) Polarization

These parameters are very interrelated because all radar system designs are compromises between conflicting requirements. These interrelationships are reviewed in the following sections and, where possible, the problems resolved.

i) Frequency Determination. In selecting an operating frequency for the radar it is necessary to review the propagation losses due to atmospheric attenuation and precipitation attenuation.

   a) Atmospheric Attenuation. In a clear atmosphere the attenuation of RF energy is principally due to oxygen content and water vapour. This small energy loss is primarily due to the heat energy absorbed by these two gases. Figure 5-1 illustrates the typical atmospheric absorption values for various frequencies. Table 5-2 summarizes these effects over a 35 km range with respect to frequency variation. Attenuation values will vary slightly according to the angle of the antenna and changes in altitude. For ground-based radars this attenuation is greatest when the antenna points along the horizon and least when pointing directly vertical. The values in Table 5-2 reveal no major difference over the frequency ranges of interest, S and C-band.

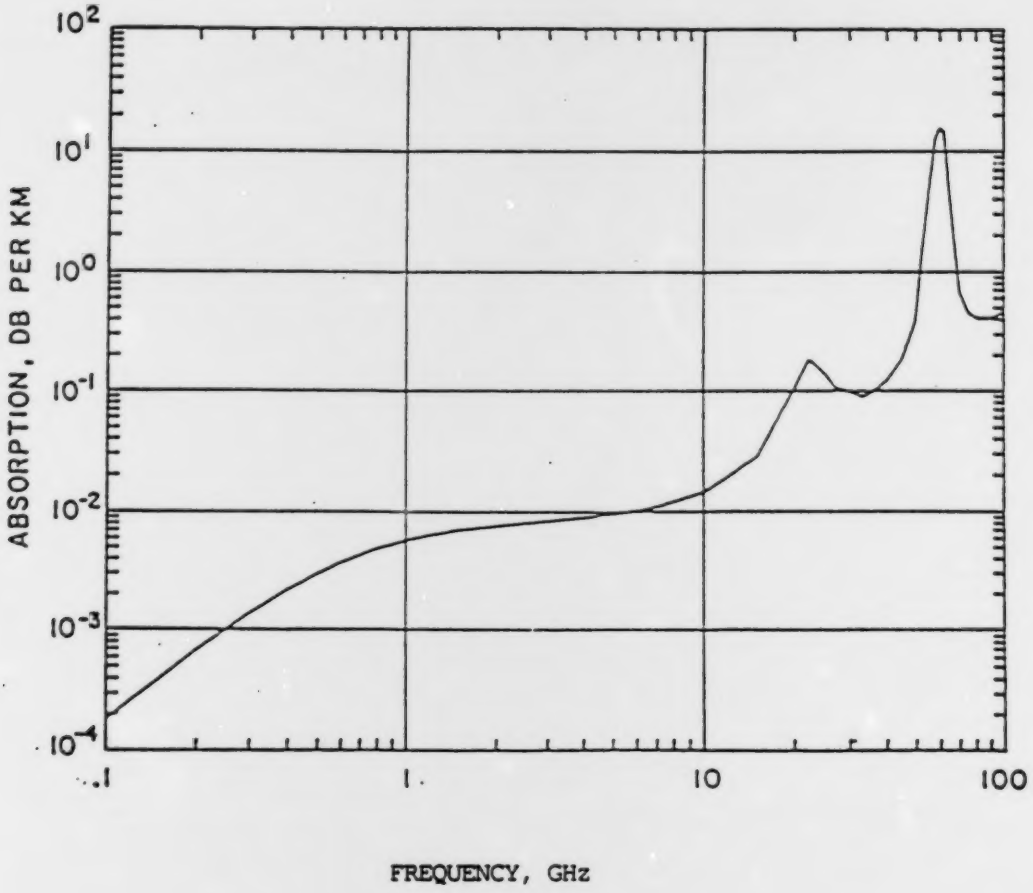

Figure 5-1 Absorption coefficients for oxygen and water vapour combined at standard sea-level temperature and pressure (from Introduction to Radar Systems, Skolnik)

Table 5-2 Atmospheric Attenuation over 35 km Two-way Path

Frequency (GHz)	Attenuation (dB/km)	2-Way Attenuation - 35 km (dB)
1	.005	0.35
3	.008	0.56
5	.01	0.70
10	.015	1.05

b) Precipitation Attenuation. Radar performance can be severely limited by precipitation attenuation. Radar energy is absorbed by the liquid water droplets and is also dissipated due to scattering of the energy outside the antenna beamwidth. This scattering contributes to signal attenuation just as absorption does. Figure 5-2 and Table 5-3 illustrate the attenuation variation over several frequency ranges for five rainfall rates.

As can be calculated from Table 5-3, the two-way attenuation for a moderate rainfall increases from 0.11 dB at 3 GHz to 4.30 dB at 10 GHz over a 35 km range. A more serious problem is that a wet microburst is usually associated with heavy rainfall resulting in extreme attentuation levels (e.g. at 10 km a 3 cm radar experiences a 20 dB loss).

The radar backscatter cross-section per unit volume is a function of wavelength. As frequency increases, so does the amount of backscatter. As a result, at the higher C-band and X-band frequencies more power will be returned to the antenna from rainfall backscatter but range coverage will not be as extensive as at lower frequencies due to the enhanced attenuation. This attenuation problem can be minimized by increasing the transmitted power levels. Another important factor to consider is that system components such as antenna dishes, waveguide, rotary joints and antenna pedestals are smaller in size at higher frequencies.

ii) PRF Determination. Two factors affect the determination of the pulse repetition frequency (PRF): the maximum range coverage of the radar and the maximum Doppler frequency to be measured.

a) Range Coverage. The maximum unambiguous range of the radar is limited by the PRF since, to be classified as unambiguous, the target echo must be received back at the radar antenna prior to the transmission of the next pulse. The standard range equation is:

$$R_{Max} = \frac{c}{2\ PRF} = \frac{c}{2} \times T_{PRF} \qquad (1)$$

Where:

c is the velocity of light
T_{PRF} is the radar pulse repetition period

The radar range is based on the two-way travel time to the target and back which accounts for the factor of two in Equation 1.

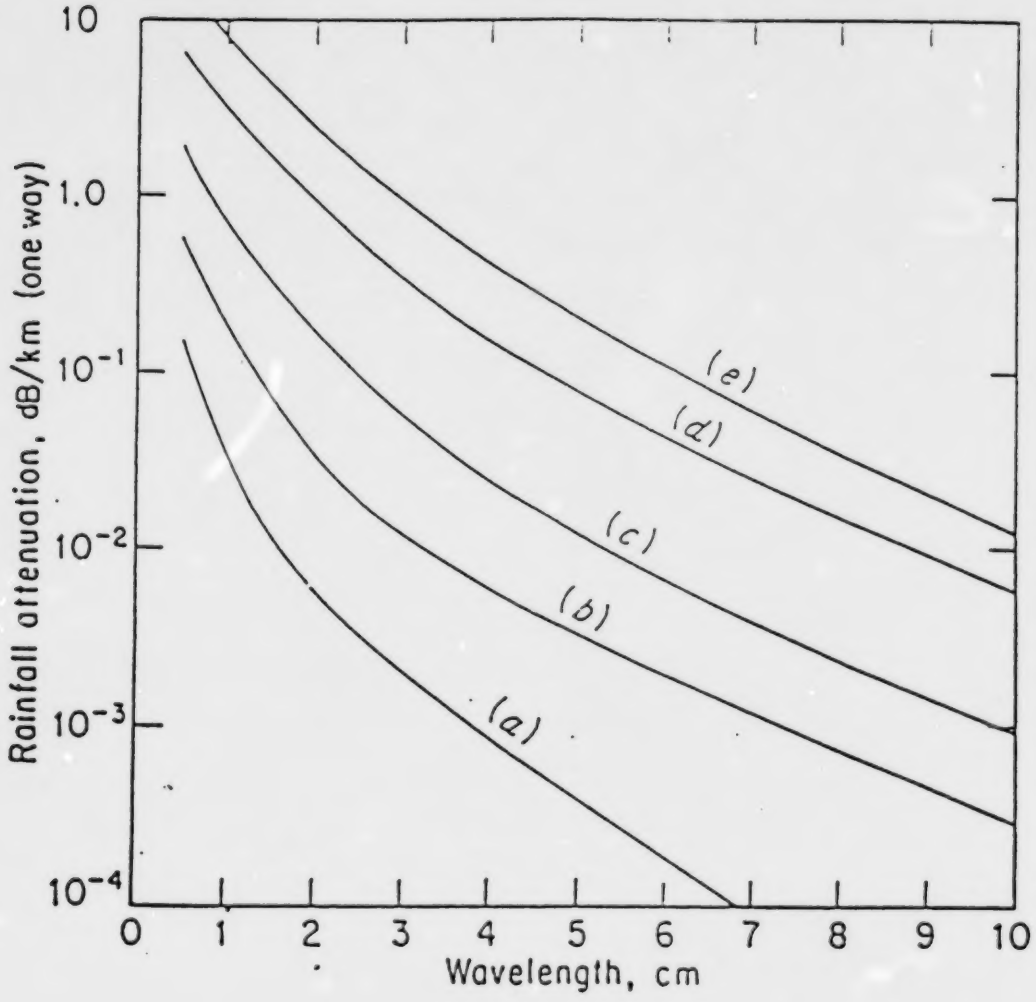

(Refer to Table 5-3 for Rainfall Type and Rates)

Figure 5-2 Attenuation versus frequency
(from Radar Range Performance Analysis, Blake)

Table 5-3 Rain attenuation with respect to frequency
(One-way Propagation)

Frequency (GHz)	λ (cm)	Attenuation (dB/km)				
		r=0.25	r=1	r=4	r=16	r=64
3	10	9.66×10^{-5}	3.92×10^{-4}	1.59×10^{-3}	6.46×10^{-3}	2.63×10^{-2}
5	6	3.02×10^{-4}	1.48×10^{-3}	7.26×10^{-3}	3.56×10^{-2}	1.74×10^{-1}
10	3	1.67×10^{-3}	1.01×10^{-2}	6.14×10^{-2}	3.72×10^{-1}	2.26×10^{0}

Where r is the rainfall rate:

	Rainfall Type	Rainfall Rate (mm/hr)
a)	Drizzle	0.25
b)	Light Rain	1.0
c)	Moderate Rain	4.0
d)	Heavy Rain	16.0
e)	Excessive Rain	> 40.0

This then equates to the following time references:

12.36 μsec/1.85 km
6.67 nsec/m

Relating these values to our range requirement of 35 km, the radar PRF becomes 4276 Hz or approximately 4300 Hz.

b) Doppler Frequency (Velocity) Coverage. The maximum unambiguous frequency is determined by the Nyquist sampling theorem which requires that the sampling rate be at least twice the maximum frequency to be measured. Since the PRF is the sampling rate, the maximum unambiguous frequency becomes:

$$F_{Max} = \frac{PRF}{2} \qquad (2)$$

However, one can relate Doppler frequency with radial velocity through the relationship:

$$f_D = \frac{2V_r}{\lambda} \qquad (3)$$

Where:

f_D is the Doppler frequency
V_r is the radial velocity
λ is the transmitted wavelength

Given a transmission frequency range of 9 to 10 GHz and the requirement to determine unambiguous velocities to 40 m/s, the frequency Doppler shift experienced at the antenna would be 2.667 kHz. This converts to a PRF of 5333 Hz which corresponds to approximately a 28 km range. In this example, the desired range coverage and Doppler velocity values are shown to be incompatible.

iii) Range-Velocity Ambiguity Interrelationships. As can be seen from the previous discussion, a compromise must be made in the unambiguous range and velocity values. If the previous equations (1,2,3) are combined, a range-velocity ambiguity function results which is of the following form:

$$R_{Max}\ V_{Max} = \frac{c\lambda}{8} \qquad (4)$$

Table 5-4 illustrates the maximum unambiguous velocity for different frequency bands over a maximum range of 35 km. As can be seen at the C-band and X-band frequencies, the required Doppler velocity of ±40 m/s is not achieved. Several techniques can be used to increase the unambiguous velocity parameter. Dual staggered pulse repetition intervals, random pulse transmissions from pulse-to-pulse and batch processing (high PRF pulses followed by a low PRF) are all possibilities for extending the effective range-velocity ambiguity. However, these techniques all require complex sophisticated signal processing in the form of duplicate Doppler processors, intricate timing controllers, large memory systems to retain data for several Pulse Repetition Intervals (PRIs), etc. with an increase in cost due to the additional hardware requirements. Because of the one million dollar ceiling on this project, a sophisticated timing and processing radar system is not justifiable. The options are then either to move lower in frequency to ensure adequate range coverage or adjust the maximum range coverage to enable adequate velocity measurement to ± 40 m/s. The following table illustrates the maximum range achievable at C and X-band frequencies if a ± 40 m/s velocity measurement is required.

Frequency	Velocity	Range
5.2 to 5.35 GHz C-band	± 40 m/s	27 km
9.6 to 10 GHz X-band	± 40 m/s	15 km

The X-band frequency coverage is too restricted and thus can be eliminated from further consideration. A C-band radar could be a possibility if a reduced range coverage of 27 km is acceptable, otherwise a S-band system would have to be implemented. In either case, a PRF of 5555 Hz would resolve the range velocity ambiguities to at least a 27 km range without requiring expensive signal processing features.

iv) Pulse Width Requirements. Since the microburst phenomena develops its maximum wind speeds 50 to 100 m above the earth's surface, the radar should be able to resolve wind velocities within this altitude range. To help facilitate any signal processing requirements by not imposing any time limitations, a 90 m range

Table 5-4 Range Velocity Ambiguities

Frequency (GHz)	R_{max} (km)	λ (m)	$R_{max}V_{max}$ (m^2/sec)	V_{max} (m/s)
1.25 - 1.35 L-Band RAMP	35	.240 - .222	8.66×10^6	247 or ± 123
2.7 - 2.85 S-Band	35	.111 - .105	4.05×10^6	115 or ± 58
5.2 - 5.35 C-Band	35	.058 - .056	2.14×10^6	61 or ± 30
9.6 - 10 X-Band	35	.031 - .030	1.14×10^6	32 or ± 16

resolution cell has been selected. This corresponds to a 0.6 μsec pulse which is easily generated by the timing controller. For a typical microburst with a core diameter of 1 to 2 km this results in approximately 11 to 22 range resolution cells across its extent.

v) Power Requirements. The power requirement to detect the microburst phenomena is a very subjective matter. Since it is likely a microburst will be accompanied with considerable rainfall, as in a wet microburst, it is logical to try to detect the relative movement of the water droplets. In attempting to quantify the required power levels to detect a microburst at a 35 km range, it is necessary to attempt to define the radar cross section. From a meteorological point of view, it is normal to consider rainfall as a large number of independent scatterers within the radar resolution cell. The contribution of all these independent scatterers is summed over this radar resolution cell which is delimited by the vertical beamwidth, the horizontal beamwidth, and the transmitted pulse duration (refer to Figure 5-3). The following radar range equation is used by meteorologists to relate power received and transmitted to rainfall rate:

$$P_r = \frac{2.4P_t \cdot G \cdot \tau \cdot r^{1.6}}{R^2 \cdot \lambda^2} \cdot 10^{-8} \qquad (5)$$

Equation 5, when rearranged to solve for P_t, becomes:

$$P_t = \frac{P_r R^2 \lambda^2}{2.4G \cdot \tau \cdot r^{1.6}} \cdot 10^{8} \qquad (6)$$

Where:

P_t is the transmitted power in watts
P_r is the received power in watts
R is the range in metres
λ is the transmitted wavelength in metres
G is the antenna gain dB
τ is the transmitted pulse length in seconds
r is the rainfall rate in mm/hr

Some assumptions are required in order to calculate this equation. The power received at the antenna is usually very small and it is not unusual for a radar receiver to have a 100 dB dynamic range with a minimum discernable signal in the region of -100 dBm.

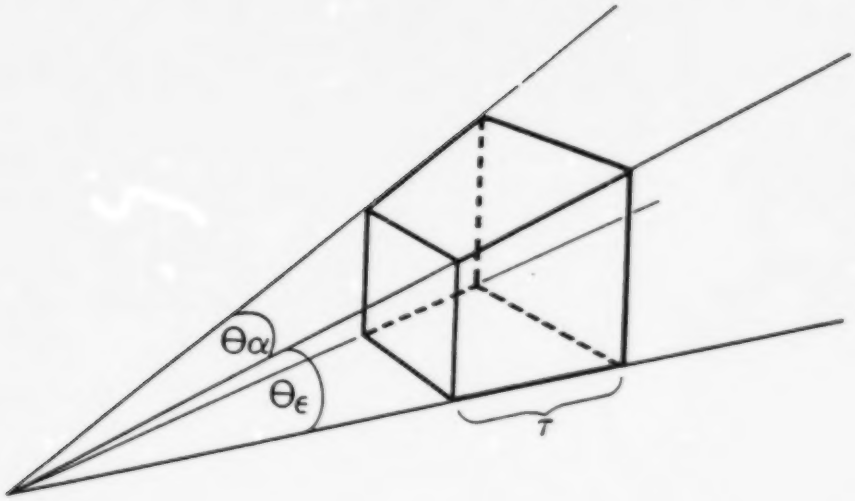

τ = Pulse Duration
θ_ε = Vertical Beamwidth
$\theta_\alpha^\varepsilon$ = Horizontal Beamwidth

Figure 5-3 Radar resolution cell to determine the radar cross section of rain

The antenna gain for a typical parabolic C-band antenna can be conservatively estimated at 30 dB. The remaining parameters have these values as already discussed:

R = 35 km
λ = 6 cm at C-band
τ = 0.6 μsec
r = 4 mm/hr for a moderate rainfall

Given these values and Equation 6, the peak transmitted power level is calculated as approximately 3.3 kw. This is an ideal case and a considerable increase in transmitted power levels is required to compensate for precipitation attenuation (wet microbursts) and the requirement to detect clear air turbulence with low backscatter (dry microbursts).

Since the pulse width is fixed due to range resolution requirements this increase in energy can only be accomplished by increasing the peak transmitted output power, unless sophisticated pulse compression techniques are used. More power will also enable greater penetration through the weather formation which becomes limited due to increased attenuation. With reference to Table 5-3, if one compares the moderate-to-excessive rainfall rate attenuation factors, it can be calculated for a return path range of 70 km there occurs an additional attenuation loss of nearly 12 dB at C-band. Thus, to maintain the range coverage of 35 km in an excessive rainfall of 64 mm/hr the peak transmitted power would need to be increased almost 15 times. If we use the previously calculated value of 3.3 kw this results in a peak power of approximately 50 kw. Thus to maintain reasonable range coverage in severe rainfall conditions and to allow for the detection of dry microbursts, peak transmitted power of levels at least 50 kw are recommended.

vi) Dry Microburst Considerations. The detection of point targets requires considerably more power than volumetric detection. The relationship for this target is

$$R^4 = \frac{P_t}{P_r} \cdot \frac{G^2 \lambda^2 \sigma}{4\pi^3} \qquad (7)$$

where σ is the cross section of the target. For a raindrop of typical size (1 mm radius) the radar cross section at 6.0 cm wavelength is approximately 5×10^{-9} m^2. If this target is viewed by a 50 kw, 6.0 cm radar with an antenna having 30 dB gain and a MDS of -100 dBm, then Equation 7 can be used to calculate the maximum range. This turns out to be approximately 519 m. Manipulating the equation shows that the detection of single drops

at ranges on the order of 35 km is in fact not feasible using any radar that it would be practical to build.

The detection of dry microbursts then depends on the reflection from refractive index discontinuities caused by the differing temperature and humidity in the downburst air compared with the normal environment at the same altitude. Bean and Dutton (1966) give the refractive index of air, N, as

$$N = (n-1)^6 = K_1 \frac{P_d}{T} + K_2 \frac{e}{T} + K_3 \frac{e}{T^2} \qquad (8)$$

where P_d is the pressure of dry air
e is the partial pressure of water vapour
K_1, K_2, K_3 are known constants.

This equation can be differentiated to give

$$\Delta N = a\Delta T + b\Delta e + c\Delta P \qquad (9)$$

For typical summer conditions (P = 1000 mb, T = 20° C, humidity 50%) we can calculate the constants a, b and c which become -1.27, +4.5 and +0.27 respectively. For the microbursts it is apparent that the biggest change in N is likely to be due to the change in e. For the parameters discussed this may result in $\Delta N = 40$. Thus the amplitude reflection coefficient

$$\frac{n_1 - n_2}{n_1 + n_2}$$

of a refractive discontinuity is of the order 40×10^{-9} and the power reflection coefficient is approximately 1.6×10^{-9}.

The radar equation for reflection from a plain discontinuity surface is given by

$$R^4 = \frac{P_t}{P_r} \cdot \frac{G^2 \lambda^2 \sigma}{64\pi^2} \cdot \left(\frac{\Delta n}{n} \right)^2 \qquad (10)$$

For the 50 kw C-band radar discussed above the detectable range is in excess of 100 km. Thus sharp discontinuities in refractive index of the magnitude thought to be produced by dry microbursts seem to be readily detectable by modest radars of the type discussed here.

vii) Polarization Options. Because raindrops are primarily spherical the backscattered energy from the rain can be severely affected by the incident energy polarization. Right and lefthand circular polarizations have been used by surveillance radars to minimize the weather backscatter received by the radar receiver. This is accomplished because a circularly polarized wave is reflected from a spherical object (raindrop) with the opposite sense of polarization. If the radar antenna is selective only to the originally transmitted polarization, the translated backscatter will be rejected by the system. Since we are interested in the backscattered energy for relative velocity measurements, the transmission of a circularly polarized wave is not acceptable. Therefore, the RF transmission of this radar should be limited to either vertical or horizontal orthogonal polarizations.

5.3.3 Antenna Scan Rate and Pattern Selection

Figure 5-4 illustrates the angle a typical microburst of 1 to 2 km core cross section would subtend at a range of 35 km. In order to adequately detect a microburst an appropriate number of pulses must be incident on the microburst within the antenna beamwidth during the time the beam scans across its azimuth extent. This is directly affected by the antenna scan rate. Table 5-5 illustrates the number of pulses on target (e.g. a microburst) for various scan rates and for the two angle limits assuming a PRF of 5555 Hz. Even at 60 rpm with a small beamwidth angle there are still a sufficient number of pulses on target to allow adequate signal processing to be performed. Since the average microburst duration is on the order of 3 minutes probability of detection increases with the antenna scan rate, due to the increase in information available for processing.

To determine the antenna scan pattern, certain microburst characteristics must be reviewed. In the initial stages of the microburst, the downdraught is descending from above and as it nears the ground the microburst begins to spread out, producing horizontal winds. Therefore, during the initial stages of microburst development, it is reasonable to perform some type of elevation cut above the area of interest in order to detect the impending downdraught. It is recommended to perform at least one elevation scan to assist in the detection of this initial microburst development. The actual scan elevation angle is dependent on the antenna beamwidth to ensure sufficient coverage of the desired area and will be discussed in a later section. However, with modern antenna pedestals, any angle is programmable and therefore does not present a problem. Several elevation cuts as proposed in the NEXRAD and TDWR systems are not appropriate because the time required for a single azimuth elevation scan (5 to 6 minutes) is too excessive to satisfy the detection time requirement for a typical microburst. Therefore, it is recommended to scan the antenna system at a high rate of up to one second per scan in an alternatively horizontal or slightly-above-horizontal scan to at least a single or double angle elevation scan.

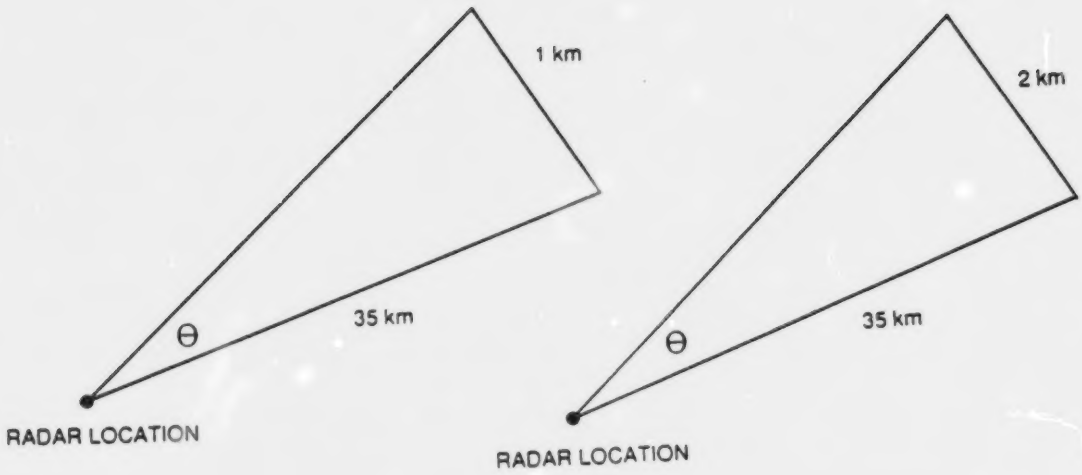

$$\Theta = \frac{1}{35} \text{ radians} = \frac{1}{35} \cdot \frac{360}{2 \cdot \pi} \text{ degrees} = 1.64 \text{ degrees}$$

$$\Theta = \frac{2}{35} \text{ radians} = \frac{2}{35} \cdot \frac{360}{2 \cdot \pi} \text{ degrees} = 3.27 \text{ degrees}$$

Figure 5-4 Typical microburst subtended angle

Table 5–5 Pulses on Target

Beamwidth 1.6°		Beamwidth 3.2°	
Antenna RPM	Pulses on Target	Antenna RPM	Pulses on Target
10 (6 sec scan)	148	10	296
20 (3 sec scan)	74	20	148
30 (2 sec scan)	50	30	100
60 (1 sec scan)	25	60	50

$$\text{Pulses on Target within Beamwidth} = \theta_{BW} \cdot \frac{PRF}{AD} \qquad (11)$$

Where:

θ is the antenna beamwidth
PRF is the selected PRF – 5555 Hz
AD is the antenna displacement at a specified scan rate

5.3.4 Functional Components

The radar system is composed of five major subsystems. These include:

i) Antenna Group
ii) Transmitter Receiver
iii) Signal Processor
iv) Timing Controller
v) Input/Output Communications
vi) Display Processor

i) Antenna Subsystem. The two major components of the antenna system are the antenna and the azimuth elevation pedestal. The antenna will be a parabolic dish which generates a pencil beam radiation pattern. Table 5-6 describes some typical electrical characteristics of these antennas over the S-band and C-band frequencies of interest. It can be seen from Table 5-6 that, as frequency and antenna size increase, overall gain is improved and the 3 dB beam width decreases. All these antennas typically have a first sidelobe level of 25 to 26 dB below the peak level. In order to match as closely as possible the 1.6 degree subtended angle of a 1 km microburst, the antenna should be selected to have a 1.8 degree beamwidth. This ensures that the antenna pattern will allow enough hits on target to enable adequate processing and yet will not be too large (2.4 m or 8 ft) causing problems with implementation and installation. This beamwidth will also maintain adequate azimuth resolution at 35 km to allow detection of adjacent microbursts if this situation ever occurs. The antenna pedestal must allow rapid scanning (possibly up to 60 rpm) and elevations to 30 degrees if the antenna is to be located as indicated in Figure 6-2 (p. 142). The antenna pedestal will contain the rotary joints to provide the coupling between the antenna and the transmitter. The antenna pedestal and associated turning apparatus must be able to operate under certain environmental characteristics relating to wind velocities and ice loading. Typical survival ratings for these parabolic antennas are:

- 200 km/hr wind velocity
- 25 mm ice loading
- -40° C to +50° C operational temperature

To prevent electrical performance degradation in the form of increased voltage standing wave ratio (VSWR), voltage breakdown, and increased attenuation, it is recommended to pressurize the waveguide run from the transmitter to the antenna feed. This is usually performed over frequencies greater than 3 GHz in the range of 21 to 55 kPa (3 to 8 lb/in^2). A self-regulating system helps maintain the waveguide pressure within these limits. The antenna pedestal also generates the appropriate analog or digital turning azimuth data.

Table 5–6 Antenna Electrical Characteristics

Frequency (GHz)	Diameter (m)	Gain (dB)	Beamwidth (degrees)
3.7 - 4.2	1.8	35	3.0
	2.4	37	2.4
4.4 - 5.0	1.8	36	2.5
	2.4	39	1.8
5.9 - 6.4	1.8	39	1.8
	2.4	41	1.4

ii) Transmitter Receiver. As already discussed, a radar transmitter capable of generating at least 50 kw of power is required. Several approaches are feasible: solid state, klystron or magnetron tube. Typical solid state modules at the S and C-band frequencies can generate up to 47 dBm (50 w). To generate the required 50 kw, hundreds of modules would be required and their respective outputs would then have to be multiplexed together. This is not only costly but also involves a large element of risk. Klystrons are 2 to 3 times more expensive than magnetrons. It appears that the magnetron is the most likely technology to satisfy the transmitter requirement. The magnetron transmitter consists of a modulator generating the specified time duration transmit pulse (0.6 μsec in length) which then excites the magnetron. The magnetron then begins to self-oscillate at its tuned frequency and remains in this state until the modulation pulse is removed. One of the main concerns with utilizing a magnetron transmitter is that the phase oscillations between each successive pulse will vary. Therefore, a small amount of transmitted RF energy is sampled by the receiver to phase lock the coherent reference signal of the phase detectors to the actual transmitted phase. The transmitter receiver will have a suitable T/R waveguide cell to protect the sensitive receiver front-end from the high power transmitted pulse. The receiver will enhance the small signals using a low noise amplifier, perform the down conversion from RF frequencies to baseband, perform the appropriate pulse matched filtering to optimize the signal-to-noise ratio, determine the target relative phase with the in-phase and quadrature phase detectors, and deliver all the appropriate signals to the digital signal processor. This transmitter receiver subsystem may be purchased as a complete unit thus minimizing development costs.

iii) Signal Processor. As shown in Figure 5-5, the initial stages of the signal processor accepts as inputs video signals from the phase detectors. This signal is then digitized by A/D converters whose dynamic range is matched to the video excursion levels from the phase detector. The sampling rate is selected such that the radar pulse of 0.6 μsec is sampled at least once over its 3dB width (note that the matched filter actually broadens the received pulse to 1.2 μsec at the pulse base). This corresponds to a sampling rate of 1.67 MHz. To facilitate the simple generation of the digitization clock by the timing controller, a 2 MHz or 500 nsec clock has been selected.

The next stage of the signal processor takes the form of a simple memory storage unit. It stores the incoming radar video in range azimuth orientation for each pulse repetition interval with a value for each range sample. The azimuth extent is determined by the complexity of the Doppler processing to follow which determines the relative velocity parameter. The state-of-the-art procedure to perform Doppler processing is to utilize the Fast Fourier Transform

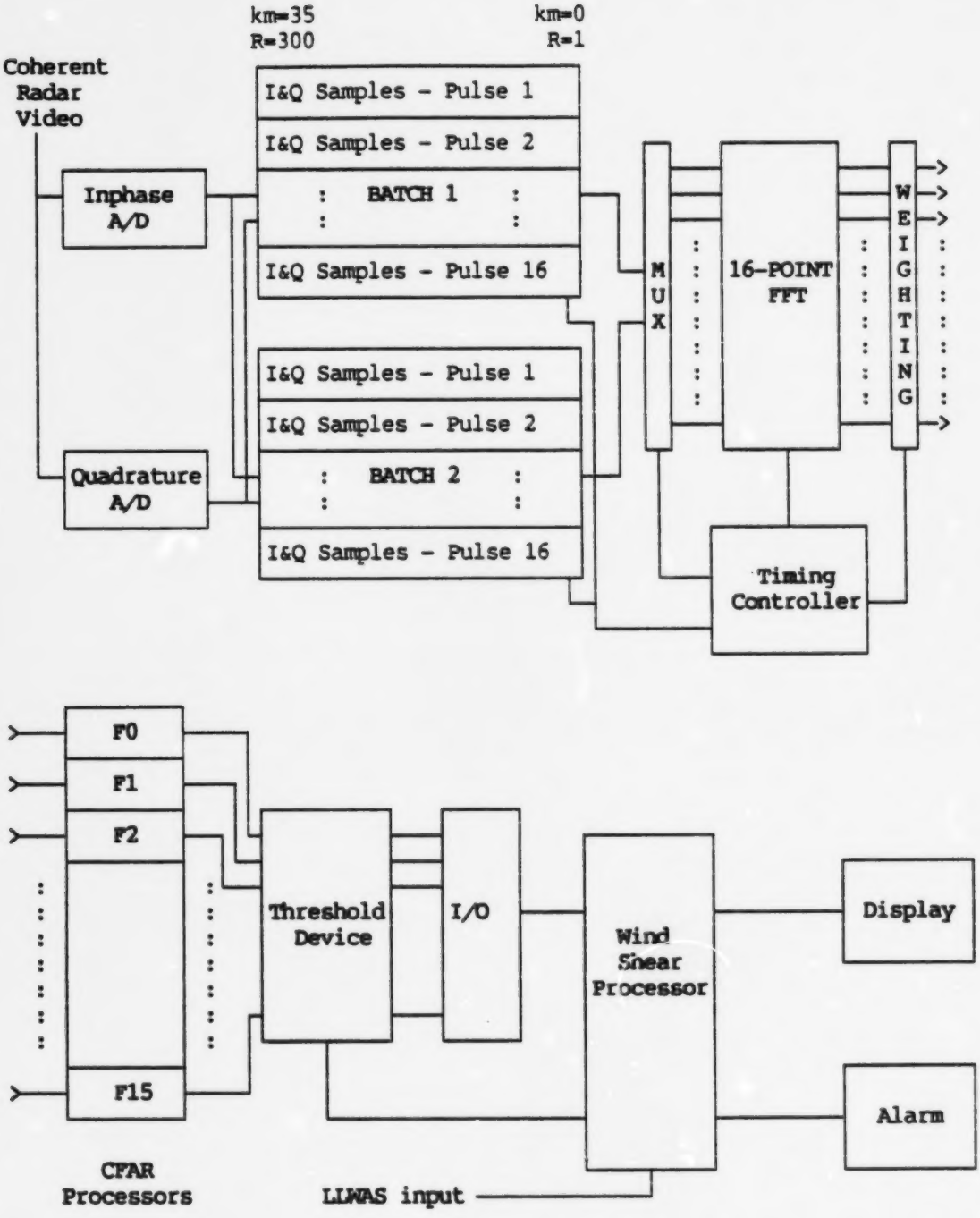

Figure 5-5 Radar processing system block diagram

(FFT) method. The initial concern is to specify the size (i.e. 16 points or 32 points) of the FFT to generate adequate velocity resolution. Other factors to consider are that processing time and the memory storage requirements will increase with FFT size. As a result, a 16 point FFT has been selected which results in a velocity resolution of each filter of 5 m/s (16 filters spread over a range of 80 m/s or ± 40 m/s). This resolution is thought to be adequate since there is no requirement to resolve any targets in the ground clutter spectrum (± 5 m/s). Two techniques are available to process the stored data by FFT methods: the sliding window approach or the batch processing procedure. The sliding window assumes a FFT calculation is performed every PRI over the past 16 radar transmissions. This gives the processor only a single pulse repetition interval to perform all the FFT calculations before the next set of incoming data is available. This has a tendency to place unnecessary processing restrictions (system timing) on the Doppler processor. The batch processor stores all 16 PRI data values and then has an entire neighbouring 16 PRI batch time to perform the calculations before being required to process this latest batch. The following calculations illustrate the basic timing requirements to perform this batch processing:

Selected PRF = 5555 Hz
PRI = 180 μsec
Selected Pulse Width = 0.6 μsec
Number of Range Cells per PRI = 300
Time for 16 PRIs = 2.88 msec

As can be seen, each batch corresponds to 2.88 msec of which there are 300 range-gated samples. This relates to completing 300 16-point FFTs within this time frame, of which each FFT must be calculated in 9.6 μsec. This is not an unreasonable time with contemporary digital technology.

In order to minimize the sidelobe spreading into adjacent velocity filters window weighting can be applied to each filter output. This is easily accomplished by adding to the filter value one half the magnitude value of each of the adjacent filter outputs. This implements a Hanning window function which causes the mainlobe response of the filter to spread slightly but reduces the sidelobe spillover to virtually nothing.

The output from the Doppler device is then fed to a Constant False Alarm Rate (CFAR) processor which is used to control the false alarm rate. This processor calculates the mean velocity of several cells on either side of the in-process cell and normalizes its value with respect to the calculated mean. The normalized in-process cell value and the mean value are then fed forward to the threshold device to determine if a target velocity threshold has

been exceeded. It is the intent to have these thresholds adaptively controlled from the user console to allow adjustment of the sensitivity of each filter performance. The threshold device also encodes the velocity filter data so as to minimize the information to be transferred on the radar data link. This is a simple comparison of the magnitude values of the filter outputs to create a four bit code indicating which filter contained the greatest velocity value for that specific range cell. This information, one four-bit value for each 300 range cells within the coherent processing interval, is then transferred to the I/O controller for transmission to the display site. It is the intent to utilize off-the-shelf CPU, memory, and communications modules with a standard bus configuration to facilitate the implementation of the CFAR processor, the threshold device, the I/O controller, and the display processor.

iv) Timing Controller. The timing controller subsystem generates all the necessary timing signals and reference clocks for the entire radar system. It is responsible for generating the main trigger PRF signal from which all range associated pulses are referenced. It generates the basic digitization clock and all the required memory management signals. It is microprocessor based with ROM based parameters to permit easy revision of any of the radar timing specifications.

v) Input/Output Communications. The communications subsystem is responsible for the management flow of information from the radar system to the operations display system which will likely be located in the control tower. It is envisioned to utilize standard communications links operating at high speed in full duplex mode. All the required communications handshaking signals and data integrity assessment checks are controlled by the communications subsystem. Depending on the quality of the operator's display a certain amount of data compression to map the radar data to the display resolution may be required. The communications subsystem will perform this data buffering and compression if required (i.e. if 300 range cells exist for every PRI, the display would require 600x600 elements to present all the radar data).

vi) Wind Shear Processor. The wind shear processor will be responsible for converting the range azimuth velocity data into scan converted X-Y display coordinates. The data presented on the display will be in colour coded presentation with respect to velocity magnitude. An associated alarm processor will coordinate the input from the LLWAS with input from the radar data threshold device. An aural as well as a visual alarm will be raised if the wind shear/microburst detection threshold has been exceeded. It is the intent, during the display processor development, to review the possibility of utilizing an expert system to assist in the wind shear/microburst detection process.

5.4 Conceptual Design Summary

The proposed wind shear detection system, as discussed, is an integrated LLWAS and Doppler radar. The LLWAS has the capability to support from 6 to 11 remote meteorological stations. The parameters of the Doppler radar are as follows:

C-band frequency

Antenna
- 1.8 to 2.4 metre dish
- 1.8° beamwidth
- 20 to 30 rpm
- radome covered

Antenna Pedestal
- 360° azimuth
- 30° elevation

Transmitter Receiver
- Power > 50 kw
- Pulse Width 0.6 μsec
- PRF 5555 Hz

Signal Processor
- 16-point FFT
- CFAR

The choice of the C-band frequency is justifiable due to the reasonable availability of transmitter components and the minimization of antenna size enabling the fast scan rates.

5.5 Overall Recommendations

1. Develop an engineering prototype with the complete transmitter receiver and signal processor. The transmitter receiver would be developed jointly with Varian Canada utilizing their MaPS technology.

   One cautionary note is that the MaPS technology is reasonably new; the klystron tube option should be given consideration but will be more expensive.

2. In order to evaluate the prototype, a repeatable test scenario is required. The capability to generate wake vortices at the NRC wind tunnel facility could provide one possible solution. The antenna could be replaced with a simple RF horn which could then be placed in the wind tunnel to determine if any reflections are returned from the wake vortex. This would greatly assist in the detection evaluation of the transmitter receiver and the signal processing unit. This system could also act as a wake vortex detector if proven successful.

3. The engineering prototype can be installed in a portable shelter with a smaller antenna and transported to a location such as Denver, Colorado to evaluate its performance against in-situ wind shear conditions.

4. An evaluation of alternate PRF patterns should be performed in order to obtain the desired 35 km range coverage with the C-band transmitter.

5. Frequency agility can enhance detectability and, with co-axial magnetrons, different frequency transmissions can be selected. An analysis should be performed to determine if this capability enhances the detection of wind shear and if it is cost effective.

6. Because transmitter output can be controlled through variations in the modulation drive, the power levels necessary to detect dry microbursts might be quantifiable. This capability exists with state-of-the-art transmitters and should be fully evaluated since these measurements would be critical in determining the radar's performance level in detecting not only dry microbursts but also the possibility of wake vortices.

7. In optimizing the Doppler processor, the advantages and disadvantages of directly using the Discrete Fourier Transform (DFT) compared to the FFT algorithm should be reviewed. It appears that, for small time to frequency transforms, the DFT is as fast or faster than the FFT algorithm. Also, for the specific application to prevent sidelobe frequency spreading, an analysis as to whether to perform the data windowing before or after the frequency transform must be performed.

8. A complete radar system specification must be prepared indicating all the system parameters (MDS, phase stabilities, clock stabilities, noise figure, etc.) as well as tolerable system losses (VSWR, mismatch losses, processing losses, etc.). This is critical to ensure the system pulse-to-pulse coherency is maintained in order to achieve the Doppler processor performance.

9. The possibility of including the processing of the radar reflectivity parameter to augment the Doppler velocity analysis should be reviewed. It is likely that the radar reflectivity measurement would offer additional information, however, the concomitant level of equipment complexity and processing that will be required needs determining.

10. The use of expert systems, to assist or possibly create a predictive capability in the detection of wind shear phenomena, needs to be thoroughly understood. The development of specific wind shear detection algorithms and their capabilities within the TDWR and NEXRAD programs should be closely monitored.

6. COST ANALYSIS

The proposed wind shear detection system is depicted in Figure 6-1. This illustrates that the incoming information is combined by the wind shear processor located at the control tower. Surveillance data from the radar site and meteorological data from the LLWAS is integrated to enable a positive detection of the wind shear phenomena. The performance criteria include a high probability of detection and minimal false alarm rate.

6.1 LLWAS Costs

The LLWAS costs have been estimated on a per meteorological station basis. This allows costing to be generated based on the number of remote stations required at each associated airport. The number of remote stations at each site will range from a minimum of six to a maximum of ten. The site costs include the meteorological sensors, support electronics and power supplies, communications networks and base station requirements. Other related, but intangible, costs must be also considered. These include costs associated with the following:

i) Land Procurement - if the meteorological station is exterior to airport boundaries.
ii) Site Preparation - a concrete base is required.
iii) Communications Link - landline equipment and installation.
iv) Tower Procurement and Installation.

The cost for an 11 station LLWAS has been estimated at $310,000.

An example of possible remote station locations at the Ottawa International Airport are depicted in Figure 6-2.

6.2 Doppler Radar Costs

The radar costs can be allocated to each major subsystem. This includes the following components:

i) Antenna Group
ii) Transmitter Receiver
iii) Signal Processor

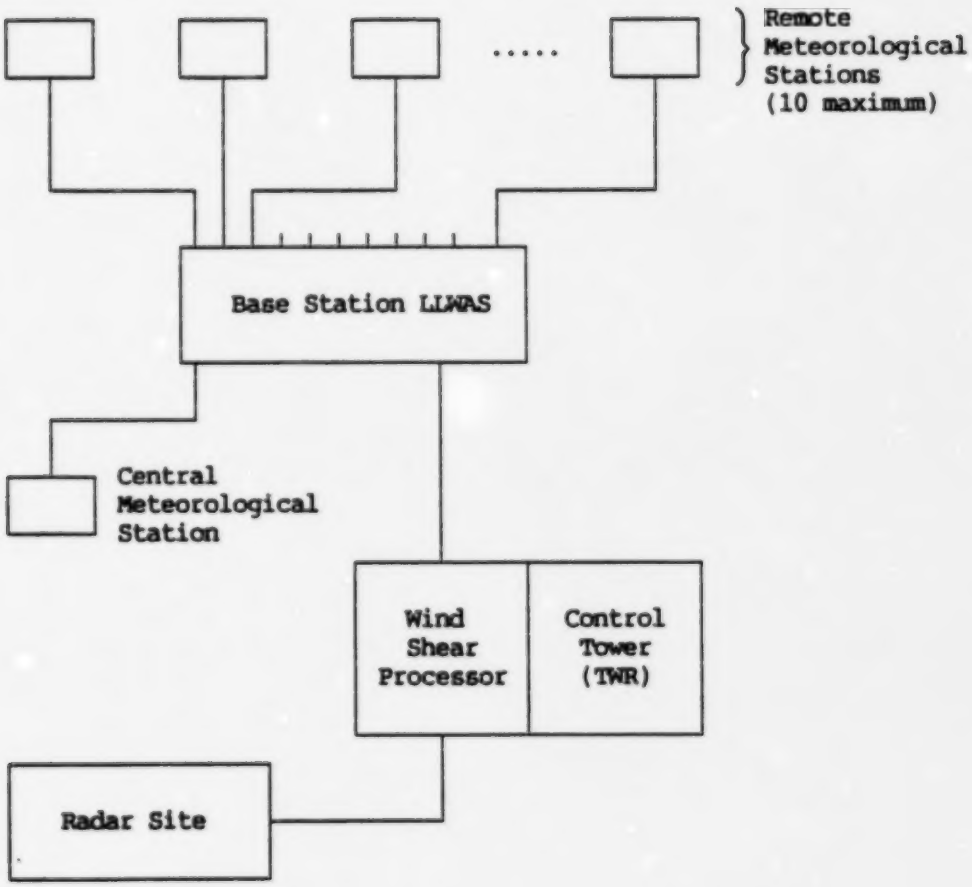

Figure 6-1 Proposed wind shear detection system

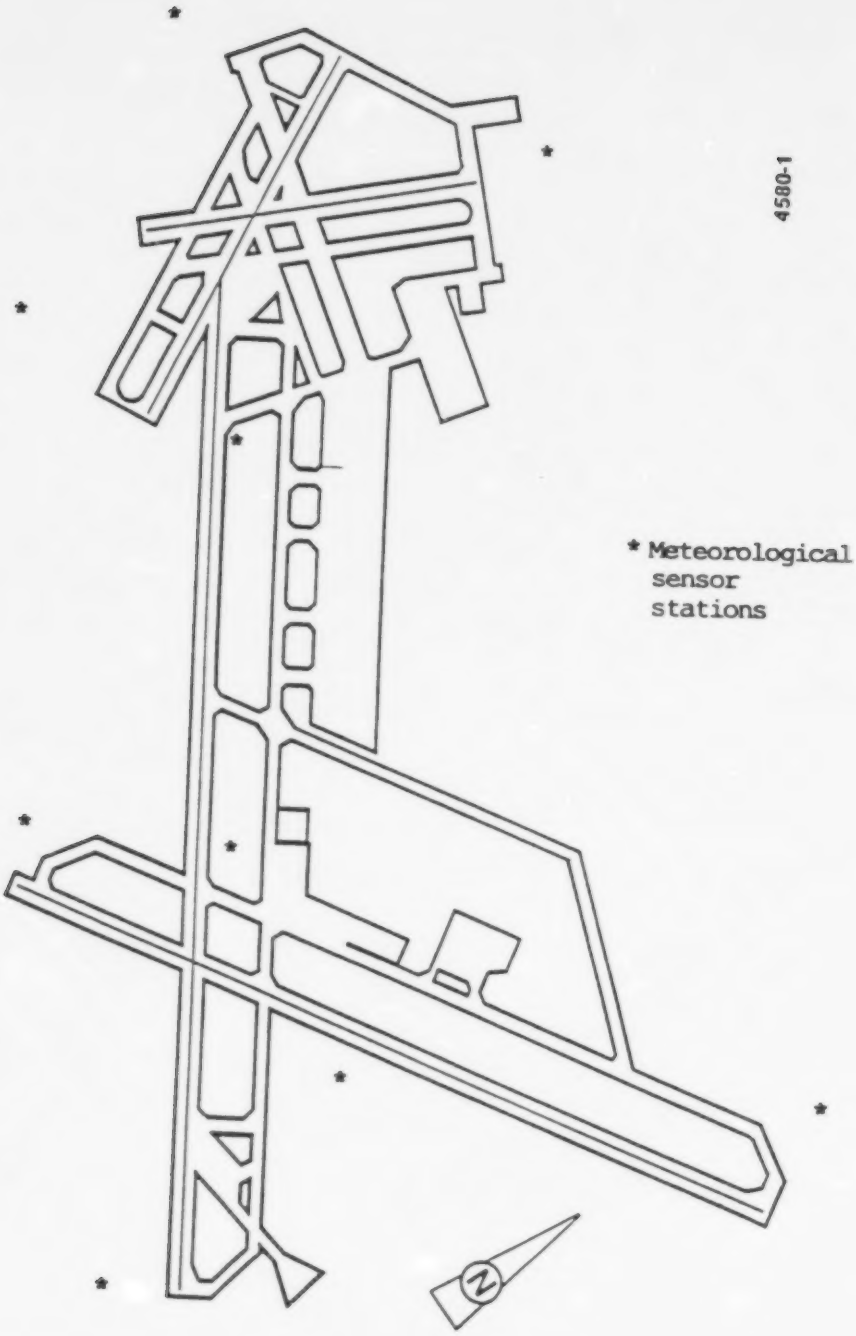

Figure 6-2 Possible remote station locations at the Ottawa International Airport

6.2.1 Antenna Group

From a costing perspective, the antenna group can be subdivided into the following major components:

i) Parabolic Dish
ii) Turning Pedestal
iii) Radome
iv) Waveguide Runs
v) Pressurization System

i) Parabolic Dish. Two C-band parabolic dishes have been costed to allow a selection of azimuth beamwidths.

Diameter (metres)	Beamwidth (degrees)	Cost (dollars)
1.8	2.5	$6,000
2.4	1.8	$7,000

The RF feed configuration for these antennas is a simple horn with a pressure window.

ii) Turning Pedestal. The antenna pedestal must have the capability to scan in azimuth and elevation, though an elevation angle of 30 degrees is likely sufficient. It must be able to support scanning rates of up to 60 rpm with appropriate synchro signals (in azimuth and elevation) to indicate positional data. It also contains suitable RF rotary joints with low VSWR to translate the RF energy to and from the antenna to the transmitter receiver. The selected antenna pedestal must allow for antenna wind and ice loading although this could be eliminated through the use of an appropriate radome. While costing the pedestal it was found that the maximum achievable turning rate was 20 to 30 rpm, in contrast with the desired 60 rpm rate.

iii) Radome. The size of the radome would be approximately 3.0 m to allow for elevation tilt angles of a 2.4 m antenna dish. These radomes will protect against the accumulation of ice and snow and significantly reduce the wind loading factor. This will also significantly reduce the operational requirements of the antenna pedestal.

iv) Waveguide Runs. Low VSWR rectangular or elliptical waveguide can be used to connect the transmitter receiver to the antenna. Appropriate gasketing and pressure windows are required where applicable. In the final selection of which waveguide type to be used, some consideration must be given to systems' losses. The following lists the losses related to waveguide runs:

Rectangular	WR159	4.70 dB/100 m
Elliptical	EW52	3.96 dB/100 m

Other considerations relate to low signal distortion (low VSWR), lower material cost, easier installation, etc. Elliptical waveguide is superior to the standard rectangular waveguide. Typical costs of the EW52 elliptical waveguide are $60/metre. It is envisioned that the radar antenna will be located close to the equipment shelter, therefore no more than 20 m should be required. The total waveguide cost then becomes $1,200.

v) Pressurization System. To prevent the possible entry of moisture into the waveguide system causing increased attenuation and VSWR, a pressurization system is recommended. The pressure within a waveguide system should be maintained at a positive level, but below the maximum pressure rating of any of the components. This maximum value is usually around the rating of 70 kPa (10 lb/in^2). These pressure systems are designed to start when the internal waveguide pressure drops to a preset low value (typically 21 kPa) and to stop when it reaches an upper limit (55 kPa). Costs for a typical pressurization system are in the region of $3,000.

6.2.2 Transmitter Receiver Group

In reviewing the costs of the transmitter receiver group, the procurement of off-the-shelf equipment was preferred as well as the purchase of as much of a complete RF system as possible. The relative prices of magnetrons to that of klystrons was found to be approximately 1:3, however, if one considers the full transmitter this drops to 1:2. Magnetron systems are simpler to modulate since they do not require floating the grid as in the klystron case. In the past, conventional magnetrons when compared to other RF tubes have had shorter operating lifetimes, however the newer co-axial configurations have been found to have comparable or better MTBF values.

The main disadvantage of using magnetrons in the past has been the lack of pulse-to-pulse coherency. However, Varian has developed a system called MaPS (Magnetron Phase Stabilizer) that provides pulse-to-pulse coherency at relatively high gains (>30 dB). This technique has been utilized in a military Ku-band MTI radar and has proven quite successful. Typical MaPS performance parameters are:

	S or C-band
Gain	> 30 dB
MTI Cancellation	> 50 dB
RMS Phase Error	0.2°
Time Jitter	< 1 nsec
Phase Locking Time	< 1 nsec

As shown, the phase locking time and the leading edge time jitter are an order of magnitude better than conventional magnetrons. This leads to an enhanced MTI improvement of approximately 16 dB. Upon review of the off-the-shelf production magnetrons it was discovered that C-band models with power output capabilities between 100 kw and 175 kw were more readily available. By adjusting the modulator drive, the magnetron output power can be modified by as much as 3 dB. The transmitter system (magnetron, modulator, STALO, power supply, and associated RF wavequide components) and the receiver system (LNA, down-converter, matched filter, phase detectors) have been costed as a delivered sub-system. Its price, estimated by Varian Canada, has been given as $300,000.

6.2.3 Signal Processor Group

The signal processor can be divided into the following subsystems to perform a cost analysis. These include:

i) A/D Converters
ii) Doppler Processor
iii) CFAR, Threshold Detector and Timing Controller
iv) Display Processor

i) A/D Converters. The level of digitization has been selected to that of 8 bits which gives approximately 48 dB of dynamic range. The byte wide amplitude data also facilitates the selection of memory ICs, digital multipliers, etc. required for the batch memory and Doppler processor. The digitizers can be purchased at board level from TRW at an approximate cost of $600. Two such boards are required in order to digitize the in-phase and quadrature channels.

ii) Doppler Processor. Most of the high speed processors reviewed (e.g. Texas Instruments, NEC, Analog Devices, etc.) exist at the integrated circuit level and would require extensive integration to develop a board level Doppler processor. However, Motorola has a new digital signal processor that is available on an application development module, the DSP56000ADS. It accepts digital input data up to the rate of 20 MHz which is more than sufficient for the A/D radar video that is digitized at a 2 MHz rate. The module also has enough internal memory to temporarily store radar batch data before Doppler processing. The interesting feature of this processor is that it can be interfaced directly to a PC which can be used to control the DSP programs of the 56000 which are executed in real time. If time-sharing or multiplexing of processors is required, the PC can control up to eight modules simultaneously. This system has been benchmarked for performing a 32-point complex FFT at 68 μsec. As the number of points decrease (16 required in our case) the number of multiplications, additions, and data moves substantially decrease. The actual relationship is N(log(N)), where N is the number of FFT points. It has been indicated that the requirement of performing a 16-point FFT within 10μsec should

not be a problem for this device. However, as a safeguard, if the single device does appear limited in its operations, multiplexed modules can simply be added to decrease the timing requirements. These modules are not expensive and cost approximately $7000 each. Therefore, in the worst case, if three multiplexed devices were required to accommodate the necessary FFT processing requirement and a PC-XT was procured as a user interface system, the total cost would be around $25,000. Figure 6-3 is a block diagram illustrating the functional flow of Motorola's DSP application development module. Note that the PC-XT is intended for development and evaluation and will not be required for production equipment.

iii) CFAR, Threshold Detector and Timing Controller. These functional subsystems will be implemented utilizing standard VME or Multibus configurations. Typical costs for the required functional PCBs are:

CPU	$ 5,000
Memory	4,000
I/O Communications	1,500
Standard Rack	2,000
Power Supply	1,000
Total	$13,500

iv) Display Processor. The display processor is responsible for the presentation of the radar data in suitable user format. It performs the required scan conversion and integration of LLWAS with the radar data. A typical scan converter with a 1024 x 1024 colour monitor can be procured for approximately $30,000.

6.2.4 Facility Shelter

The radar equipment shelter located adjacent to the antenna structure can be procured with its own electrical system, ventilation system, forced air heating, and equipment racks. A typical 3x6x3 m shelter constructed from fiberglass-reinforced polyester costs approximately $18,000.

6.3 Canadian Industry Capability

Table 6-1 lists the Canadian manufacturers and vendors who have the relevant experience to be considered as suppliers for the identified subsystems.

6.4 Cost Summary

Table 6-2 contains a cost summary for a single detection system. Total system production costs are estimated to be $934,000 per system, and non-recurring development costs are estimated to be $810,000 for all airport systems.

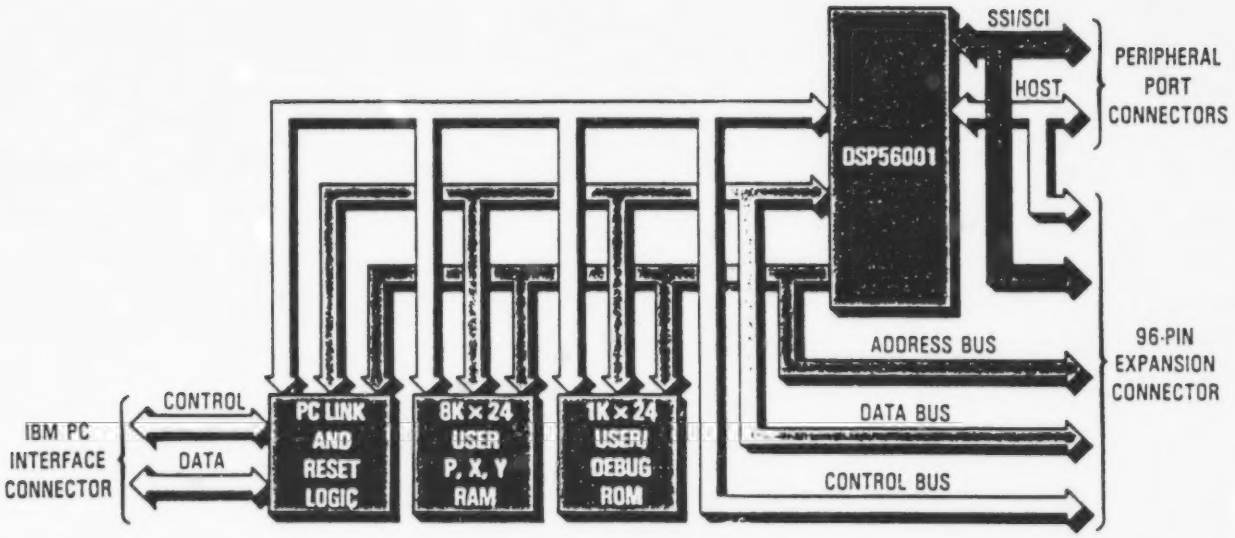

Figure 6-3 Block diagram of DSP application development module (Motorola)

Table 6-1 Canadian Suppliers and Vendors

Sub-system	Supplier or Vendor
Antenna	Andrew Antenna Company Whitby, Ontario
Radome	ICL Engineering Limited, Richmond, B.C.
Waveguide, Pressurization System	Andrew Antenna Company
Antenna Pedestal	McGill Weather Observatory Ste. Anne de Bellevue, P.Q. Andrew Antenna Company through U.S. subsidiary Kintec Ltd.
Transmitter/Receiver	Varian Canada, Ottawa, Ontario
Display Processor	MacDonald Dettwiler Richmond, British Columbia
Radar Shelter	Andrew Antenna Company

Table 6-2 Cost Summary

Sub-system	Cost ($)
Antenna Group	
Antenna	7,000
Antenna Pedestal	200,000
Waveguide	1,200
Pressurization System	3,000
Radome	25,000
Shelter	18,000
Total	**254,200**
Transmitter Receiver Group	
Magnetron MaPS System and Receiver with 30 MHz IF Output	280,000
Phase Detectors and Matched Filter	20,000
Total	**300,000**
Signal Processor Group	
A/D Converters	1,200
FFT Processor	25,000
CFAR, Threshold Detection and Timing Controller	13,500
Display Processor	30,000
Total	**69,700**
LLWAS	
Complete 11 Station System	310,000
Total	**310,000**
Total System Production Costs	**934,000**
Non-Recurring Engineering Development Costs	
Transmitter Receiver	280,000
Signal Processor	150,000
Antenna and Pedestal	70,000
Display Processor	310,000
Total	**810,000**

7. CONCLUSIONS AND RECOMMENDATIONS

The following conclusions summarize the findings of this feasibility study to determine possible technical approaches for the detection, analysis, and advance warning of wind shear conditions, specifically microbursts, in and around Canadian airports.

1. Future work in this area would benefit from an analysis of wind shear/microburst data collected at Canadian airports.

2. The microburst phenomena is not easily characterized by a definitive set of meteorological parameters.

3. Several technologies exist for measuring and monitoring various meteorological parameters but there is no single technology capable of meeting Transport Canada's requirements for wind shear/microburst detection.

4. Doppler radar and LLWAS systems provide the best complimentary capabilities to solve this requirement.

5. The proposed wind shear/microburst detection system can be built with a large complement of off-the-shelf components from Canadian companies.

6. It appears feasible to be able to install a wind shear detection system at an airport for $1,000,000. Initially, however, approximately $1,000,000 in non-recurring engineering costs would be required to develop such a system.

7.1 Recommendations

The following recommendations outline areas to be initially addressed in order to develop a solution to the wind shear/microburst detection problem.

1. Install an LLWAS system at a Canadian airport for collecting meteorological data on wind shear/microbursts. This will help to determine the extent of the wind shear problem in Canada.

2. Develop and evaluate (laboratory and in-situ) a prototype integrated Doppler radar/LLWAS.

3. Define suitable wind shear detection algorithms for use in a detection system, with consideration given to expert systems and developments in the NEXRAD and TDWR systems.

REFERENCES - SECTION 2

1. Transport Canada, General Specification for Procurement of Electronic Equipment, TP 3131, Facility Engineering and Systems Development Branch.

2. Transport Canada, Land Use in the Vicinity of Airports, TP 1247, Air Navigation Systems Requirements Branch.

REFERENCES - SECTION 3

1. International Civil Aviation Organization. Wind Shear, 1987, 183 pp., International Civil Aviation Organization Circular No. 186-AN/122.

2. Ralph E. Huschke (Editor). Glossary of Meteorology, American Meteorology Society, 1959, Third printing 1980.

3. Lansford, H. The Might of the Microburst, Air and Space, August/September 1986, pp. 43-54.

4. Mathews, T. and Hicks, R.B. Doppler Sodar Measurements of Wind Climatology of Calgary, Alberta Environment Report 84/28, 149 pp.

5. Fujita, T.T. The Downburst, Microburst, and Macroburst, Satellite and Mesometeorology Research Project (SMRP), University of Chicago Press, Chicago, Illinois, 1985, 122 pp.

6. Bohun, R. A Discourse Concerning the Origin and Properties of Wind, W. Hall, Oxford, England, 1671.

7. Byers, H.R., Braham, R.R. Jr. The Thunderstorm, United States Government Printing Office, 1949, 287 p.p.

8. Wakimoto, R.M. The Life Cycle of Thunderstorm Gust Fronts as viewed with Doppler Radar and Rawinsonde Data, Montreal Weather Review, Montreal, Quebec, Vol. 110, 1982, pp. 1060 - 1082.

9. Fujita, T.T. Private communication. 1986.

10. Fujita, T.T., McCarthy, J. Application of Mesoscale Analysis to Aviation Weather, Proceedings 1987 Weather Conference, Boston, Mass., American Meteorological Society.

11. Transport Canada, Microbursts - A Review, Transport Canada, Air Navigation Technology Development.

12. Environment Canada, Principal Station Data - Winnipeg Int'l A PSD-11, A publication of the Canadian Climate Program, 1983.

13. Bedard, A.J. Jr., LeFebvre, T.J. Surface Measurements of Gust Fronts and Microbursts during the JAWS Project: Statistical Results and Implications for Wind Shear Detection, Prediction and Modelling, National Oceanic and Atmospheric Administration Technical Memorandum, United States Department of Commerce, April 1986, ERL WPL-135.

14. Baker, Dr. C.B., Gilmore, D.W., McCall, R. LLWAS: An Integral Part of the U.S. Wind Shear Safety Programme, International Civil Aviation Organization Bulletin, March 1986, p. 11.

15. Bennett, J. Automated Weather Observing System Passes San Jose Trial, Airport Services Management, February 1987, p. 47.

16. Andrews, K.C. AWOS Operational Scan Capabilities Already Are Being Expanded, International Civil Aviation Organization Bulletin, April 1987, p. 24.

17. Radian Corporation. New Radar Profiles Atmospheric Cross-Section, International Civil Aviation Organization Bulletin, April 1986, p. 15.

18. Radian Corporation. Introducing CAPSONDE, Technical Design and First Results June 1985, Radian Technical Description, June 1985, 12 pp.

19. Johnston, B.C. Wind Shear Detection: A Report on the First Such Airborne Warning Device to be Commercially Certified, International Civil Aviation Bulletin, March 1986, p. 14.

20. Safe Flight Instrument Corporation. Airborne Wind Shear Alert System Enhances Landing/Takeoff Safety, Air Transport World, September 1981.

21. Safe Flight Instrument Corporation. Wind Shear Development Provides Timely Warning, Aviation Week and Space Technology, March 1981.

22. Safe Flight Instrument Corporation. Safe Flight's Automatic Family, Product Analysis, Business and Commercial Aviation, October 1984.

23. Greene, Dr. L.M., Low Altitude Wind Shear Protection can be Attained, International Civil Aviation Bulletin, April 1986, p. 10.

24. Rahr, W. Wind Shear: Solving the Problem for Today and Tomorrow, International Civil Aviation Bulletin, April 1987, p. 14.

25. Bilbro, J.W., DeMarzio, D.F., Johnson, S., Jones, W. Airborne Doppler Lidar Measurements, Applied Optics, November 1986, p. 3952.

26. Pilots Glean Shear Information From Operational LLWAS Tests, Aviation Week and Space Technology, 24 August 1987, p. 25.

27. Manufacturers Urge Interim Implementation of Warning Function, Aviation Week and Space Technology, 22 September 1986, p. 78.

28. The Menacing Microburst, The Institute of Electrical and Electronics Engineers, Inc., November 1986, p. 50.

29. Wieler, J.G. NEXRAD: A Doppler Weather Radar for Aviation Use, International Civil Aviation Organization Bulletin, September 1986, p. 28.

30. Campbell, W.C., Chadwick, R.B., Moran, K.P., Strauch, R.G. Meterological Applications of the FM Doppler Radar, National Oceanic and Aviation Administration Technical Memorandum, United States Department of Commerce, December 1975, ERL 351-WPL 44.

31. Vaisala Inc. DigiCora MW11 - Technical Data, Vaisala Inc. Marketing Literature.

32. Radian Corporation. Echosonde PS/2 Doppler Acoustic Sounding System, Radian Internal Technical Literature, 10 pp.

33. Fage, J.M., Huguet, P. Doppler Sodar can provide Timely Wind Shear Warning, International Civil Aviation Organization, April 1985, pp. 26 - 28.

34. Wind Shear Detector, Aviation Consumer, 1 March 1981, p. 22.

35. Danzier, A., Fage, J.M. Research Continues On Sodar Wind Shear Detector, International Civil Aviation Organization Bulletin, October 1986, p. 29.

36. Groff, G. Tomorrow's Weather: New Accuracy In Forecasting, High Technology, April 1986, p. 27.

37. Koepp, F., Krichbaumer, W.A. Experimental or Theoretical Doppler-Lidar Signatures of Aircraft Wake Vortices, DFVLR Institute of Optoelectronics.

38. Bilbro, J.W., Craig, G.D., George, R.W., Jeffreys, H.B., Manero, P.J., Weaver, E.A. Laser Doppler Vortex Measurements at John F. Kennedy International Airport, Proceedings of the Airport Wake Vortices Conference, 15 - 17 March 1977, pp. 81 - 105.

39. Banic, J., Houston, J.D., Sizgoric, S., Ulitsky,A. Raman Lidar System for Methane Gas Concentration Measurements, Applied Optics, Vol. 25, 1 July 1986, p. 2115.

40. Mundle, J. Uses for Laser Anemometry in Aviation are Widening, International Civil Aviation Organization Bulletin, April 1987, p. 17.

41. Kapp, F., Schwiesow, R.L., Werner, C. Influence of Clouds and Fog on LDA Wind Measurements, Applied Optics, Vol 23., 1 August 1984, p. 2482.

42. Hall, F.F., Hardesty, R.M., Lawrence, T.R., Post, M.J. Doppler Lidar Studies of Atmospheric Wind Field Dynamics, National Oceanic and Atmospheric Administration Technical Memorandum, United States Department of Commerce, Wave Propogation Laboratory.

Accident. When used in reference to an Aircraft Accident Investigation an accident is defined as follows. An occurrence associated with the operation of an aircraft which takes place between the time any person boards the aircraft with the intention of flight until such time as all such persons have disembarked, in which:

a) a person is fatally or seriously injured as a result of:

- being in the aircraft, or
- direct contact with any part of the aircraft, including parts which have become detached from the aircraft, or
- direct exposure to jet blast,

except where the injuries are from natural causes, self-inflicted or inflicted by other persons, or when the injuries are to stowaways hiding outside the areas normally available to the passengers and crew; or

b) the aircraft sustains damage or structural failure which:

- adversely affects the structural strength, performance or flight characteristics of the aircraft, and

- would normally require major repair or replacement of the affected component,

except for engine failure or damage, when the damage is limited to the engine, its cowlings or accessories; or for damage limited to propellers, wing tips, antennas, tires, brakes, fairings, small dents or puncture holes in the aircraft skin; or

c) the aircraft is missing or completely inaccessible.

Note 1. - For statistical uniformity only, an injury resulting in death within thirty days of the date of the accident, is classified as a fatal injury by ICAO.

Note 2. - An aircraft is considered to be missing when the official search has been terminated and the wreckage has not been located.

Coriolis Force. An "apparent" force which acts on moving particles in a non-inertial coordinate reference system. In meteorology this applies to air moving in relation to the rotating earth. In the northern (southern) hemisphere the "apparent" force acts to the right (left) when viewed along the motion. In order to account for the deflection due to the earth's rotation an

"apparent" force has to be introduced. The force is named after Gustave-Gaspard Coriolis, a French mathematician who first described the effect in 1835.(1)

Downburst. A strong downdraught which induces an outflow of damaging winds on or near the ground.(1)

Geostrophic Wind. The horizontal wind velocity for which the horizontal component of the coriolis force exactly balances the **horizontal pressure gradient force** (see below) so that the wind blows parallel to the isobars.(1)

Gust Front. The leading edge of the cold air from a convective cloud downdraught which reaches ground level and spreads outwards, undercutting the surrounding warmer air.(1)

Horizontal Pressure Gradient Force. The horizontal component of the force which acts on air particles due to the variation in pressure in space. The force acts perpendicular to the isobars from high to low pressure.(1)

Horizontal Wind Shear. Change of horizontal wind direction and/or speed with horizontal distance, as would be determined by two or more anemometers mounted at the same height along a runway.(1)

Incident. When used in reference to an Aircraft Accident Investigation an incident is defined as follows. An occurrence, other than an accident, associated with the operation of an aircraft which affects or could affect the safety of operation.

Macroburst. A large downburst with its outburst wind extending in excess of 4 km (2.5 miles) in horizontal dimension. An intense macroburst often causes wide spread, tornado-like damage. Damaging winds, lasting 5 to 30 minutes, could be as high as 60 m/s (134 mph).(5)

Microburst. A strong localized downdraught which induces a sudden outflow of damaging winds on or near the ground with a horizontal extent between 0.4 and 4 km.(1)

Nowcast. A description of current weather and a forecast for up to two hours ahead.(1)

Turbulence. Eddy motions in the atmosphere which are functions of both time and space.(1)

Wind Shear. The local variation of the wind vector or any of its components in a given direction. The vertical shear can be expressed in terms of the height , $\delta V/\delta z$, or of pressure, $\delta V/\delta p$, as the vertical coordinate. If the wind is geostrophic, the vertical shear is given by the thermal-wind equation. The wind shear at a point is said to be cyclonic or anticyclonic according to whether the sense of rotation from the wind vector to the shear vector at the point is cyclonic or anticyclonic.(2)

BIBLIOGRAPHY

AeroEnvironment Inc. Model 2000 Doppler Acoustic Sounding System, AeroEnvironment Inc. Marketing Information.

Andre and Mahot. The Nocturnal Surface Inversion and Influence of Clear Air Radiative Cooling, Journal of Atmospheric Science, April 1982.

Austin, G.L., Bellon, A., Dionne, P., Roch, M. On the Interaction between Radar and Satellite Image Nowcasting Systems and Mesoscale Numerical Models, Proceedings of the Symposium on Mesoscale Analysis and Forecasting, Vancouver, 17 - 19 August 1987, pp. 225 - 228, ESA SP-282.

Badner, J. Low Level Wind Shear, A Critical Review, National Oceanic and Atmospheric Administration Technical Memorandum, April 1979, 80 pp., NWS FCST-23.

Baker, Dr. C.B., Gilmore, D.W., McCall, R. LLWAS: An Integral Part of the U.S. Wind Shear Safety Programme, International Civil Aviation Organization Bulletin, March 1986, pp. 11 - 13.

Bedard, A.J. Jr., LeFebvre, T.J. Surface Measurements of Gust Fronts and Microbursts during the JAWS Project: Statistical Results and Implications for Wind Shear Detection, Prediction and Modelling, National Oceanic and Atmospheric Administration Technical Memorandum, United States Department of Commerce, April 1986, ERL WPL-135.

Bedard, A.J. Jr. The Dulles International Airport Wind Shear Detection System - Statistical Results, Conference on Atmsopheric Environment of Aerospace Systems and Applied Meteorology, American Meteorological Society, New York, New York, 14 - 16 November 1978, pp. 57 - 66.

Beran, D.W. Acoustics: A New Approach for Monitoring the Environment Near Airports, National Oceanic and Atmospheric Administration Technical Memorandum, United States Department of Commerce, Wave Propogation Laboratory, Boulder, Colorado, 12 August 1971, COM-72-10726.

Bilbro, J.W., Burnham, D.C., Hallock, J.N., Harris, C., Weaver, E.A. Pulsed Laser Doppler Measurements of Wind Shear, Bulletin of the American Meteorological Society, Vol. 60, No. 9, September 1979, p. 1061.

Bohun, R. A Discourse Concerning the Origin and Properties of Wind, W. Hall, Oxford, England, 1671.

Bonewitz, J.D. NEXRAD - Weather Radar for the Future.

Brennan, W.T. Advisory Circular, United States Department of Transportation, 20 January 1983, pp. 1 - 7.

Brown, H.A. Specification of Slant Visual Wind Shear with an Offset Tower Observation System, Ninth Conference on Aerospace and Aeronautical Meteorology, American Meteorological Society, Omaha, Nebraska, 6 - 9 June 1983, pp. 241 - 246.

Browning and Foote. Airflow and Hail Growth in Supercell Storms, Quarterly Journal of the Royal Meteorological Society, London, England, July 1976.

Byers, H.R., Braham, R.R. Jr. The Thunderstorm, United States Government Printing Office, 1949, 287 p.p.

Byers, R.L., Kane, T.J., Zhou, B. Potential for Coherent Doppler Wind Velocity Lidar using Meodymium Lasers, Applied Optics, 1 August 1984, p. 2477.

Carbone, R., Fujita, T.T., McCarthy, J., Wilson, J. Doppler Weather Radar Applications to Terminal and EnRoute Air Traffic Control.

Carswell, A.I. Lidar Measurements of the Atmosphere, Canadian Journal of Physics, Vol. 61, No. 2, 1983, p. 378 - 395.

Chadwick, R.B., Jordan, J., Detman, T. Radar Detection of Wingtip Vortices, Ninth Conference on Aerospace and Aeronautical Meteorology, American Meteorological Society, Omaha, Nebraska, 6 - 9 June 1983, pp. 235 - 240.

Chang, H.P., Elmare, K.L., Frost, W., McCarthy, J. A High Resolution Spatial and Temporal Multiple Doppler Analysis of a Microburst and Its Application to Aircraft Flight Simulation, Journal of Climate and Applied Meteorology, Vol. 25, 1986, p. 1398.

Charba, J. Application of Gravity Current Model to Analysis of Squall-Line Gust Front, Montreal Weather Review, 1974, p. 102.

Cherna, E., Bellon, A., Austin, G.L., Kilambi, A. An Objective Technique for the Delineation and Extrapolation of Thunderstorms from GOES Satellite Data, Journal of Geophysical Research, Vol. 90, No. D4, 30 June 1985, pp. 6203-6210.

Christie and Muirhead. Solitary Waves: A Hazard to Aircraft Operating at Low Altitudes, Australian Meteorological Magazine, June 1983.

Clark, M. United States Criteria for Selecting Airports for Doppler Radar Installation, 1986, p. 1-6.

Coping with Microbursts, Air Transport World, January 1985, p. 46.

DeLaMarche, A., Lee, T.Y., Lewis, W., Offi, D.L. Test and Evaluation of the Airport Radar Wind Shear Detection System, Final Report, February 1982, DOT/FAA/RD-81/85.

DeLaMarche, A., Lee, T.Y., Lewis, W., Oliver, R.G. Test and Evaluation of the Radar Thunderstorm Turbulence Detection System (Phase 1), July 1982, 24 pp., DOT/FAA/RD-82/22.

Dill, R.A. Latest Developments in Doppler Weather Radar, The Institute of Electrical and Electronics Engineering, Inc., International Radar Conference.

Donzier, A., Fage, J.M. Research Continues on Sodar Wind Shear Detection, International Civil Aviation Organization Bulletin, October 1986, pp. 29 - 31.

Doviak, R.J. Doppler Weather Radar for Forecasting and Warning, National Severe Storm Laboratory.

Doviak, R.J., Koscielny, A.J., Robin, R.M. Doppler Weather Radar for Profiling and Mapping Winds in the Prestorm Environment, Institute of Electrical and Electronics Engineers, Inc., Transactions on Geoscience and Remote Sensing, Vol. GE-21, No. 1, January 1983, p. 25.

Doviak, R.J., Lee, J.T. Field Program Operations - Turbulence and Gust Front Studies, November 1981, 34 pp., DOT/FAA/RD-81/108.

Doviak, R.J., Sirmans, D.S., Zrnic, D.S. Doppler Weather Radar, Proceedings of the Institute of Electrical and Electronics Engineers, Inc., Vol. 67, No. 11, November 1979, p. 1522.

Dunkin, J.A., Harris, C.E. Clear Weather Laser Radar, Electro/81 Proceedings, Session 34, 1981, p. 34/3.

Ellis and Keenan. Development of Wind Shear Models and Determination of Wind Shear Hazards, Federal Aviation Administration, January 1978, FAA Report No. FAA-RD-79-119.

Emmitt, G.D. Ground Based CO2 Doppler Lidar Wind Measurements of Winds in the Vicinity of Cumulus Convection, Ninth Conference on Aerospace and Aeronautical Meteorology, American Meteorological Society, Omaha, Nebraska, 6 - 9 June 1983, pp. 257 - 258.

Fage, J.M., Huguet, P. Doppler Sodar can provide Timely Wind Shear Warning, International Civil Aviation Organization, April 1985, pp. 26 - 28.

Federal Aviation Administration. Criteria for Operational Approval of Airborne Wind Shear Alerting and Flight Guidance Systems, 7 November 1983, 50 pp., FAA Advisory Circular 120-41.

Federal Aviation Administration. Thunderstorms, 20 January 1983, 7 pp., FAA Advisory Circular 00-24B.

Federal Aviation Administration. Low Level Wind Shear, 23 January 1979, 17 pp., FAA Advisory Circular 00-50A.

Frost, W., Kessel, P.A., Turkel, B.S. Feasibility Study of a Procedure to Detect and Warn of Low Level Wind Shear, Scientific and Technical Information Branch, NASA, 1981, 80 pp., NASA Contractor Report 3480.

Fujita, T.T. Microburst Wind Shear at New Orleans International Airport Kenner, Louisiana on July 9, 1982, Satellite and Meteorology Research Project 199, University of Chicago, 12 January 1983, 39 pp.

Fujita, T.T. Private communication. 1986.

Fujita, T.T. The Downburst, Microburst, and Macroburst, Satellite and Mesometeorology Research Project (SMRP), University of Chicago Press, Chicago, Illinois, 1985, 122 pp.

Fujita, T.T. Tornadoes and Downbursts in the Context of Generalized Planetary Scales, Journal of Atmsopheric Science, Vol. 38, 1981, pp. 1511 - 1534.

Fujita, T.T., Byers, H.R. Spearhead Echo and Downburst in the Crash of an Airliner, Montreal Weather Review, Vol. 105, p. 129 - 146.

Fujita, T.T., Caracena, F. An Analysis of Three Weather-Related Aircraft Accidents, Bulletin of the American Meteorological Society, Vol. 58, pp. 1164 - 1181.

Fujita, T.T., McCarthy, J. Application of Mesoscale Analysis to Aviation Weather, Proceedings 1987 Weather Conference, Boston, Mass., American Meteorological Society.

Fujita, T.T., Wakimoto, R.M. Five Scales of Airflow Associated with a Series of Downbursts on 16 July 1980, Montreal Weather Review, Vol. 109, pp. 1438 - 1456.

Fujita, T.T., Wakimoto, R.M. Microburst in JAWS depicted by Doppler Radars, PAM and Aerial Photographs, Preprint Volume, 21st Conference on Radar Meteorology, American Meteorological Society, Edmonton, Alberta, September 1983.

Goss, D. Beaver County Tower First With Doppler Radar, Journal of Air Traffic Control, October - December 1985, pp. 39 - 41.

Greene, L.M. Low Altitude Wind Shear Protection Can Be Attained, International Civil Aviation Organization, April 1986, pp. 10 - 13.

Griffith, M.S. Jr., McAnally, M.A., Peterman, K.R. Low Level Wind Shear Detection, Radian Corporation, 16 pp.

Heald & Mahot. The Dependence of Boundary Layer Shear on Diurnal Variation of Stability, Journal of Atmospheric Science, August 1981.

Hopkins, H. Microburst, Flight International, 29 September 1984, pp. 812 - 817.

Huguet, M.P., Zanelli, R., Fage, J.M. Low Level Wind Shear Detection System for Airport Landing Approach Areas using the Bertin Doppler Acoustic Sounder (SODAR), First International Conference on Aviation Weather System, American Meteorological Society, Montreal, Quebec, 4 - 6 May 1981, p. 87 - 92.

International Civil Aviation Organization. Wind Shear, 1987, 183 pp., International Civil Aviation Organization Circular No. 186-AN/122.

Jasperson. The Limiting Accuracy of Wind Profiles obtained by Tracking Rising Balloons, Journal of Applied Meteorology, June 1982.

Jelalian, A.V. Laser Radar Systems, Electro/81 Proceedings, Session 34, 1981, p. 34/1.

Joffre. Power Laws and the Empirical Representation of Speed and Directional Shears, Journal of Applied Meteorology, August 1984.

Klass, P.J. FAA Tests of Wind Shear Detection Systems Continue, Aviation Week and Space Technology, 2 August 1985, p. 18.

Klehr, J.T. Wind Shear Simulation Enters the Fourth Dimension, International Civil Aviation Organization Bulletin, May 1986, pp. 23 - 27.

Kirchner, M.E. Approaches to the Wind Shear Problem, Journal of Air Traffic Control, January - March 1986, pp. 7 - 11.

Korhonen, O. An Operation Wind Shear and Inversion Warning System for Helsinki-Vantaa Airport, First International Conference on Aviation Weather Systems, American Meteorological Society, Montreal, Quebec, 4 - 6 May 1981, pp. 121 - 124.

Krauspe, P., Swolinsky, M., Vorsmann, P. Wind Determination and Wind Shear Detection from Flight Test and Airline Flight Data, First International Conference on Aviation Weather Systems, American Meteorological Society, Montreal, 4 - 6 May 1981, pp. 79 - 86.

Kropfli, R.A. A Microburst Observed by High Resolution Dual-Doppler Radar, Preprints, 23rd Conference on Radar Meteorology, American Meteorological Society, Snowmass, pp. J109-J112.

Lansford, H. The might of the microburst, Air and Space, August/September 1986, pp. 43-54.

Lansford, H. Terminal Weather, Flight International, 23 May 1987, pp. 44 - 48.

Laser Radar comes out of the Laboratory, High Technology, August 1987, p. 50.

Lee, J.T. Turbulence and Wind Shear Experiments Related to Aircraft Operation in the Terminal Area, First International Conference on Aviation Weather Systems, American Meteorological Society, Montreal, Quebec, 4 - 6 May 1981, pp. 93 - 102.

Lee, J.T., Doviak, R.J. Field Program Operations - Turbulence and Gust Front Studies, National Technical Information Service, Springfield, Virginia, 1981, pp. 1 - 34.

Lewis, W., Oliver, R.G., DeLaMarche, A., Lee, T.V. Test and Evaluation of the Radar Thunderstorm Turbulence Detection System (Phase I), National Technical Information Service, Springfield, Virginia, pp. 1 - 24.

Lincoln Laboratory, Massachusetts Institute of Technology, Weather Radar Studies, Quarterly Technical Summary, 30 June 1985, 68 pp., AD-A165 221.

Luers and Haines. The Effect of Heavy Rain on Wind Shear Attributed Accidents, American Institute of Aeronautics and Astronautics, St. Louis, Missouri, January 1981.

Mathews, T. and Hicks, R.B. Doppler Sodar Measurements of Wind Climatology of Calgary, Alberta Environment Report 84/28, 149 pp.

McCarthy, J., Wilson, J.W. The Classify, Locate and Avoid Wind Shear (CLAWS) Project at Denver's Stapleton International Airport: Operational Testing of Terminal Weather Hazard Warnings with an Emphasis on Microburst Wind Shear, Preprint, Second International Conference on the Aviation Weather System, American Meteorological Society, Montreal, Quebec, 19 - 21 June 1985, pp. 247 - 256.

McCarthy, J., Wilson, J.W. The Microburst as a Hazard to Aviation, 2nd International Nowcasting Symposium, Norrkoping, Sweden, 1984.

McCarthy, J., Wilson, J.W., Fujita, T.T. The Joint Airport Weather Studies Project, Bulletin of the American Meteorological Society, Vol. 63, pp. 15 - 22.

McCarthy, J., Wilson, J.W. The Joint Airport Weather Studies Project (JAWS), First International Conference on Aviation Weather Systems, American Meteorological Society, Montreal, Quebec, 4 - 6 May 1981, pp. 103 - 110.

McLure, H.R. Hazardous Weather Detection and Warning Systems, United States General Accounting Office, 1987, pp. 1 - 8.

Microburst, Flight International, 29 September 1984, p. 812.

Moncrieff. Comments on Nor-Western Thunderstorm Structure, Weather, London, England, January 1986.

National Research Council. Low-Altitude Wind Shear and its Hazard to Aviation, National Academy Press, Washington, D.C., 1983, 161 p.p.

Offi, D.L., Lewis, W., Lee, T., DeLaMarche, A. Test and Evaluation of the Airport Radar Wind Shear Detection System, National Technical Information Service, Springfield, Virginia, 1982, pp. 1 - 32.

Ott, J. Inquiry Focuses on Wind Shear as Cause of Delta L-1011 Crash, Aviation Week and Space Technology, 12 August 1985, pp. 16 - 19.

Peterson. A Triple Doppler Radar Analysis of a Discretely Propagating Multicell Convective Storm, Journal of Atmospheric Science, October 1984.

Radian Corporation. Introducing CAPSONDE, Radian Corporation Marketing Information.

Rahr, W. Wind Shear: Solving the Problem for Today and Tomorrow, International Civil Aviation Bulletin, April 1987, pp. 14 - 16.

Raytheon Corporation. CAT Lidar Wind Shear Studies, Technical Report, prepared for George C. Marshall Space Flight Centre, March 1978, 33 pp.

Reed, A. Coping with Microbursts, 1/85 Air Transport World, 1985, pp. 46 - 48.

Rosner, N.L. Meteorological Modelling to Predict Real Time Extreme Wind Shear Situations, Conference on Atmospheric Environment of Aerospace Systems and Applications Meteorology, American Meteorological Society, 14 - 16 November 1978, New York, New York, pp. 83 - 86.

Rotunno and Klemp. On the Rotation and Propogation of Simulated Supercell Thunderstorms, Journal of Atmospheric Science, February 1985.

Shrager, J.J. Wind Shear: A Literature Search, Analysis and Annotated Bibliography, United States Department of Transportation/Federal Aviation Administration, Systems Research and Development Service, Washington, D.C., 1977, Final Report No. FAA-RD-76-114.

Simpson et al. Observations and Mechanisms of GATE Waterspouts, Journal of Atmospheric Science, April 1986.

Snow and Pauley. On the Thermodynamic Method of Etimating Maximum Tornado Wind Speeds, Journal of Climatology and Applied Meteorology, October 1984.

Sperry Corporation. Wind Profiler System, Sperry Corporation Marketing Information, 1986.

Srivasta. A Simple Model of Evaporatively Driven Downdraught: Application to Microburst, Journal of Atmospheric Science, May 1985.

Stewart. The Atmospheric Boundary Layer, Third IMO lecture, World Meteorlogical Organization, 1979, No. 523.

Terminal Weather, Flight International, 23 May 1987, p. 44.

Thorpe. Thunderstorm Dynamics: A Challenge to the Physicist, Weather, London, England, April 1981.

Transport Canada, General Specification for Procurement of Electronic Equipment, TP 3131, Facility Engineering and Systems Development Branch.

Transport Canada, Land Use in the Vicinity of Airports, TP 1247, Air Navigation Systems Requirements Branch.

Trunov, O.K. Wind Shear Revisited, International Civil Aviation Bulletin, October 1986, pp. 26 - 28.

Uccellini, L.W., Brill, K.F., Petersen, R.A., Keyser, D., Aune, R., Kocin, P.J., des Jardins, M. A Report on the Upper-Level Wind Conditions Preceding and During the Shuttle Challenger (STS 51L) Explosion, American Meteorological Society, Vol. 67, No. 10, October 1986, pp. 1248 - 1265.

Uthe, E.E. Alpha-1/Alarm Airborne Lidar Systems and Measurements, Ninth Conference on Aerospace and Aeronautical Meteorology, American Meteorological Society, Omaha, Nebraska, 6 - 9 June 1983, pp. 229 - 234.

Vaisala Inc. Shaping the Future in Upper Air Observations - the DigiCORA Automatic Rawinsonde Set, Vaisala Inc., Marketing Information, 1984.

Viezee, W., Collis, R.T.H., Lawrence, J.D. Jr. An Investigation of Mountain Waves with Lidar Observations, Journal of Applied Meteorology, Vol. 12, 1972, pp. 140 - 148.

Wakimoto, R.M. Forecasting Dry Microburst Activity Over the High Plains, Montreal Weather Review, Montreal, Quebec, Vol. 113(7), 1985, pp. 1131 - 1143.

Wakimoto, R.M. The Life Cycle of Thunderstorm Gust Fronts as viewed with Doppler Radar and Rawinsonde Data, Montreal Weather Review, Montreal, Quebec, Vol. 110, 1982, pp. 1060 - 1082.

Watson, G. Wind Shear Detection, Wings Newsmagazine, September 1987, pp. 36 - 37.

Wei-Kuo Tao and Simpson. Cloud Interactions and Merging: Numerical Simulations, Journal of Atmsopheric Science, October 1984.

Wilson, J.W., Roberts, R.D., Kessinger, C., McCarthy, J. Microburst Wind Structure and Evaluation of Doppler Radar for Wind Shear Detection, Journal of Climatology and Applied Meteorology, Vol. 23, 1984, pp. 898 - 915.

Wilson, J.W., Roberts, R.D. Evaluation of Doppler Radar for Airport Wind Shear Detection, Preprint, Conference on Radar Meteorology, American Meteorological Society, Edmonton, Alberta, Vol. 21, September 1983.

Wolfson. Doppler Radar Observations of an Oklahoma Downburst, Preprint, 21st Conference on Radar Meteorology, American Meteorological Society, Edmonton, Alberta, Vol. 21, 1983.